# REPORT DOCUMENTATION PAGE

*Form Approved*
*OMB No. 074-0188*



| 1. AGENCY USE ONLY (Leave blank) | 2. REPORT DATE | 3. REPORT TYPE AND DATES COVERED |
|---|---|---|
| | April 2004 | Annual Summary (1 Apr 2000 - 30 Mar 2004) |

**4. TITLE AND SUBTITLE**

Biochemical Analysis of the BRCA2 Protein Complex

**5. FUNDING NUMBERS**

DAMD17-00-1-0146

**6. AUTHOR(S)**

Jun Qin, Ph.D.

**7. PERFORMING ORGANIZATION NAME(S) AND ADDRESS(ES)**

Baylor College of Medicine
Houston, TX 77030

E-Mail: jqin@bcm.tmc.edu

**8. PERFORMING ORGANIZATION REPORT NUMBER**

**9. SPONSORING / MONITORING AGENCY NAME(S) AND ADDRESS(ES)**

U.S. Army Medical Research and Materiel Command
Fort Detrick, Maryland 21702-5012

**10. SPONSORING / MONITORING AGENCY REPORT NUMBER**

**11. SUPPLEMENTARY NOTES**

**12a. DISTRIBUTION / AVAILABILITY STATEMENT**

Approved for Public Release; Distribution Unlimited

**12b. DISTRIBUTION CODE**

**13. ABSTRACT (Maximum 200 Words)**

This linked career development award and idea award (CDA part) aims at relieving my administrative duties to acquire molecular biology skills in biology research.

I have learned all the molecular biology techniques in accordance to Task 1 and 2 as stated in the Statement of Work. I have also learned biochemistry and cell biology techniques including protein complex purification, indirect immuno-staining and functional assays for activation of the S-phase and G2/M checkpoints.

This career development award has allowed me to finish the transition from a mass spectrometrist who concentrates on methodology development to a biologist who works on important problems that are related to breast cancer and other human disease. During the award period, I have published 5 papers as a corresponding author and many papers as a collaborator. I have obtained 3 R01 grants from NIH to study the molecular mechanism of DNA damage checkpoint activation, which is important for suppression of breast cancer development.

**14. SUBJECT TERMS**

Breast Cancer

**15. NUMBER OF PAGES**

51

**16. PRICE CODE**

| 17. SECURITY CLASSIFICATION OF REPORT | 18. SECURITY CLASSIFICATION OF THIS PAGE | 19. SECURITY CLASSIFICATION OF ABSTRACT | 20. LIMITATION OF ABSTRACT |
|---|---|---|---|
| Unclassified | Unclassified | Unclassified | Unlimited |

AD_____

Award Number: DAMD17-00-1-0146

TITLE: Biochemical Analysis of the BRCA2 Protein Complex

PRINCIPAL INVESTIGATOR: Jun Qin, Ph.D.

CONTRACTING ORGANIZATION: Baylor College of Medicine
Houston, TX 77030

REPORT DATE: April 2004

TYPE OF REPORT: Annual Summary

PREPARED FOR: U.S. Army Medical Research and Materiel Command
Fort Detrick, Maryland 21702-5012

## Table of Contents

## Introduction

This linked career development award and idea award (CDA part) aims at relieving my administrative duties to acquire molecular biology skills in biology research. Since my background is chemistry and physics, I need to learn the basic molecular biology skills to carry out breast cancer research. For four years of career development, I have been working under the guidance of Dr. Steve Elledge and other faculty members in Baylor College of Medicine to learn molecular biology. I was able to learn ahead of the schedule as stated in the approved statement of work. I also have substantially expanded my learning experience to other techniques that are also necessary for breast cancer research. For the last four years, I have been working on the bench and have contributed data to all papers published from my lab.

## Body

Since I have already reported the learning experience of molecular biology in the last three annual reports, I will not give a detailed description here. Instead, I will focus on the research projects that I have contributed directly in a significant way.

I concentrate on two areas of research, (1) DNA damage/repair and (2) heterochromatin maintenance. In the area of DNA damage response, we first reported the identities of the members of a group of proteins that associate with BRCA1 to form a large complex that we have named BASC (BRCA1-associated genome surveillance complex). This complex includes tumor suppressors and DNA damage repair proteins MSH2, MSH6, MLH1, ATM, BLM, and the RAD50-MRE11-NBS1 protein complex. In addition, DNA replication factor C (RFC), a protein complex that facilitates the loading of PCNA onto DNA, is also part of BASC. We find that BRCA1, the BLM helicase, and the RAD50-MRE11-NBS1 complex colocalize to large nuclear foci that contain PCNA when cells are treated with agents that interfere with DNA synthesis. The association of BRCA1 with MSH2 and MSH6, which are required for transcription-coupled repair, provides a possible explanation for the role of BRCA1 in this pathway. Strikingly, all members of this complex have roles in recognition of abnormal DNA structures or damaged DNA, suggesting that BASC may serve as a sensor for DNA damage. Several of these proteins also have roles in DNA replication-associated repair. Collectively, these results suggest that BRCA1 may function as a coordinator of multiple activities required for maintenance of genomic integrity during the process of DNA replication and point to a central role for BRCA1 in DNA repair.

Subsequently, we tested our genome surveillance hypothesis and found that SMC1 is a downstream effector in the ATM/NBS1 branch of the human S-phase checkpoint. Structural maintenance of chromosomes (SMC) proteins (SMC1, SMC3) are evolutionarily conserved chromosomal proteins that are components of the cohesin complex, necessary for sister chromatid cohesion. These proteins may also function in DNA repair. Here we report that SMC1 is a component of the DNA damage response network that functions as an effector in the ATM/NBS1-dependent S-phase checkpoint pathway. SMC1 associates with BRCA1 and is phosphorylated in response to IR in an ATM- and NBS1-dependent manner. Using mass spectrometry, we established that ATM phosphorylates S957 and S966 of SMC1 in vivo. Phosphorylation of S957 and/or S966 of SMC1 is required for activation of the S-phase checkpoint in response to IR. We also discovered that the phosphorylation of NBS1 by ATM is required for the phosphorylation of SMC1, establishing the role of NBS1 as an adaptor in the ATM/NBS1/SMC1 pathway. The ATM/CHK2/CDC25A pathway is also involved in the S-phase checkpoint activation, but this pathway is intact in NBS cells. Our results indicate that the ATM/NBS1/SMC1 pathway is a separate branch of the S-phase checkpoint pathway, distinct from the ATM/CHK2/CDC25A branch. Therefore, this work establishes the ATM/NBS1/SMC1 branch, and provides a molecular basis for the S-phase checkpoint defect in NBS cells.

Finally, we show that MSH2 and ATR form a signaling module and regulate two branches of the damage response to DNA methylation. The mismatch repair proteins function upstream in the DNA damage signaling pathways induced by the DNA methylating agent N-methyl-N'-nitro-N-nitrosoguanidine (MNNG). We report that MSH2 (MutS homolog 2) protein interacts with the ATR (ATM- and Rad3-related) kinase to form a signaling module and regulate the phosphorylation of Chk1 and SMC1 (structure maintenance of

chromosome 1). We found that phosphorylation of Chk1 by ATR also requires checkpoint proteins Rad17 and replication protein A. In contrast, phosphorylation of SMC1 by ATR is independent of Rad17 and replication protein A, suggesting that the signaling pathway leading to SMC1 phosphorylation is distinct from that mediated by the checkpoint proteins. In addition, both MSH2 and Rad17 are required for the activation of the S-phase checkpoint to suppress DNA synthesis in response to MNNG, and phosphorylation of SMC1 is required for cellular survival. These data support a model in which MSH2 and ATR function upstream to regulate two branches of the response pathway to DNA damage caused by MNNG.

In the area of DNA repair, we concentrate on the single strand break repair (SSBR) pathway. We found a new XRCC1 (X-ray cross complementation protein 1) containing protein complex and evaluated its role in cellular survival to MMS (methyl methane sulfonate). SSBR is important for maintaining genome stability and homeostasis. Current SSBR model derived from in vitro reconstituted reaction suggests that the SSBR complex mediated by X-ray repair cross complimenting protein 1 (XRCC1) is assembled sequentially at the site of damage. In this study, we provide biochemical data to demonstrate that there exist two preformed XRCC1 protein complexes in cycling HeLa cells. One contains known enzymes that are important for SSBR, including DNL3, PNK, and Pol β; the other is a new complex that contains DNL3, and the Ataxia with Oculomotor Apraxia type 1 (AOA) gene product Aprataxin. We report the characterization of the new XRCC1 complex. XRCC1 is phosphorylated in vivo and in vitro by CK2, and CK2 phosphorylation of XRCC1 on S518, T519 and T523 largely determines Aprataxin binding to XRCC1 though its FHA domain. Acute loss of Aprataxin by small RNA interference renders HeLa cells sensitive to MMS by a mechanism of shortened half life of XRCC1. Thus, Aprataxin plays one role to maintain the steady state protein level of XRCC1. Collectively, these data provide insights to the SSBR molecular machinery in the cell and point to the involvement of Aprataxin in SSBR, thus linking SSBR to the neurological disease AOA.

In the area of heterochromatin maintenance, we first found differential association of products of alternative transcripts of the candidate tumor suppressor ING1 with the mSin3/HDAC1 transcriptional corepressor complex. The candidate tumor suppressor ING1 was identified in a genetic screen aimed at isolation of human genes whose expression is suppressed in cancer cells. It may function as a negative growth regulator in the p53 signal transduction pathway. However, its molecular mechanism is not clear. The ING1 locus encodes alternative transcripts of p47 (ING1a), p33 (ING1b), and p24 (ING1c). Here we report differential association of protein products of ING1 with the mSin3 transcriptional corepressor complex. p33 (ING1b) associates with Sin3, SAP30, HDAC1, RbAp48, and other proteins, to form large protein complexes, whereas p24 (ING1c) does not. The ING1 immune complexes are active in deacetylating core histones in vitro, and p33 (ING1b) is functionally associated with HDAC1-mediated transcriptional repression in transfected cells. Our data provide basis for a p33 (ING1b)-specific molecular mechanism for the function of the ING1 locus.

Later, we identified components of a pathway maintaining histone modification and heterochromatin protein 1 binding at the pericentric heterochromatin in mammalian cells. Heterochromatin is a higher order chromatin structure that is important for transcriptional silencing, chromosome segregation, and genome stability. The establishment and maintenance of heterochromatin is regulated not only by genetic elements but also by epigenetic elements that include histone tail modification (e.g. acetylation and methylation) and DNA methylation. Here we show that the p33ING1-Sin3-HDAC complex as well as DNA methyltransferase 1 (DNMT1) and DNMT1-associated protein 1 (DMAP1) are components of a pathway required for maintaining proper histone modification and heterochromatin protein 1 binding at the pericentric heterochromatin. p33ING1 and DMAP1 interact physically and co-localize to heterochromatin in the late S phase, and both are required for heterochromatin protein 1 binding to heterochromatin. Although the p33ING1-Sin3-HDAC and DMAP1-DNMT1 complexes are recruited independently to pericentric heterochromatin regions, they are both required for deacetylation of histones and methylation of histone H3 at lysine 9. These data support a cooperative model for histone deacetylation, methylation, and DNA methylation in maintaining pericentric heterochromatin structure throughout cell divisions.

## Key Research Accomplishments

- We found BASC, a super complex of BRCA1-associated proteins involved in the recognition and repair of aberrant DNA structures.
- We found that SMC1 is a downstream effector in the ATM/NBS1 branch of the human S-phase checkpoint.
- We found that MSH2 and ATR form a signaling module and regulate two branches of the damage response to DNA methylation.
- We found a new XRCC1 (X-ray cross complementation protein 1) containing protein complex and demonstrated its role in cellular survival to MMS (methyl methane sulfonate).
- We found differential association of products of alternative transcripts of the candidate tumor suppressor ING1 with the mSin3/HDAC1 transcriptional corepressor complex.
- We identified components of a pathway maintaining histone modification and heterochromatin protein 1 binding at the pericentric heterochromatin in mammalian cells

## Reportable Outcomes

1. Five papers describing the above findings have been published (see appendix) and one paper is being reviewed in Molecular and Cellular Biology.
2. Three R01 grants (the one addressing the function of BRCA1 has been renewed, and the other addresses human S-phase checkpoint).
3. Many expression vectors, cell lines, and antibodies were generated.

## Conclusions

I have learned many molecular biology techniques and other techniques that are crucial for breast cancer research. This career development award has allowed me to finish the transition from a mass spectrometrist who concentrates on methodology development to a biologist who works on important problems that are related to Breast cancer and other human disease. With the help of this award, I have published 5 papers as a corresponding author and many papers as a collaborator, and I have obtained 3 R01 grants from NIH to study the molecular mechanism of DNA damage checkpoint activation, which is important for suppression of breast cancer development.

## References

None.

## Appendices

Five published papers in PDF form.

# BASC, a super complex of BRCA1-associated proteins involved in the recognition and repair of aberrant DNA structures

Yi Wang,[1,2,6] David Cortez,[1,3,6] Parvin Yazdi,[1,2] Norma Neff,[5] Stephen J. Elledge,[1,3,4] and Jun Qin[1,2,7]

[1]Verna and Mars McLean Department of Biochemistry and Molecular Biology, [2]Department of Cellular and Molecular Biology, [3]Howard Hughes Medical Institute, and [4]Department of Molecular and Human Genetics, Baylor College of Medicine, Houston, Texas 77030 USA; [5]Laboratory of Molecular Genetics, New York Blood Center, New York, New York 10021 USA

**We report the identities of the members of a group of proteins that associate with BRCA1 to form a large complex that we have named BASC (BRCA1-associated genome surveillance complex). This complex includes tumor suppressors and DNA damage repair proteins MSH2, MSH6, MLH1, ATM, BLM, and the RAD50–MRE11–NBS1 protein complex. In addition, DNA replication factor C (RFC), a protein complex that facilitates the loading of PCNA onto DNA, is also part of BASC. We find that BRCA1, the BLM helicase, and the RAD50–MRE11–NBS1 complex colocalize to large nuclear foci that contain PCNA when cells are treated with agents that interfere with DNA synthesis. The association of BRCA1 with MSH2 and MSH6, which are required for transcription-coupled repair, provides a possible explanation for the role of BRCA1 in this pathway. Strikingly, all members of this complex have roles in recognition of abnormal DNA structures or damaged DNA, suggesting that BASC may serve as a sensor for DNA damage. Several of these proteins also have roles in DNA replication-associated repair. Collectively, these results suggest that BRCA1 may function as a coordinator of multiple activities required for maintenance of genomic integrity during the process of DNA replication and point to a central role for BRCA1 in DNA repair.**

[*Key Words*: BASC; BRCA1; DNA repair; DNA structure; cancer]

Received January 21, 2000; revised version accepted March 2, 2000.

Two general classes of cancer genes have been identified (Kinzler and Vogelstein 1997). The first class consists of genes that control cell proliferation and tumor growth such as growth factors, cyclin-dependent kinase (Cdk) regulators such as cyclins, Cdk inhibitors (CKIs) and the retinoblastoma protein, apoptotic factors, and angiogenesis factors. These genes, when mutated or overproduced, promote the inappropriate accumulation of cells. The second class consists of genes that control the stability of the genome and prevent the accumulation of mutations in the first class of genes. These genes are called antimutators or caretaker genes and include DNA repair proteins, cell cycle checkpoint regulators, and genes that maintain the fidelity of chromosome segregation. Many genes of the second class have been identified, including the mismatch-repair genes, *MSH2* and *MLH1*, which are linked to hereditary nonpolyposis colorectal cancer (Kinzler and Vogelstein 1996); the breast cancer susceptibility genes 1 and 2 (*BRCA1* and *BRCA2*; Futreal et al. 1994; Miki et al. 1994); the *ATM* gene, which is mutated in the cancer predisposition syndrome ataxia telangiectasia (AT; Savitsky et al. 1995); and the XP excision repair genes that are responsible for xeroderma pigmentosum. Other genetic disease genes that function in genome maintenance include *NBS1*, the gene mutated in Nijmegen breakage syndrome (NBS; Carney et al. 1998), *BLM*, which encodes a RecQ type DNA helicase and is mutated in Blooms' syndrome (Ellis et al. 1995), and *MRE11*, which is mutated in a variant of AT (Stewart et al. 1999). These proteins all function in DNA metabolism and repair. In addition, there is evidence that several of these proteins also participate in cell cycle checkpoint functions that halt cell cycle progression in the presence of damaged DNA (Shiloh and Rotman 1996; Jongmans et al. 1997).

BRCA1 contains an amino-terminal RING finger domain, a carboxy-terminal BRCT domain, and a SQ cluster domain (SCD) (Bork et al. 1997; Cortez et al. 1999). Disruption of the *BRCA1* gene in mice causes embryonic lethality (Hakem et al. 1996; Gowen et al. 1996). Tar-

[6]These authors contributed equally.
[7]Corresponding author.
E-MAIL jqin@bcm.tmc.edu; FAX (713) 798-1625.

geted deletion of exon 11 of *BRCA1* in mouse mammary epithelial cells results in mammary tumor formation after long latency and genetic instability characterized by aneuploidy, chromosomal rearrangements, or alteration of p53 transcription (Xu et al. 1999a). The BRCA1 protein abundance is cell cycle regulated with low levels in $G_0$ and $G_1$ cells that increase as cells enter S phase (Chen et al. 1996; Ruffner and Verma 1997). BRCA1 localizes to nuclear foci during S phase that rapidly disperse when cells are treated with DNA damaging agents (Scully et al. 1997b). The BRCA1 protein is hyperphosphorylated in response to DNA damage and DNA replication blocks. Genetic evidence indicates that BRCA1 is required for transcription-coupled repair of oxidative DNA damage (Gowen et al. 1998) and homologous recombination in response to double-strand breaks (Moynahan et al. 1999). In addition, BRCA1 has been implicated in $G_2$/M checkpoint control (Xu et al. 1999).

Biochemical evidence also supports a role for BRCA1 in DNA damage repair. BRCA1 is associated and colocalized with the DNA repair protein hRad51 (Scully et al. 1997c). BRCA1 associates with and is phosphorylated by the ATM protein kinase, a global regulator of the DNA damage response (Cortez et al. 1999). In addition, BRCA1 associates with the RAD50–MRE11–NBS1 complex, which functions in homologous recombination, nonhomologous end joining, meiotic recombination, and telomere maintenance (Zhong et al. 1999).

To further understand the function of BRCA1, we used immunoprecipitation and mass spectrometry to identify BRCA1-associated proteins. We found that BRCA1 resides in a large multisubunit protein complex of tumor suppressors, DNA damage sensors, and signal transducers that we have named BASC for BRCA1-associated genome surveillance complex.

## Results

### *Biochemical purification and mass spectrometric identification of BRCA1-associated proteins*

To facilitate the purification of the BRCA1 complex by antibody affinity, we raised two rabbit polyclonal antibodies against GST–BRCA1 1021–1552 (Ab80) and GST–BRCA1 1501–1861 (Ab81) produced in *Escherichia coli*. These antibodies were affinity purified using the respective antigens and shown to recognize a ~220-kD BRCA1 protein by Western blotting and immunoprecipitation.

We purified BRCA1-associated proteins from unfractionated HeLa nuclear extracts by one-step immunoprecipitation with antibodies Ab80, Ab81, or the commercial carboxy-terminal epitope antibody C-20. After extensive washing in NETN buffer, the immunoprecipitates were eluted, separated by SDS-PAGE, and detected by Coomassie blue staining (Fig. 1A). Then, we sequenced all proteins that were just visible by Coomassie blue staining by mass spectrometry (Ogryzko et al. 1998).

Nonspecific immunoprecipitating proteins were identified by immunoprecipitation with pre-immune serum and nonrelevant antibodies such as an anti-GST antibody followed by mass spectrometric sequencing. Proteins that are common to both anti-BRCA1 immunoprecipitates and negative controls are designated as nonspecific binding proteins. To identify proteins that may be cross-reacting to antibodies Ab80 and Ab81, we carried out immunoprecipitation in high detergent-containing buffers such as RIPA with the same antibodies. Under these conditions, most of the truly associated proteins will be completely or partially dissociated, whereas the cross-reacting proteins and BRCA1 will be immunoprecipitated.

In total, 40 proteins (excluding nonspecific-binding and cross-reacting proteins) were identified from Ab80, Ab81, and C-20 immunoprecipitates by mass spectrometry. As expected, we found several known BRCA1-interacting proteins such as BRCA1-associated RING domain protein (BARD1) and histone deacetylase 1 (HDAC1; Wu et al. 1996; Yarden and Brody 1999). Then, we focused our effort on the characterization of proteins that are involved in DNA damage repair (listed in Table 1 and described below) while the rest of the proteins await further characterization.

### *BRCA1 associates with multiple DNA repair proteins to form BASC*

One band that migrates at ~150 kD from an anti-BRCA1 (C-20) immunoprecipitation was identified as RAD50. During the course of this study, a second group independently reported the association of RAD50 and BRCA1 (Zhong et al. 1999). A band in the Ab81 immunoprecipitate that migrates slightly slower on SDS-PAGE than BRCA1 was determined to be the protein kinase ATM, consistent with our previous observations (Cortez et al. 1999). In addition to the RAD50 complex and ATM, we also identified a 160-kD band from the Ab80 IP as BLM, the RecQ helicase (see Fig. 1B). Using a database search program PROWL (http://prowl.rockefeller.edu), the mass of the parent peptide (m/z 812, 2+ charged) and the masses of fragments we identified a sequence $^{41}$TSSDNNVSVTNNSVAK$^{56}$, which is unique to BLM. Protein bands migrating at 160 kD from the Ab80 and C-20 immunoprecipitations were identified as MSH6. A 100 kD protein band from the Ab80 IP was identified as MSH2, and protein bands with molecular masses of 90 kD from Ab80 and Ab81 immunoprecipitates were identified as MLH1. Three bands that migrate at 140, 37, and 34 kD from both Ab80 and Ab81 immunoprecipitations were determined to be three subunits of the replication factor C (RFC) complex (p140, p37, and p34, respectively). These results are summarized in Table 1.

To confirm that the proteins identified by mass spectrometry did interact with BRCA1 and to determine the binding interrelationship among all the associated proteins, we carried out multiple reciprocal co-immunoprecipitations with antibodies against these proteins. As shown in Figure 2 (A,B), anti-BRCA1 antibodies co-immunoprecipitate RFC (p140), MSH6, BLM, ATM, and

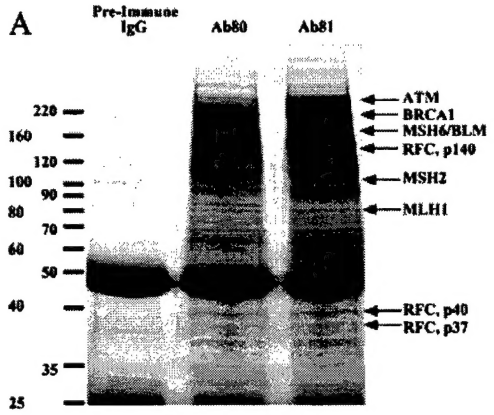


**Figure 1.** Immunoprecipitation of BRCA1-associated proteins and identification by mass spectrometry. (*A*) Immunoprecipitates of BRCA1-associated proteins using antibodies Ab80 and Ab81 were resolved on a 4%–20% gradient SDS–polyacrylamide gel and stained with Coomassie blue. Labeled protein bands were identified by mass spectrometry. (*B*) A representative MS/MS spectrum that identifies the 160-kD band from Ab80 immunoprecipitate as the RecQ DNA helicase BLM.

RAD50. Multiple independent BRCA1 antibodies (polyclonal Ab80, Ab81, and C-20, and monoclonal D-9) also co-immunoprecipitate MSH2, MLH1, MRE11 and NBS1 (data not shown). In addition, antibodies to ATM, RAD50, MSH2, and BLM reciprocally immunoprecipitate BRCA1 (Fig. 2C,D). The presence of MRE11 and NBS1 in the BRCA1 complex was confirmed by immunoblotting (Fig. 2D and data not shown). Moreover, we also found that antibodies to ATM, MSH6, MLH1, BLM, and RFC could immunoprecipitate RFC, MSH6, and BLM (Fig. 2A); antibodies to RAD50, MRE11, ATM, MSH2, MLH1, BLM, and RFC could immunoprecipitate ATM and RAD50 with the exception that RFC did not immunoprecipitate ATM (Fig. 2B), although antibodies to ATM did immunoprecipitate RFC (Fig. 2A); and antibodies to NBS1 could immunoprecipitate BLM, RAD50, MRE11, and ATM (Fig. 2D and data not shown). In summary, nearly all of these BRCA1-associated proteins can co-immunoprecipitate each other. Thus, BRCA1 and these DNA repair and checkpoint signaling proteins may reside in the same protein complex.

To further confirm that these proteins reside in a complex with BRCA1 and to estimate the size of the complex, we performed a two-step fractionation of the nuclear extracts using a DEAE ion-exchange column and a Superose 6 gel-filtration column. BRCA1 elutes at 0.2, 0.3, and 0.4 M KCl from a step-eluted DEAE column. The 0.3 M KCl fraction that contains the majority of cellular BRCA1 as detected by Western blotting was further separated on a Superose 6 gel-filtration column. BRCA1 was eluted exclusively in the void volume. All the associated DNA repair proteins were detected in multiple fractions from the DEAE column and as multiple peaks from the gel-filtration column, but all of them could be detected co-eluting with BRCA1 in the void volume in the 0.3 M KCl fraction (Fig. 2E), thus establishing that this BRCA1-containing complex is >2 MD.

To exclude the possibility that this BRCA1 complex is organized by DNA or RNA instead of through protein–protein interactions, we treated the nuclear extracts with DNaseI, RNase A, or ethidium bromide before performing the co-immunoprecipitation experiments. We could not detect any significant difference in protein associations between treated and untreated nuclear extracts (data not shown).

Taken together, these results suggest that BRCA1 and these identified BRCA1-associated proteins are likely in the same protein complex and, therefore, may function in the same DNA damage response pathway.

**Table 1.** *DNA repair proteins identified with mass spectrometry from immunoprecipitations of different BRCA1 antibodies*

| SDS-PAGE (kD) | Ab80 | Ab81 | C20 |
|---|---|---|---|
| 350 | | ATM | |
| 220 | BRCA1 | BRCA1 | BRCA1 |
| 160 | MSH6, BLM | | MSH6 |
| 150 | | | RAD50 |
| 140 | RFC, p140 | RFC, p140 | |
| 100 | MSH2 | | |
| 90 | MLH1 | MLH1 | |
| 40 | RFC, p40 | RFC, p40 | |
| 37 | RFC, p37 | RFC, p37 | |

### *Colocalization of BRCA1 and BLM before and after exposure to DNA damage and replication blocks*

To examine when and where BASC may function, we analyzed the localization of these proteins in untreated cells and cells exposed to DNA-damaging agents and DNA replication inhibitors. We found that, in untreated cells, the BLM protein has several staining patterns that often occur within the same cell including a diffuse nucleoplasmic staining, brighter patches of staining, and

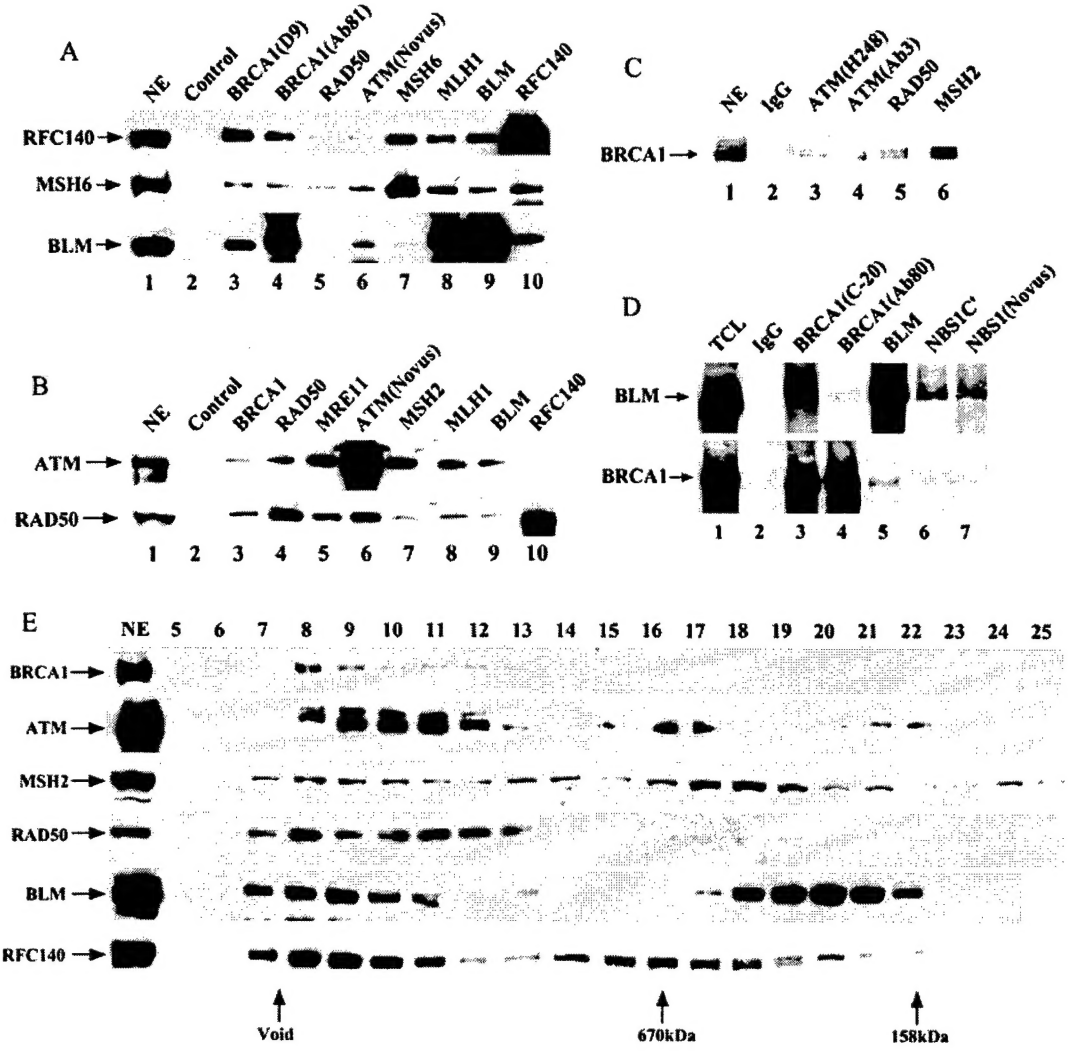


**Figure 2.** BRCA1-associated proteins that form a BASC. (*A–D*) Components of the BASC coimmunoprecipitate. Immunoprecipitations were done with HeLa nuclear extracts (NE) (*A–C*) and 293T whole-cell extracts (TCL) (*D*). Antibodies and immunoprecipitation/Western conditions are described in the Materials and Methods section. (*E*) BRCA1 resides in a large complex of >2 MD. Components of the BASC complex cofractionate on DEAE and Superose 6 columns. HeLa nuclear extracts were fractionated and step eluted (0.2–0.4 M KCl) on a DEAE column. The majority of BRCA1 eluted in the 0.3 M fraction. The 0.3 M fraction was fractionated further on a Superose 6 gel filtration column. BRCA1 was detectable only in the void volume (>2 MD). Other components of BASC were detected as multiple peaks; all contain one peak in the void volume that co-elutes with BRCA1. Other peaks of smaller sizes exist independent of BRCA1. The majority of the RAD50 complex that is independent of BRCA1 elutes in the 0.2 M KCl on the DEAE column.

bright discrete foci (Fig. 3B,E). BRCA1 foci partially overlap with the bright BLM foci but rarely with the BLM patches (Fig. 3A–F). The amount of BRCA1 and BLM colocalization is greatly increased in a subset of cells following treatment with hydroxyurea (HU) for 6–8 hr (Fig. 3G–L). The HU-induced relocalization of BLM and BRCA1 appears to be specific for cells that are in mid- to late S phase or $G_2$ at the time of HU addition as the foci are rarely observed following synchronization of the cells in early S phase or $G_1$ (data not shown). This result may also explain why a relatively small percentage of asynchronous populations of cells (~10%) show this relocalization following HU treatment. Exposure of cells to ionizing radiation also causes a more subtle redistribution of BLM into an increased number of nuclear foci in some cells that partially overlap with BRCA1 foci (Fig. 3M–O).

### *Two distinct localization patterns of the RAD50–MRE11–NBS1 complex in response to DNA damage*

BRCA1 partially colocalizes with the RAD50–MRE11–NBS1 complex in a subset of cells that are exposed to ionizing radiation and then allowed to recover for vari-

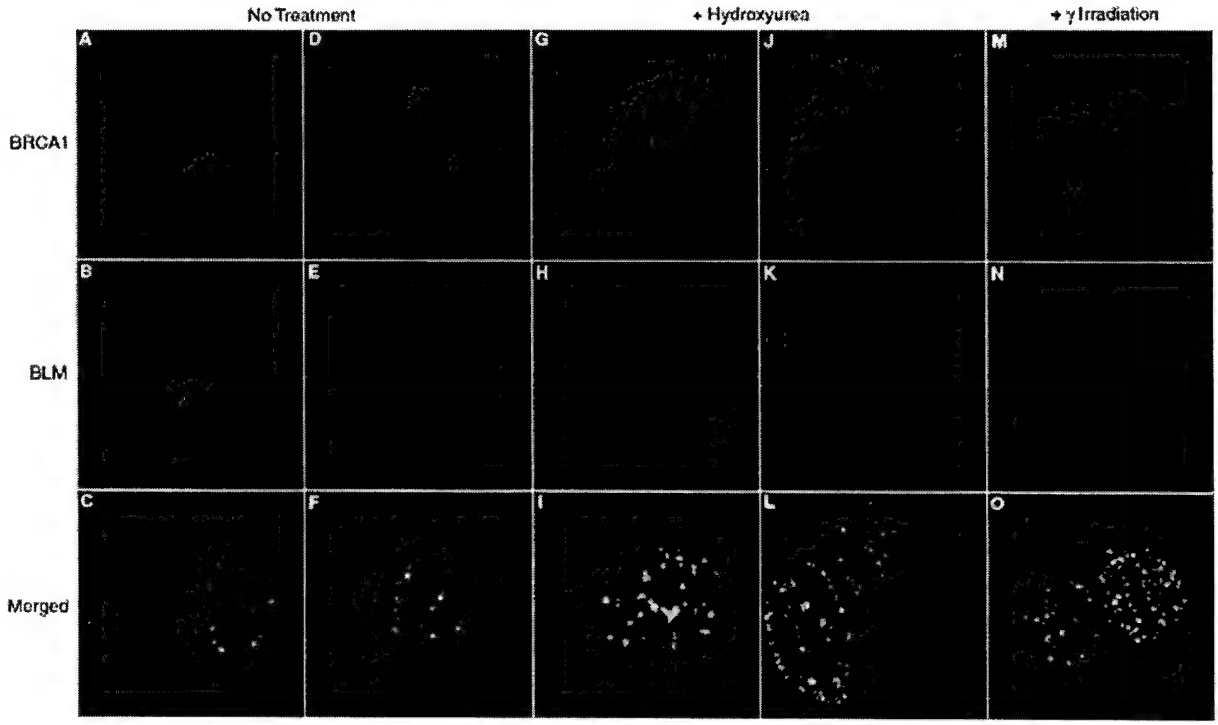


**Figure 3.** Colocalization of BRCA1 with BLM before and after exposure to genotoxic agents. (*A–F*) Asynchronous, logarithmically growing MCF7 cells were fixed with methanol/acetone and stained with antibodies to BRCA1 (Ab-1, Calbiochem) and BLM followed by the appropriate FITC and Cy3-conjugated secondary antibodies. (*G–L*) Cells were treated with 1 mM HU for 6–8 hr followed by fixation and staining. (*M–O*) Cells were exposed to 12 Gy of γ-irradiation and incubated for 8 hr prior to fixation and staining. Confocal images were captured at 1260× magnification.

ous times (2–8 hr) (Fig. 4; data not shown). However, we often found cells that displayed little if any detectable BRCA1 signal but strong RAD50–MRE11–NBS1 foci. Further examination revealed two distinct localization patterns for these proteins after treatment with ionizing radiation. Cells that formed bright, discrete RAD50–MRE11–NBS1 foci often expressed too little BRCA1 to be visualized by immunofluorescence (Fig. 4, D–F and P–R). Cells that formed bright BRCA1 foci also exhibited RAD50–MRE11 foci but also showed a more diffuse nucleoplasmic RAD50–MRE11 staining as well. In many cases, the RAD50–MRE11 foci in these cells did overlap significantly with BRCA1 foci.

Because BRCA1 expression peaks in S phase, we tested whether these two staining patterns reflected cell cycle regulation. MCF-7 cells were synchronized by serum starvation and re-addition of serum. Then, we irradiated the cells immediately ($G_0/G_1$ cells) or waited 24 hr to allow the cells to progress into S phase and then irradiated them. The cells were fixed and stained 5 hr after irradiation. This procedure causes the cells to either arrest at the $G_1$ DNA damage checkpoint or the $G_2$/M DNA damage checkpoint. We observed that bright RAD50–MRE11 foci and low BRCA1 staining were specific to the $G_1$-arrested cells whereas diffuse nucleoplasmic and focal RAD50–MRE11 staining accompanied by the bright BRCA1 foci were specific to cells irradiated in S phase (Fig. 4, G–L and S–X). The highest level of colocalization between BRCA1 and RAD50–MRE11 was seen in the bright foci among the S phase-irradiated cells.

### *The RAD50 complex properly localizes in BRCA1-deficient HCC1937 cells*

We also examined how RAD50 foci relocalize in BRCA1-deficient HCC1937 cells. Before treatment of the cells, we observed RAD50–MRE11–NBS1 foci in ~11% of the cells using antibodies to each of these components (Fig. 5A,D). After treatment of the cells with 12 Gy of ionizing radiation, we observed an increase in the number of RAD50–MRE11–NBS1 foci-containing cells to ~60%, which is consistent with the response in BRCA1-proficient cell lines (Fig. 5B,E; Maser et al. 1997). Transient transfection of wild-type BRCA1 driven by either a CMV promoter or a LTR promoter had no effect on the percentage of cells that displayed the focal staining pattern within the transfected population (data not shown). As this result appears to be in direct contradiction to previously published data (Zhong et al. 1999), we obtained HCC1937 cells from three different sources to confirm its reproducibility. Two of the sources behaved virtually identically as reported above. The cells from the third source showed a reduced increase in foci formation after ionizing radiation, but in no case did transfection of

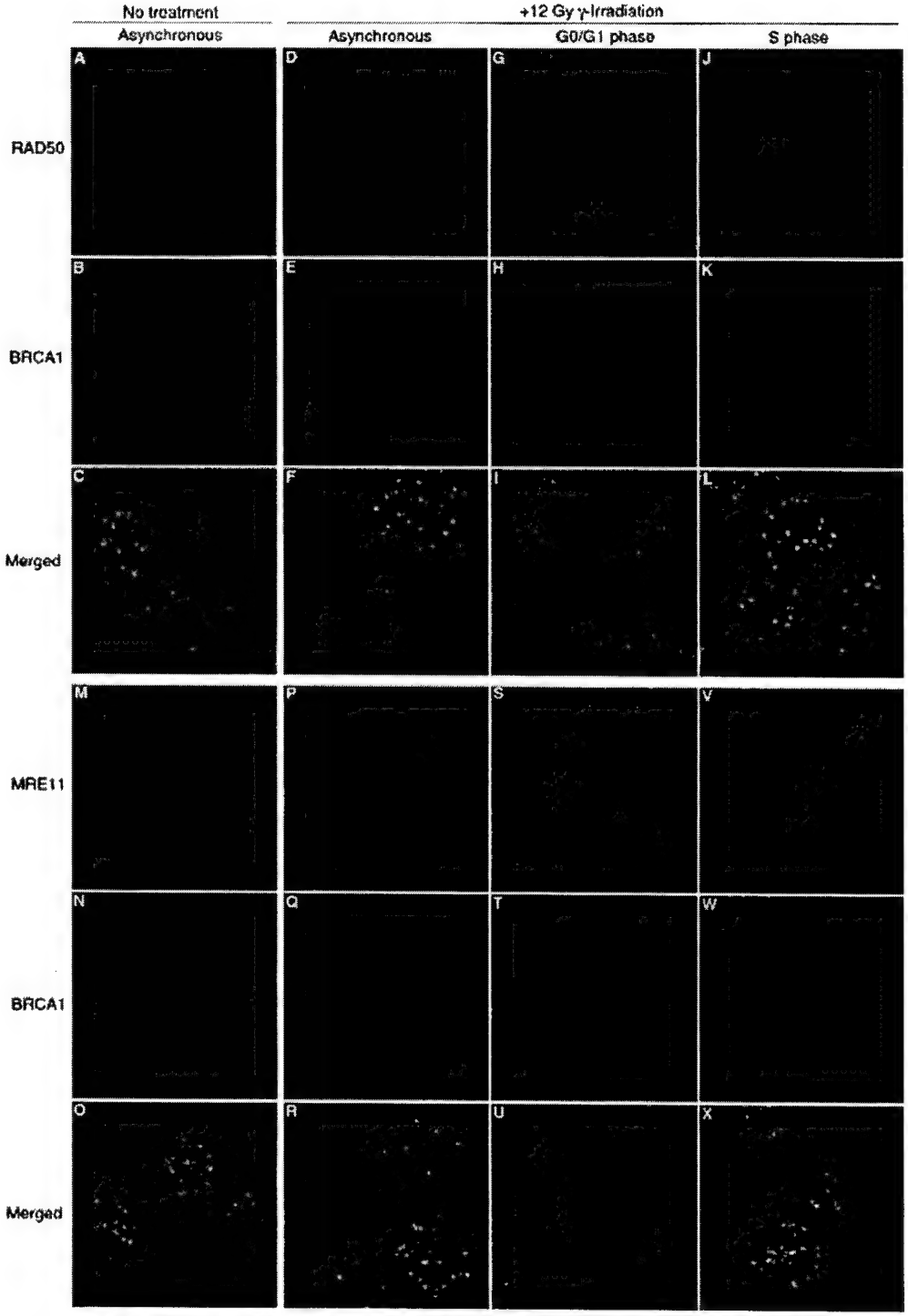


**Figure 4.** Cell cycle dependent colocalization of BRCA1 with the MRE11–RAD50–NBS1 complex after ionizing radiation. (*A–C,M–O*) Asynchronous MCF7 cells were fixed and stained with (*A–C*) anti-RAD50 and anti-BRCA1 or (*M–O*) anti-MRE11 and anti-BRCA1 antibodies. Asynchronous (*D–F,P–R*), $G_0/G_1$ arrested (*G–I,S–U*), or S-phase synchronized (*J–L,V–X*) MCF7 cells were exposed to 12 Gy of γ-irradiation then incubated for 5 hr prior to fixation and immunostaining. Appropriate FITC or Cy3-conjugated secondary antibodies were used for indirect visualization of the epitopes. Confocal images were captured on a Bio-Rad confocal microscope at 1260× magnification.

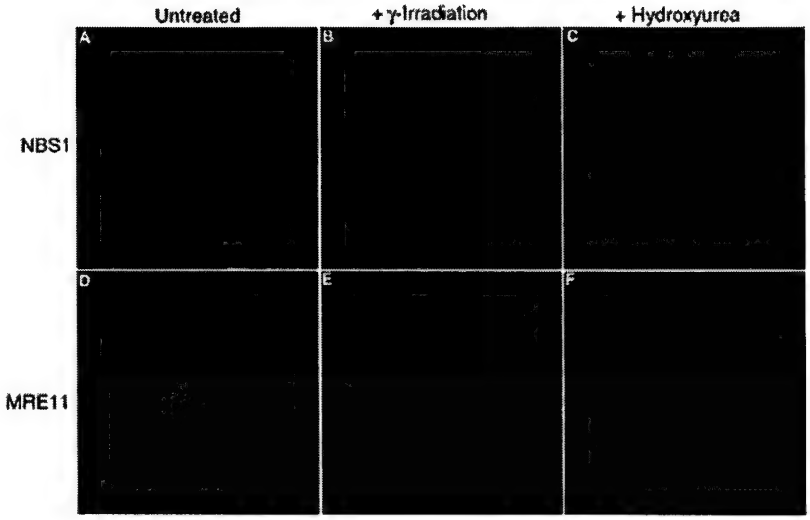


**Figure 5.** Relocalization of the RAD50–MRE11–NBS1 complex following exposure to ionizing radiation or HU is independent of BRCA1. Exponentially growing HCC1937 cells were either left untreated (*A,D*), exposed to 12 Gy of ionizing radiation followed by an 8-hr incubation (*B,E*), or treated with 1 mM HU for 8 hr (*C,F*). Cells were fixed and stained with antibodies to NBS1 (Novus) or MRE11 (Novus) as indicated. (*A,D*) Cells without foci; (*B,C,E,F*) cells that contain foci. Confocal images were captured at 1260× magnification. The percentage of cells with foci in each condition was determined by scoring cells as positive if they contained >10 foci. In each experiment, >200 cells were counted.

wild-type BRCA1 have any effect. Similar results have been obtained by others (D. Livingston, pers. comm.).

### *BLM colocalizes with BRCA1 and the RAD50–MRE11–NBS1 complex to replication forks in cells treated with inhibitors of replication*

Significantly, the RAD50 complex also redistributes to large foci in a subset of asynchronous cells exposed to HU (Fig. 6). We confirmed that this redistribution is to the same location as the BRCA1 and BLM proteins by staining cells simultaneously for RAD50 and BRCA1 (Fig. 6A–C), MRE11 and BRCA1 (Fig. 6D–F), MRE11 and BLM (Fig. 6G–I), or RAD50 and BLM (Fig. 6J–L). The relocalization of the RAD50–MRE11–NBS1 complex after HU treatment does not appear to require BRCA1 function as we observed an increase (from 11% to 23%) in the percentage of HCC1937 cells displaying a focal RAD50–MRE11–NBS1 staining after HU treatment for 8 hr (Fig. 5C,F). This increase is consistent with the ~10% increase observed in HU-treated cells containing wild-type BRCA1.

BRCA1 has been shown previously to colocalize with PCNA at replication forks in a small subset of late S phase cells exposed to ionizing radiation (Scully et al. 1997a). Therefore, we examined whether the BLM–BRCA1–MRE11–RAD50 nuclear domains that formed in response to HU treatment were also at replication forks. Staining with PCNA and BRCA1, PCNA and BLM, or PCNA and RAD50 confirmed that this BRCA1 complex does redistribute to PCNA-positive replication forks after HU treatment (Fig. 7).

## Discussion

In this study we have partially purified the BRCA1 protein complex and identified its components using mass spectrometry. We found that all cellular BRCA1 protein resides in a large protein complex(s) (>2 MD) consistent with previous studies using sedimentation analysis (Scully et al. 1997a). We characterized a group of BRCA1-associated proteins that form what we refer to as a BASC. This work not only reinforces the current view of the involvement of BRCA1 in DNA damage repair but also allows us to propose two testable models for the function of BASC and the function of BRCA1 within BASC (see below). Furthermore, the fact that many proteins in BASC are themselves tumor suppressors suggests that interference with the function of BASC may be a central event in tumorigenesis.

### *BASC, a super complex of DNA repair protein complexes*

The BASC characterized in this paper contains at least 15 subunits. In addition to BRCA1, ATM, and BLM, BASC contains four subprotein complexes including the RAD50–MRE11–NBS1 complex, the MSH2–MSH6 heterodimer, the MLH1–PMS2 heterodimer (the presence of PMS2 is inferred) and the RFC complex (five subunits total, of which three were detected by mass spectrometric analysis, and two are hypothesized to be present on the basis of known interactions with the first three). All of the BRCA1-associated proteins reported here also form smaller, stable subcomplexes independent of BRCA1 as evidenced by column fractionation. The relatively low abundance of the BRCA1 protein suggests that these other subcomplexes may have functions independent of BRCA1. BRCA1 may regulate the functions of these subcomplexes for a specialized repair function, or perhaps these complexes confer special properties to BRCA1.

The assembly of BRCA1 with different proteins may be a dynamic process changing throughout the cell cycle and within subnuclear domains. Thus, the associated proteins that we have identified may represent multiple distinct complexes that assemble and disassemble at

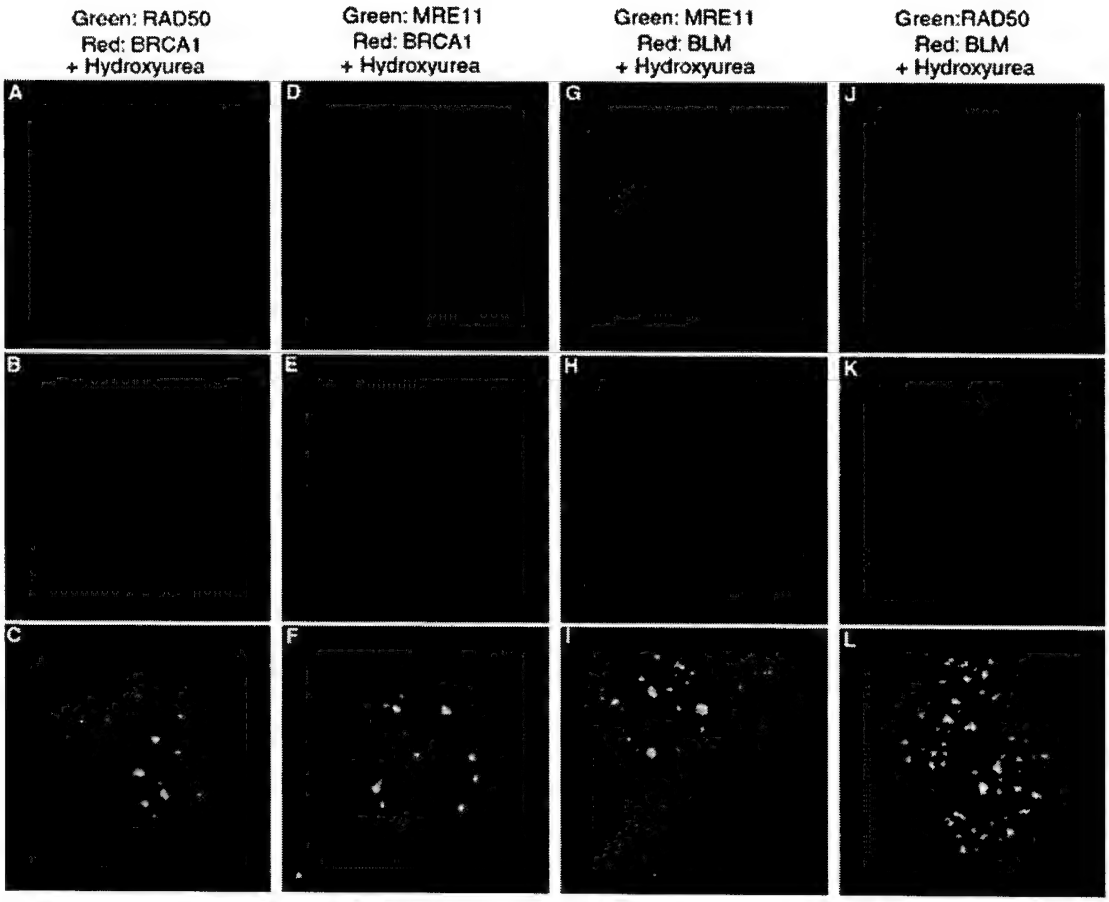


**Figure 6.** Colocalization of RAD50, MRE11, BRCA1, and BLM following treatment of cells with HU. Asynchronous MCF7 cells were treated with 1 mM HU for 4–8 hr. Cells were fixed and stained with the following antibodies: (*A–C*) anti-RAD50 (13B3, GeneTex) and anti-BRCA1 (Ab-2, Neomarkers); (*D–F*) anti-MRE11 (12D, GeneTex) and anti-BRCA1 (Ab-2 NeoMarkers); (*G–I*) anti-MRE11 (12D7 GeneTex); and affinity-purified polyclonal anti-BLM; (*J–L*) anti-RAD50 (13B3, GeneTex) and affinity-purified polyclonal anti-BLM. Confocal images were captured at 1260× magnification. It should be noted that the majority of cells after HU treatment did not appear significantly different from the untreated cells. However, ~10% showed redistribution into nuclear foci as represented in these images.

various sites of BRCA1 function such as DNA double-strand breaks and stalled replication forks. However, because we were able to co-immunoprecipitate many of these DNA repair proteins in BASC with each other, it is likely that this BASC functions coordinately on DNA. In our analysis, we have not found BRCA2 and RAD51, two proteins that were previously reported to interact with BRCA1 (Chen et al. 1998; Scully et al. 1997c). The reason for this result is not clear at present. These proteins may be displaced by the three antibodies that we used, which were all raised against different segments of the carboxyl-terminus of BRCA1 (amino acids 1021–1861). As shown in Table 1 and Figure 1, BRCA1-associated proteins are immunoprecipitated to different extents by different antibodies, possibly due to competition for binding-site accessibility. Alternatively, these proteins may be substoichiometric components of BASC whose abundance is below the level detectable by Coomassie blue and mass spectrometry.

### *Is BASC a DNA structure surveillance machine?*

An intriguing feature of these BRCA1-associated DNA repair proteins is that they each possess the ability to bind abnormal DNA structures, such as double-strand breaks, base-pair mismatches, Holliday junctions, cruciform DNA, template–primer junctions, and telomere repeat sequences (Uchiumi et al. 1996; Alani et al. 1997; Bennett et al. 1999; Marsischky et al. 1999). Therefore, these proteins have the potential to act as sensors of these structures. The RAD50–MRE11–NBS1 complex and the checkpoint kinase ATM may be sensors for DNA double-strand breaks as they interact with these breaks and are regulated by them (Maser et al. 1997; Smith et al. 1999; Stewart et al. 1999). The mismatch repair proteins may act as sensors of abnormal DNA structures caused both by distortions of the helix by mismatches and chemical alterations of the helix by cisplatin, DNA-methylating agents, and other chemicals. The

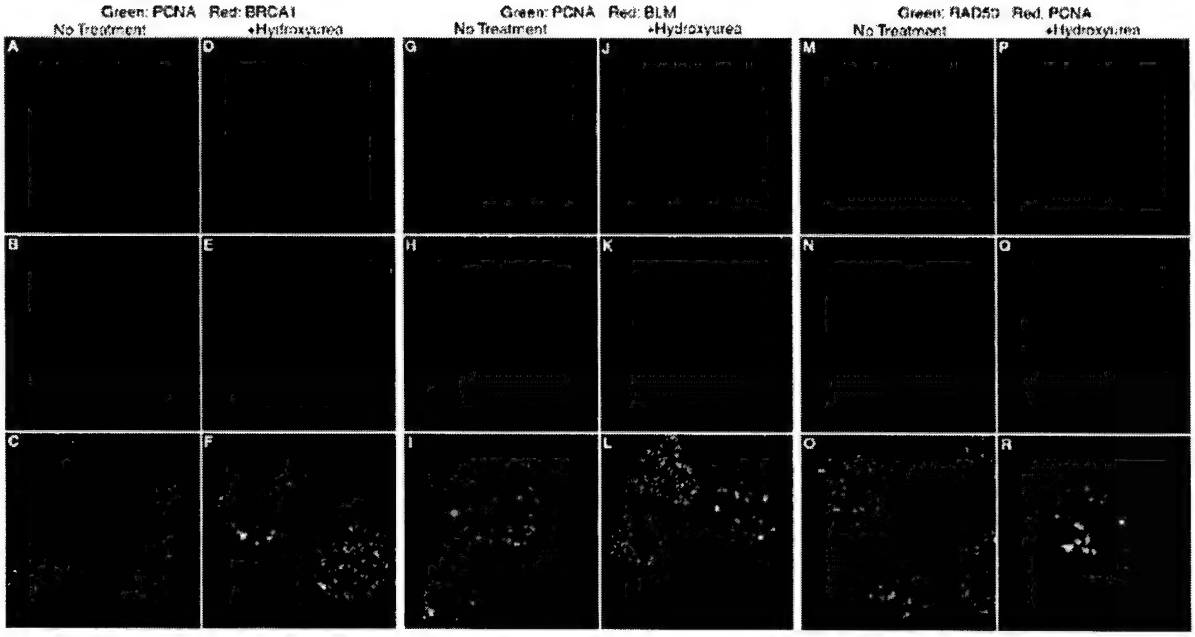


**Figure 7.** Colocalization of BLM, BRCA1, and RAD50 with PCNA following treatment with HU. Cells were left either untreated or exposed to 1 mM HU for 7 hr. Then, cells were fixed by methanol/acetone treatment and stained by indirect immunofluorescence with the following primary antibodies: (*A–F*) anti-PCNA (PC10, Santa Cruz) and anti-BRCA1 (Ab-2, Neomarkers); (*G–L*) anti-PCNA (PC10, Santa Cruz) and anti-BLM; (*M–R*) anti-PCNA (FL261, Santa Cruz) and anti-RAD50 (GeneTex). Appropriate Cy3- or FITC-conjugated secondary antibodies were used and confocal images were captured at 1260× magnification. It should be noted that the majority of cells after HU treatment did not appear significantly different from the untreated cells. However, ~10% showed redistribution into nuclear foci as represented in these images.

tyrosine kinase c-Abl regulates p73 in the apoptotic response to cisplatin-induced DNA damage in a MLH1-dependent manner (Gong et al. 1999). Furthermore, treatment of cells with methylating agents results in p53 phosphorylation that is dependent on the presence of functional MSH2–MSH6 and MLH1 proteins (Duckett et al. 1999). These observations implicate the mismatch repair system in the initial step of a damage-signaling cascade that leads to activation of the DNA damage response. In addition, the MSH2–MSH6 heterodimer binds not only to mismatched DNA, but also has affinity for Holliday junctions (Alani et al. 1997; Marsischky et al. 1999) thereby acting as potential sensors of recombination and replication fork damage. The BLM DNA helicase may be a sensor of abnormal double-stranded DNA structures during replication. Its yeast ortholog Sgs1 binds a variety of abnormal DNA structures including forked DNA, synthetic cruciforms, and telomeric G4 DNA in vitro (Bennett et al. 1999). In addition, the Sgs1 helicase has been shown to act upstream of Rad53 in the DNA replication checkpoint (Frei and Gasser 2000). The RFC complex is known to bind the 3′ end of an elongating DNA primer and to recruit PCNA onto DNA polymerase δ, serving the role of the clamp loader in replication and a potential sensor of gapped DNA. Rfc3 mutant *Schizosaccharomyces pombe* cells are sensitive to HU, methanesulfonate, gamma irradiation, and UV irradiation. Phosphorylation of Chk1 and the replication checkpoint are deficient in Rfc3 mutant cells (Shimada et al. 1999). Work in budding yeast has also revealed a role for RFC in DNA repair and S-phase checkpoint regulation, suggesting that the RFC complex plays a direct role in sensing the state of DNA (Sugimoto et al. 1996; Noskov et al. 1998).

In addition to these built-in sensors, BASC also has signal transducers including the ATM kinase, the ATR kinase (B. Abraham, pers. comm.), and possibly other proteins that have not yet been identified. The initial effector may be BRCA1 itself, which is hyperphosphorylated in response to various types of DNA damage by multiple kinases including ATM (Cortez et al. 1999). Other proteins within BASC, such as NBS1 and MRE11, may also be targets for the ATM kinase (Kim et al. 1999). Thus, it is conceivable that the function of BRCA1 in the context of BASC is as a scaffold protein that organizes different types of DNA damage sensors, then serves as an effector in response to DNA damage to coordinate repair. A role for BASC as a surveillance machine is consistent with the observation that BRCA1 is associated constitutively with these DNA damage sensors and signal transducers. When aberrant DNA structures occur, in theory, BASC could respond rapidly to signal the DNA damage response. Phosphorylation of components of BASC by signal transducers such as ATM may regulate the repair functions of these proteins. In addition, the signal transducers could activate cell cycle checkpoints through

phosphorylation and activation of the p53 and Chk proteins (Banin et al. 1998; Canman et al. 1998; Matsuoka et al. 1998).

### *A role for BASC in postreplicational repair*

Another common feature of the repair proteins associated with BRCA1 is their roles in DNA postreplicational repair. Many of these proteins function directly in DNA replication or repair of damage that can occur at replication forks. The RAD50–MRE11–NBS1 complex is involved in repair of double-strand breaks generated at stalled replication forks (Haber 1998). We have previously identified mutants in the *Saccharomyces cerevisiae* homolog of RAD50 and NBS1 (Xrs2) as mutants sensitive to the replication inhibitor HU (Allen et al. 1994). HU treatment induces sister chromatid exchange (SCE) and mutants in BLM have high levels of spontaneous SCE. Furthermore, the *S. pombe* homolog of BLM was initially identified on the basis of its extreme sensitivity to HU (Stewart et al. 1997) further supporting a role in repair of replication errors. RFC complexes are also clearly involved in replicational repair of DNA damage and mutants in yeast that are sensitive to HU have been identified (Sugimoto et al. 1996; Noskov et al. 1998; Shimomura et al. 1998; Shimada et al. 1999). Mismatch repair proteins would also be required not only to check the fidelity of newly synthesized DNA during repair processes, but also to recognize and initiate repair of abnormal structures generated at the site of collapsed replication forks. Given the roles of these proteins in replicational repair and the fact that BRCA1 expression, phosphorylation, and localization all peak or change during S phase, it is tempting to speculate that BRCA1 might act to coordinate the repair and surveillance functions of these proteins at sites of DNA replicational stress. The resolution of aberrant DNA structures that occur during DNA replication likely occurs through a tightly regulated process that is linked to the actions of the replication machinery. BRCA1 might act to funnel certain types of damage through particular pathways. For example, it could identify a broken replication fork, allow BLM and mismatch repair proteins to unwind and remove inappropriate DNA helical conformations, then allow the RAD50–MRE11–NBS1 complex to initiate homologous recombinational repair, and finally load the RFC complex to recruit DNA polymerase to complete repair. Although speculative, this model is consistent with the observation that BRCA1-deficient cells are hypersensitive to DNA-damaging and replication blocking agents (Abbott et al. 1999; Scully et al. 1999). It should be noted that a role in directing repair does not rule out a role for this complex as a sensor and signal transducer.

The colocalization of BLM and BRCA1 with PCNA further suggests a role in replicational repair. The relocalization of BRCA1, BLM, and RAD50–MRE11–NBS1 after HU treatment appears to be specific to mid to late S phase cells. This observation could indicate a specific requirement for these proteins in the replication/repair of late replicating DNA. Alternatively, it may be that the number of active replication forks and the size of DNA replication factories early in S phase simply are not large enough to produce the large immunostaining domains of these proteins. The association may occur throughout S phase to resolve problems associated with DNA metabolism, and HU may simply amplify the number of problems sufficiently to observe an accumulation of the proteins at intranuclear domains of replication.

The identification of the RAD50 complex in BASC provides further support for the role of BRCA1 in control of homologous recombination (Moynahan et al. 1999). The role of BRCA1 in this process is currently unknown. Although it was previously published that cells deficient for BRCA1 fail to properly regulate and localize the RAD50 complex in response to DNA damage (Zhong et al. 1999), we could not find such a role for BRCA1 in our studies. Analysis of three different sources of HCC1937 cells defective for BRCA1, including the cells analyzed by Zhong and colleagues showed BRCA1-independent foci formation. Our results suggest that BRCA1 is not required to localize the RAD50 complex in response to DNA damage and may carry out a different role with respect to this complex. The cell cycle-regulated colocalization of BRCA1 with the RAD50 complex suggests that it may regulate the type of repair activity that functions to repair double-strand break lesions.

### *Association of mismatch repair proteins with BRCA1 may explain the role of BRCA1 in transcription-coupled repair*

The identification of multiple mismatch repair proteins associated with BRCA1 provides support for genetic observations that BRCA1 is required for transcription-coupled repair of oxidation induced damage (Gowen et al. 1998). Previously it was noted that MSH2-deficient cell lines have a defect in transcription-coupled repair for both UV-induced and oxidation-induced DNA damage (Mellon et al. 1996). The association of BRCA1 with MSH2–MSH6 and MLH1–PMS2 suggests that the defective transcription-coupled repair in BRCA1$^{-/-}$ cells may arise from deregulation of mismatch repair genes or an inability of the mismatch repair genes to signal the presence of damage to BRCA1. We also examined colocalization of mismatch repair proteins (MSH2 and MLH1) with BRCA1 by immunofluorescence. The mismatch repair proteins stain the nucleus uniformly before DNA damage and do not show a detectable change upon DNA damage (ionizing radiation and HU treatment). We reason that even if there are foci formed in response to DNA damage, which is not known at present, the intense uniform nucleoplasm staining might mask the foci formed for these mismatch repair proteins. Therefore, it is not presently possible to judge colocalization of mismatch repair proteins with BRCA1 in nuclear foci. It is possible that the mismatch repair proteins use their association with BRCA1, which is known to interact with RNA

polymerase (Scully et al. 1997a), to identify the transcribed strand for preferential repair. Alternatively, this association may instruct BRCA1 to prevent active transcription complexes from disrupting repair of the transcribed strand. This connection may provide insight for the initiation of mechanistic studies aimed at understanding the mechanism of transcription-coupled repair.

The molecular dissection of BASC presented here has provided significant insights into the role of BRCA1 in the process of DNA repair. Knowledge of the composition of this complex has allowed us to propose two models for the role of this complex in the cell, as a sensor of abnormal DNA structures and/or as a regulator of the post-replicational repair process. This knowledge sets the stage for the dissection of the significance of the presence of the individual members of this complex and the elucidation of their roles in the preservation of genomic stability and tumor suppression.

## Materials and methods

### *Nuclear extract fractionation*

HeLa-S3 nuclear extracts prepared according to the standard Dignam protocol were first loaded on a DEAE column equilibrated with 20 mM Tris-HCl (pH 8.0), 100 mM KCl, and 0.5 mM DTT and step-eluted in 0.2 M KCl, 0.3 M KCl and 0.4 M KCl, all in the equilibration buffer. The 0.3 M fraction was then applied to a Superose 6 (Pharmacia) column equilibrated with 20 mM HEPES (pH 7.5), 0.2 M KCl and 0.5 mM DTT. Fractions were collected and an equal volume from each fraction was loaded onto a 4%–12% SDS–polyacrylamide gel.

### *Immunoprecipitation, Western blotting, and antibodies*

Large scale immunoprecipitation was carried out with unfractionated HeLa nuclear extracts. From 50 to 100 μg of affinity-purified antibodies as indicated was added to 5 ml of HeLa nuclear extracts (~10 mg/ml) and rotated for 2 hr at 4°C. Two hundred microliters of protein A–Sepharose beads (50% slurry) was added to the mixture and rotated for an additional 2 hr. The immunoprecipitates were then washed in 10 ml of NETN [20 mM Tris-HCl (pH 8.0), 0.1 M NaCl, 1 mM EDTA, 0.5% NP-40] three times. The precipitated proteins were eluted into Laemmli buffer and separated on a 4%–20% SDS–polyacrylamide gel.

For immunoprecipitation/Western analysis, immunoprecipitation was done in essentially the same manner, except in a smaller scale. Briefly, 100 μl of nuclear extracts, 5 μg of antibody, and 15 μl of protein A beads were used in each reaction. The wash was done with 1 ml of NETN three times. Samples were separated on 4%–12% SDS–polyacrylamide gels, transferred to nitrocellulose membranes by semi-dry method, and probed with the appropriate antibodies.

The primary antibodies used in this work were as follows: rabbit polyclonal Ab80 and Ab81 were raised in rabbits against GST–BRCA1 1021–1552 and GST–BRCA1 1501–1861, respectively. GST–BRCA1 fusion proteins were produced in *E. coli*. Ab80 and Ab81 antibodies were affinity purified using the respective antigens following a conventional affinity-purification protocol. Affinity-purified rabbit polyclonal anti-NBS1C′ antibody was raised against a carboxy-terminal NBS1 peptide: CDDLFRYNPYLKRRR conjugated to KLH. Rabbit anti-BLM polyclonal antibody was prepared as described (Neff et al. 1999). Commercial anti-BRCA1 antibodies were D-9, C-20 (mouse monoclonal and rabbit polyclonal, respectively, Santa Cruz), Ab-2 (rabbit polyclonal, NeoMarker), and Ab-1 (monoclonal, CalBiochem). Other antibodies were rabbit polyclonal anti-ATM (Novus), mouse monoclonal anti-ATM-2C1 (GeneTex), rabbit polyclonal anti-ATM (H248, Santa Cruz, Ab-3, CalBiochem), mouse monoclonal anti-RAD50-13B3 (GeneTex), rabbit polyclonal anti-NBS1 (Novus), rabbit polyclonal anti-MRE11 (Novus), mouse monoclonal anti-MRE11-12D7 (GeneTex), goat polyclonal anti-MSH6 (GTBP, N-20, Santa Cruz), rabbit polyclonal anti-MSH2 (N-20, Santa Cruz), rabbit polyclonal anti-hMLH1 (C-20, Santa Cruz), mouse monoclonal anti-PCNA (PC10 and FL261, Santa Cruz), and mouse monoclonal anti-RFC p140 (kind gift from Dr. Bruce Stillman, Cold Spring Harbor Laboratory, Cold Spring Harbor, NY).

### *Identification of proteins by mass spectrometry*

Protein sequencing using mass spectrometry was carried out as described with the exception that $O^{18}$-labeled $H_2O$ was omitted (Ogryzko et al. 1998). Briefly, the Coomassie blue stained protein band was in-gel digested with trypsin, and the recovered peptides were analyzed using an electrospray ion trap mass spectrometer (LCQ, Finnigan MAT, San Jose, CA) coupled on-line with a capillary HPLC (Magic 2002, Michrom BioResources, Auburn, CA) to acquire mass spectrometry/mass spectrometry (MS/MS) spectra. A 0.1 × 50 mm-MAGICMS C18 column (5-μm particle diameter, 200 Å pore size) with mobile phases of A (methanol:water:acetic acid, 5 : 94 : 1) and B (methanol:water:acetic acid, 85 : 14 : 1) was used. Data derived from the MS/MS spectra were used to search a compiled protein database that was composed of the protein database NR and a six-reading frame translated EST database to identify the protein by use of the program PROWL, which is publicly available (http://prowl.rockefeller.edu).

### *Immunofluorescence*

Indirect immunofluorescence was performed by growing cells on glass coverslips in 35-mm dishes. Fixation and permeabilization were performed with either 100% methanol at -20°C for 20 min followed by 100% acetone at -20°C for 20 seconds or 3% paraformaldehyde followed by 0.5% triton X-100. Some samples were blocked with BSA or normal donkey serum. Staining was performed with antibodies diluted in PBS at 37°C for 20–30 min. Cy3-, Texas Red-, or FITC-conjugated secondary antibodies were obtained from Jackson Immunoresearch Laboratories and Amersham. Images were captured on a Zeiss microscope with a Bio-Rad confocal imaging system.

## Acknowledgments

We are grateful to Drs. Robert Roeder and Yoshihiro Nakatani for HeLa nuclear extracts, Dr. John Petrini for sharing Nbs1 antibodies, Dr. Bruce Stillman for providing anti-RFC140 antibodies, and Dr. David Livingston for sharing unpublished results. We also thank Tim H. Lee for technical assistance. D.C. is a Fellow of the Jane Coffin Childs Memorial Fund for Medical Research. This work was supported by grants GM44664 and Q1187 (Welch) to S.J.E. S.J.E. is an investigator with the Howard Hughes Medical Institute.

The publication costs of this article were defrayed in part by payment of page charges. This article must therefore be hereby marked "advertisement" in accordance with 18 USC section 1734 solely to indicate this fact.

## References


Abbott, D.W., M.E. Thompson, C. Robinson-Benion, G. Tomlinson, R.A. Jensen, and J.T. Holt. 1999. BRCA1 expression restores radiation resistance in BRCA1-defective cancer cells through enhancement of transcription-coupled DNA repair. *J. Biol. Chem.* **274:** 18808–18812.

Alani, E., S. Lee, M.F. Kane, J. Griffith, and R.D. Kolodner. 1997. Saccharomyces cerevisiae MSH2, a mispaired base recognition protein, also recognizes Holliday junctions in DNA. *J. Mol. Biol.* **265:** 289–301.

Allen, J.B., Z. Zhou, W. Siede, E.C. Friedberg, and S.J. Elledge. 1994. The SAD1/RAD53 protein kinase controls multiple checkpoints and DNA damage-induced transcription in yeast. *Genes & Dev.* **8:** 2401–2415.

Banin, S., L. Moyal, S. Shieh, Y. Taya, C.W. Anderson, L. Chessa, N.I. Smorodinsky, C. Prives, Y. Reiss, Y. Shiloh, and Y. Ziv. 1998. Enhanced phosphorylation of p53 by ATM in response to DNA damage. *Science* **281:** 1674–1677.

Bennett, R.J., J.L. Keck, and J.C. Wang. 1999. Binding specificity determines polarity of DNA unwinding by the Sgs1 protein of S. cerevisiae. *J. Mol. Biol.* **289:** 235–248.

Bork, P., K. Hofmann, P. Bucher, A.F. Neuwald, S.F. Altschul, and E.V. Koonin. 1997. A superfamily of conserved domains in DNA damage-responsive cell cycle checkpoint proteins. *FASEB J.* **11:** 68–76.

Canman, C.E., D.S. Lim, K.A. Cimprich, Y. Taya, K. Tamai, K. Sakaguchi, E. Appella, M.B. Kastan, and J.D. Siliciano. 1998. Activation of the ATM kinase by ionizing radiation and phosphorylation of p53. *Science* **281:** 1677–1679.

Carney, J.P., R.S. Maser, H. Olivares, E.M. Davis, M. Le Beau, J.R. Yates, L. Hays, W.F. Morgan, and J.H. Petrini. 1998. The hMre11/hRad50 protein complex and Nijmegen breakage syndrome: Linkage of double-strand break repair to the cellular DNA damage response. *Cell* **93:** 477–486.

Chen, J., D.P. Silver, D. Walpita, S.B. Cantor, A.F. Gazdar, G. Tomlinson, F.J. Couch, B.L. Weber, T. Ashley, D.M. Livingston, and R. Scully. 1998. Stable interaction between the products of the BRCA1 and BRCA2 tumor suppressor genes in mitotic and meiotic cells. *Mol. Cell* **2:** 317–328.

Chen, Y., A.A. Farmer, C.F. Chen, D.C. Jones, P.L. Chen, and W.H. Lee. 1996. BRCA1 is a 220-kDa nuclear phosphoprotein that is expressed and phosphorylated in a cell cycle-dependent manner. *Cancer Res.* **56:** 3168–3172.

Cortez, D., Y. Wang, J. Qin, and S.J. Elledge. 1999. Requirement of ATM-dependent phosphorylation of BRCA1 in the DNA damage response to double-strand breaks. *Science* **286:** 1162–1166.

Duckett, D.R., S.M. Bronstein, Y. Taya, and P. Modrich. 1999. hMutSα- and hMutLα-dependent phosphorylation of p53 in response to DNA methylator damage. *Proc. Natl. Acad. Sci.* **96:** 12384–12388.

Ellis, N.A., J. Groden, T.Z. Ye, J. Straughen, D.J. Lennon, S. Ciocci, M. Proytcheva, and J. German. 1995. The Bloom's syndrome gene product is homologous to RecQ helicases. *Cell* **83:** 655–666.

Frei, C. and S.M. Gasser. 2000. The yeast Sgs1p helicase acts upstream of Rad53p in the DNA replication checkpoint and colocalizes with Rad53p in S-phase-specific foci. *Genes & Dev.* **14:** 81–96.

Futreal, P.A., Q. Liu, D. Shattuck-Eidens, C. Cochran, K. Harshman, S. Tavtigian, L.M. Bennett, A. Haugen-Strano, J. Swensen, and Y. Miki. 1994. BRCA1 mutations in primary breast and ovarian carcinomas. *Science* **266:** 120–122.

Gong, J.G., A. Costanzo, H.Q. Yang, G. Melino, W.G.J. Kaelin, M. Levrero, and J.Y. Wang. 1999. The tyrosine kinase c-Abl regulates p73 in apoptotic response to cisplatin-induced DNA damage. *Nature* **399:** 806–809.

Gowen, L.C., B.L. Johnson, A.M. Latour, K.K. Sulik, and B.H. Koller. 1996. Brca1 deficiency results in early embryonic lethality characterized by neuroepithelial abnormalities. *Nat. Genet.* **12:** 191–194.

Gowen, L.C., A.V. Avrutskaya, A.M. Latour, B.H. Koller, and S.A. Leadon. 1998. BRCA1 required for transcription-coupled repair of oxidative DNA damage. *Science* **281:** 1009–1012.

Haber, J.E. 1998. The many interfaces of Mre11. *Cell* **95:** 583–586.

Hakem, R., J.L. de la Pompa, C. Sirard, R. Mo, M. Woo, A. Hakem, A. Wakeham, J. Potter, A. Reitmair, F. Billia, E. Firpo, C.C. Hui, J. Roberts, J. Rossant, and T.W. Mak. 1996. The tumor suppressor gene Brca1 is required for embryonic cellular proliferation in the mouse. *Cell* **85:** 1009–1023.

Jongmans, W., M. Vuillaume, K. Chrzanowska, D. Smeets, K. Sperling, and J. Hall. 1997. Nijmegen breakage syndrome cells fail to induce the p53-mediated DNA damage response following exposure to ionizing radiation. *Mol. Cell Biol.* **17:** 5016–5022.

Kim, S.T., D.S. Lim, C.E. Canman, and M.B. Kastan. 1999. Substrate specificities and identification of putative substrates of ATM kinase family members. *J. Biol. Chem.* **274:** 37538–37543.

Kinzler, K.W. and B. Vogelstein. 1996. Lessons from hereditary colorectal cancer. *Cell* **87:** 159–170.

———. 1997. Cancer-susceptibility genes. Gatekeepers and caretakers. *Nature* **386:** 761–763.

Marsischky, G.T., S. Lee, J. Griffith, and R.D. Kolodner. 1999. Saccharomyces cerevisiae MSH2/6 complex interacts with Holliday junctions and facilitates their cleavage by phage resolution enzymes. *J. Biol. Chem.* **274:** 7200–7206.

Maser, R.S., K.J. Monsen, B.E. Nelms, and J.H. Petrini. 1997. hMre11 and hRad50 nuclear foci are induced during the normal cellular response to DNA double-strand breaks. *Mol. Cell. Biol.* **17:** 6087–6096.

Matsuoka, S., M. Huang, and S.J. Elledge. 1998. Linkage of ATM to cell cycle regulation by the Chk2 protein kinase. *Science* **282:** 1893–1897.

Mellon, I., D.K. Rajpal, M. Koi, C.R. Boland, and G.N. Champe. 1996. Transcription-coupled repair deficiency and mutations in human mismatch repair genes. *Science* **272:** 557–560.

Miki, Y., J. Swensen, D. Shattuck-Eidens, P.A. Futreal, K. Harshman, S. Tavtigian, Q. Liu, C. Cochran, L.M. Bennett, and W. Ding. 1994. A strong candidate for the breast and ovarian cancer susceptibility gene BRCA1. *Science* **266:** 66–71.

Moynahan, M.E., J.W. Chiu, B.H. Koller, and M. Jasin. 1999. Brca1 controls homology-directed DNA repair. *Mol. Cell* **4:** 511–518.

Neff, N.F., N.A. Ellis, T.Z. Ye, J. Noonan, K. Huang, M. Sanz, and M. Proytcheva. 1999. The DNA helicase activity of BLM is necessary for the correction of the genomic instability of bloom syndrome cells. *Mol. Biol. Cell* **10:** 665–676.

Noskov, V.N., H. Araki, and A. Sugino. 1998. The RFC2 gene, encoding the third-largest subunit of the replication factor C complex, is required for an S-phase checkpoint in Saccharomyces cerevisiae. *Mol. Cell. Biol.* **18:** 4914–4923.

Ogryzko, V.V., T. Kotani, X. Zhang, R.L. Schlitz, T. Howard, X.J. Yang, B.H. Howard, J. Qin, and Y. Nakatani. 1998. Histone-like TAFs within the PCAF histone acetylase complex. *Cell* **94:** 35–44.

Ruffner, H. and I.M. Verma. 1997. BRCA1 is a cell cycle-regulated nuclear phosphoprotein. *Proc. Natl. Acad. Sci.*

**94:** 7138–7143.

Savitsky, K., A. Bar-Shira, S. Gilad, G. Rotman, Y. Ziv, L. Vanagaite, D.A. Tagle, S. Smith, T. Uziel, and S. Sfez. 1995. A single ataxia telangiectasia gene with a product similar to PI-3 kinase. *Science* **268:** 1749–1753.

Scully, R., S.F. Anderson, D.M. Chao, W. Wei, L. Ye, R.A. Young, D.M. Livingston, and J.D. Parvin. 1997a. BRCA1 is a component of the RNA polymerase II holoenzyme. *Proc. Natl. Acad. Sci.* **94:** 5605–5610.

Scully, R., J. Chen, R.L. Ochs, K. Keegan, M. Hoekstra, J. Feunteun, and D.M. Livingston. 1997b. Dynamic changes of BRCA1 subnuclear location and phosphorylation state are initiated by DNA damage. *Cell* **90:** 425–435.

Scully, R., J. Chen, A. Plug, Y. Xiao, D. Weaver, J. Feunteun, T. Ashley, and D.M. Livingston. 1997c. Association of BRCA1 with Rad51 in mitotic and meiotic cells. *Cell* **88:** 265–275.

Scully, R., S. Ganesan, K. Vlasakova, J. Chen, M. Socolovsky, and D.M. Livingston. 1999. Genetic analysis of BRCA1 function in a defined tumor cell line. *Mol. Cell* **4:** 1093–1099.

Shiloh, Y. and G. Rotman. 1996. Ataxia-telangiectasia and the ATM gene: Linking neurodegeneration, immunodeficiency, and cancer to cell cycle checkpoints. *J. Clin. Immunol.* **16:** 254–260.

Shimada, M., D. Okuzaki, S. Tanaka, T. Tougan, K.K. Tamai, C. Shimoda, and H. Nojima. 1999. Replication factor C3 of Schizosaccharomyces pombe, a small subunit of replication factor C complex, plays a role in both replication and damage checkpoints. *Mol. Biol. Cell* **10:** 3991–4003.

Shimomura, T., S. Ando, K. Matsumoto, and K. Sugimoto. 1998. Functional and physical interaction between Rad24 and Rfc5 in the yeast checkpoint pathways. *Mol. Cell. Biol.* **18:** 5485–5491.

Smith, G.C., N. Divecha, N.D. Lakin, and S.P. Jackson. 1999. DNA-dependent protein kinase and related proteins. *Biochem. Soc. Symp.* **64:** 91–104.

Stewart, E., C.R. Chapman, F. Al-Khodairy, A.M. Carr, and T. Enoch. 1997. rqh1+, a fission yeast gene related to the Bloom's and Werner's syndrome genes, is required for reversible S phase arrest. *EMBO J.* **16:** 2682–2692.

Stewart, G.S., R.S. Maser, T. Stankovic, D.A. Bressan, M.I. Kaplan, N.G. Jaspers, A. Raams, P.J. Byrd, J.H. Petrini, and A.M. Taylor. 1999. The DNA double-strand break repair gene hMRE11 is mutated in individuals with an ataxia-telangiectasia-like disorder. *Cell* **99:** 577–587.

Sugimoto, K., T. Shimomura, K. Hashimoto, H. Araki, A. Sugino, and K. Matsumoto. 1996. Rfc5, a small subunit of replication factor C complex, couples DNA replication and mitosis in budding yeast. *Proc. Natl. Acad. Sci.* **93:** 7048–7052.

Uchiumi, F., T. Ohta, and S. Tanuma. 1996. Replication factor C recognizes 5'-phosphate ends of telomeres. *Biochem. Biophys. Res. Commun.* **229:** 310–315.

Wu, L.C., Z.W. Wang, J.T. Tsan, M.A. Spillman, A. Phung, X.L. Xu, M.C. Yang, L.Y. Hwang, A.M. Bowcock, and R. Baer. 1996. Identification of a RING protein that can interact in vivo with the BRCA1 gene product. *Nat. Genet.* **14:** 430–440.

Xu, X., K.U. Wagner, D. Larson, Z. Weaver, C. Li, T. Ried, L. Hennighausen, A. Wynshaw-Boris, and C.X. Deng. 1999a. Conditional mutation of Brca1 in mammary epithelial cells results in blunted ductal morphogenesis and tumour formation. *Nat. Genet.* **22:** 37–43.

Xu, X., Z. Weaver, S.P. Linke, C. Li, J. Gotay, X.W. Wang, C.C. Harris, T. Ried, and C.X. Deng. 1999b. Centrosome amplification and a defective G2-M cell cycle checkpoint induce genetic instability in BRCA1 exon 11 isoform-deficient cells. *Mol. Cell* **3:** 389–395.

Yarden, R.I. and L.C. Brody. 1999. BRCA1 interacts with components of the histone deacetylase complex. *Proc. Natl. Acad. Sci.* **96:** 4983–4988.

Zhong, Q., C.F. Chen, S. Li, Y. Chen, C.C. Wang, J. Xiao, P.L. Chen, Z.D. Sharp, and W.H. Lee. 1999. Association of BRCA1 with the hRad50-hMre11-p95 complex and the DNA damage response. *Science* **285:** 747–750.

# SMC1 is a downstream effector in the ATM/NBS1 branch of the human S-phase checkpoint

**Parvin T. Yazdi,[1] Yi Wang,[1] Song Zhao,[2] Nimitt Patel,[1] Eva Y.-H.P. Lee,[2] and Jun Qin[1,3]**

[1]Verna and Marrs McLean Department of Biochemistry and Molecular Biology and Department of Molecular and Cellular Biology, Baylor College of Medicine, Houston, Texas 77030, USA; [2]Department of Molecular Medicine/Institute of Biotechnology, The University of Texas Health Science Center at San Antonio, San Antonio, Texas 78245, USA

**Structural maintenance of chromosomes (SMC) proteins (SMC1, SMC3) are evolutionarily conserved chromosomal proteins that are components of the cohesin complex, necessary for sister chromatid cohesion. These proteins may also function in DNA repair. Here we report that SMC1 is a component of the DNA damage response network that functions as an effector in the ATM/NBS1-dependent S-phase checkpoint pathway. SMC1 associates with BRCA1 and is phosphorylated in response to IR in an ATM- and NBS1-dependent manner. Using mass spectrometry, we established that ATM phosphorylates S957 and S966 of SMC1 in vivo. Phosphorylation of S957 and/or S966 of SMC1 is required for activation of the S-phase checkpoint in response to IR. We also discovered that the phosphorylation of NBS1 by ATM is required for the phosphorylation of SMC1, establishing the role of NBS1 as an adaptor in the ATM/NBS1/SMC1 pathway. The ATM/CHK2/CDC25A pathway is also involved in the S-phase checkpoint activation, but this pathway is intact in NBS cells. Our results indicate that the ATM/NBS1/SMC1 pathway is a separate branch of the S-phase checkpoint pathway, distinct from the ATM/CHK2/CDC25A branch. Therefore, this work establishes the ATM/NBS1/SMC1 branch, and provides a molecular basis for the S-phase checkpoint defect in NBS cells.**

[*Key Words*: DNA damage response; S-phase checkpoint; phosphorylation; SMC1; ATM; NBS1]

Received December 18, 2001; revised version accepted January 16, 2002.

Cells have an intricate signaling network that deals with genomic insults (Weinert 1998; Zhou and Elledge 2000). This signaling network in response to DNA damage is composed of interacting signal transduction pathways, each consisting of sensors, transducers, and effectors. Sensors detect damaged DNA and signal to transducers. Transducers amplify and relay the signal to effectors. Effectors then execute the cellular response to elicit cell cycle checkpoint activation, DNA repair or apoptosis. Many tumor suppressor proteins are components of the DNA damage signaling network, underscoring the importance of this network to cancer development.

Proteins that serve as sensors are not well defined. Prime candidates are three groups of proteins that contain functional motifs: (1) PCNA-like proteins Rad1/Rad9/Hus1, (2) RFC-like proteins Rad17/RFC2–5, and (3) BRCT domain-containing proteins Rad9/DPB11 in *Saccharomyces cerevisiae* and Crb2/Rhp9/Cut5 in *Schizosaccharomyces pombe* (the mammalian counterparts are not known, but the breast cancer tumor suppressor protein BRCA1 and a protein called 53BP1 are candidates; Zhou and Elledge 2000). The double-stranded break (DSB) repair protein complex MRE11/RAD50/NBS1 (M/R/N) is also hypothesized to be a sensor, as it localizes to the region of DSBs in response to ionizing radiation (IR) (Maser et al. 1997; Nelms et al. 1998; Mirzoeva and Petrini 2001). The central signal transducer in response to IR is the checkpoint kinase ATM, the protein product of the gene mutated in ataxia-telangiectasia (A-T) (Shiloh and Rotman 1996). ATM is responsible for the activation of the $G_1$, S, and $G_2$/M checkpoints (Shiloh 2001). Tumor suppressor proteins p53 and CHK2 serve as effectors and are phosphorylated and activated by ATM to induce $G_1$ and $G_2$/M cell cycle arrest (Banin et al. 1998; Canman et al. 1998; Matsuoka et al. 1998).

The defective S-phase checkpoint is defined by radioresistant DNA synthesis (RDS). In S-phase checkpoint proficient cells, the rate of DNA synthesis decreases in response to IR. This decrease occurs to a lower extent in S-phase checkpoint defective cells. A-T and NBS (derived from the Nijmegen breakage syndrome) cells were first noted for this defect (Painter and Young 1980). One pathway involved in the activation of the S-phase checkpoint is ATM/CHK2/CDC25A (Falck et al. 2001). ATM activates CHK2, and CHK2 phosphorylates the cell cycle

[3]Corresponding author.
E-MAIL jqin@bcm.tmc.edu; FAX (713) 798-1625.
Article and publication are at http://www.genesdev.org/cgi/doi/10.1101/gad.970702.

regulator CDC25A, leading to its degradation through the polyubiquitination-mediated proteolysis pathway. ATM also phosphorylates NBS1 to activate the S-phase checkpoint (Gatei et al. 2000; Lim et al. 2000; Wu et al. 2000; Zhao et al. 2000), but the downstream effectors are not known, and the relationship between the NBS1 pathway and the ATM/CHK2/CDC25A pathway is not clear. BRCA1, which is believed to function in DNA damage response and transcription regulation, is also required for activation of the S-phase checkpoint (Xu et al. 2001), and is also phosphorylated by ATM in response to IR (Cortez et al. 1999).

Structural maintenance of chromosomes (SMC) proteins are evolutionarily conserved chromosomal proteins. SMC proteins contain coiled-coil domains flanked by globular N- and C-terminal domains, and are divided in the central region by a flexible hinge domain. SMC1 and SMC3 are components of the cohesin complex, which is necessary for sister chromatid cohesion (Guacci et al. 1997; Michaelis et al. 1997; Losada et al. 1998). SMC1 and SMC3 are believed to form a heterodimer in an antiparallel fashion, in which the C-terminal coiled-coil domain of SMC1 interacts with the N-terminal coiled-coil domain of SMC3 (Strunnikov and Jessberger 1999). Cohesion between sister chromatids must be coordinated with DNA replication because cohesion is established during DNA replication (Uhlmann and Nasmyth 1998). The cohesin complex also functions in DNA repair, and is required for postreplicative DSB repair in *S. cerevisiae* (Sjogren and Nasmyth 2001). A mutation in one subunit of the cohesin complex in *S. pombe*, Rad21, renders cells sensitive to DNA damage (Birkenbihl and Subramani 1992).

We report here that SMC proteins are components of the DNA damage response network. ATM phosphorylates SMC1 in response to IR in an NBS1-dependent manner, and the phosphorylation of SMC1 is required for S-phase checkpoint activation. Our data show that SMC1 is a downstream effector in the ATM/NBS1 branch of the S-phase checkpoint pathway. We also show that NBS1 serves as an adaptor in the ATM/NBS1/SMC1 pathway. The ATM/CHK2/CDC25A pathway is intact in NBS cells. Therefore, the ATM/NBS1/SMC1 pathway defines a separate branch of the S-phase checkpoint that is distinct from the ATM/CHK2/CDC25A pathway.

## Results

### *SMC1 associates with BRCA1 and is phosphorylated in response to IR*

We recently partially purified and identified a BRCA1-containing protein complex, BASC, which contains several components of the DNA damage response network, including ATM, NBS1, and BLM, the protein product of the gene mutated in Bloom syndrome (Wang et al. 2000). We speculated that BASC functions as a human genome surveillance complex. We report here that SMC1 and SMC3 are two additional proteins that associate with BRCA1 (data not shown). To confirm the association, we immunoprecipitated SMC1 from HeLa nuclear extracts (NE) and detected BRCA1 by Western blotting. An irrelevant antibody against SGT1 did not coimmunoprecipitate BRCA1 (Fig. 1a). This protein interaction is not mediated by DNA, as SMC1 coimmunoprecipitated BRCA1 from NE that were treated with 1.2 μg/mL ethidium bromide to disrupt protein–DNA interactions (Fig. 1a, last lane).

Because BASC contains many proteins that function in DNA damage signaling, we examined whether SMC1 was posttranslationally modified in cells that were treated with IR. A slower-migrating band was observed for SMC1 (Fig. 1b, lane 3), indicating that SMC1 may be phosphorylated in response to IR. Phosphatase treatment of the cell lysate eliminated the top band (Fig. 1b, lane 4), showing that SMC1 was, indeed, phosphorylated. SMC1 can also be phosphorylated in response to a DNA replication block (HU treatment), but with much slower kinetics than BRCA1 (Fig. 1b; data not shown), suggesting that different kinases are involved. These observations support the notion that SMC1 may be a component of the DNA damage response network.

### *SMC1 phosphorylation is defective in ATM- and NBS1-deficient cells*

To delineate the interrelationship between SMC1 and the components of the BRCA1 network, we studied the phosphorylation of SMC1 in cell lines that are wild type or defective in the individual components of the BRCA1 network. Phosphorylation of SMC1 was detected in both

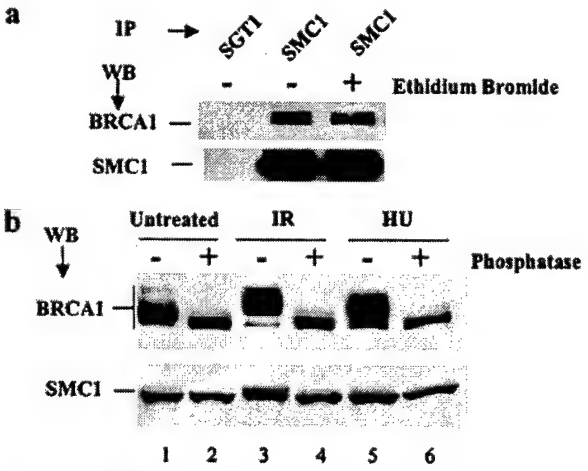


**Figure 1.** SMC1 associates with BRCA1 and is phosphorylated in response to IR. (*a*) Coimmunoprecipitation of BRCA1 and SMC1 in HeLa NE and NE treated with 1.2 μg/mL ethidium bromide. SGT1 is an irrelevant antibody serving as a negative control. (*b*) Phosphorylation of SMC1 in response to IR. T24 cells were left untreated, irradiated with 10 Gy of IR and incubated for 2 h, or treated with 1 mM hydroxyurea (HU) for 8 h. Cell lysates before and after treatment with 20 U/μL λ protein phosphatase were analyzed by Western blotting.

human cancer and primary cell lines as early as 15 min after IR treatment (Fig. 2a; data not shown). The A-T cell line GM05849 was defective in SMC1 phosphorylation in response to IR (Fig. 2a,b).

Because NBS1 functions in the ATM pathway, we examined the dependence of SMC1 phosphorylation on NBS1. Defective phosphorylation of SMC1 was also observed in cells defective in NBS1 (GM 07166 and JS; Fig.

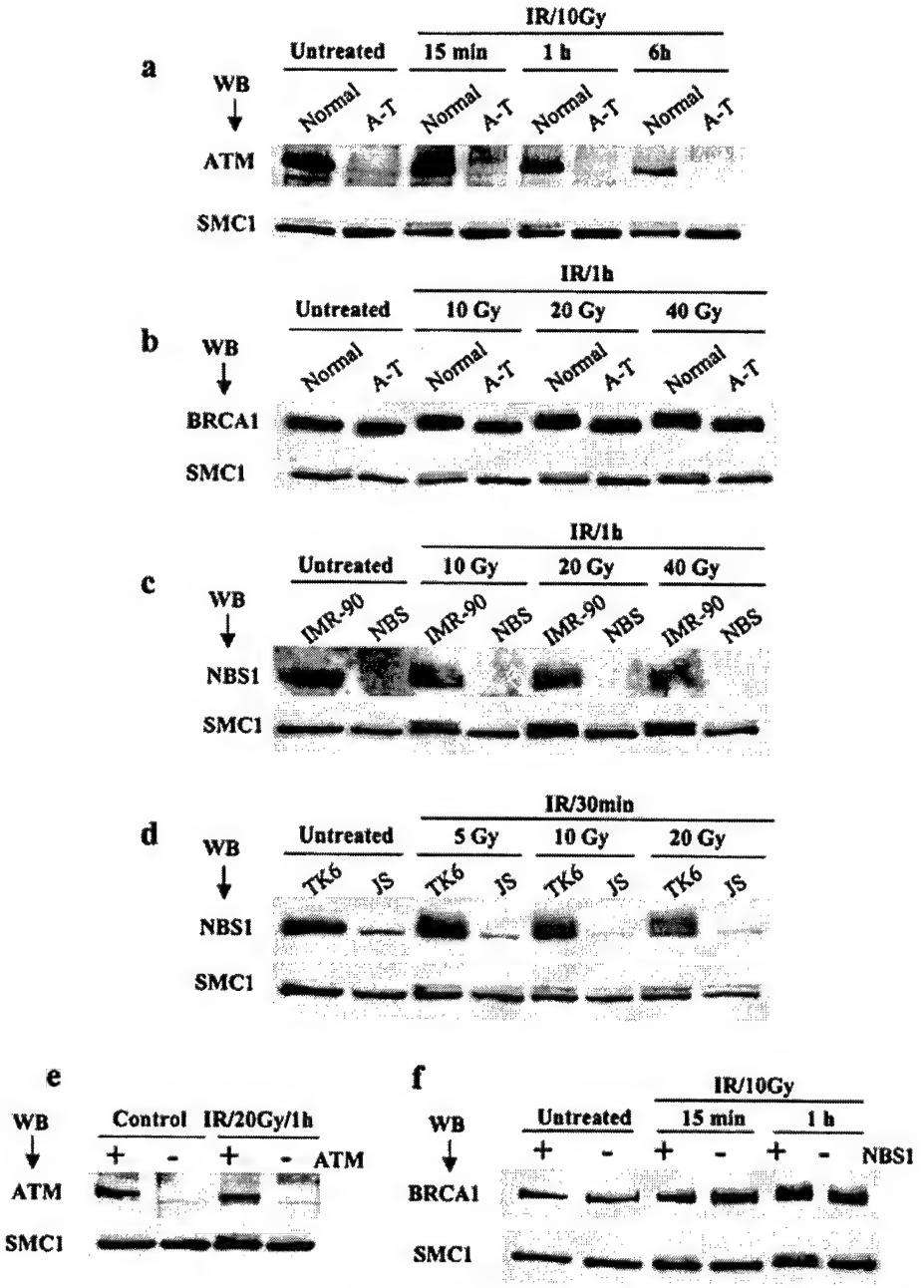


**Figure 2.** Phosphorylation of SMC1 in response to IR is ATM- and NBS1-dependent. (*a*) Comparison of SMC1 phosphorylation kinetics in normal (GM00637) and A-T (GM05849) cell lines. Cells were irradiated with 10 Gy and incubated for indicated time periods. Cell lysates were analyzed by Western blotting. (*b*) Comparison of SMC1 phosphorylation in normal and A-T cells as a function of IR dosage. After receiving the indicated IR dosages, cells were incubated for 1 h. (*c,d*) Comparison of SMC1 phosphorylation in normal (IMR-90 and TK6) and NBS1-defective cells (GM07166 and JS). (*e*) Dependence of SMC1 phosphorylation on ATM. ATM fibroblasts FT169A and their ATM cDNA-complemented derivative cell line YZ5 were irradiated and analyzed for SMC1 phosphorylation. (*f*) Dependence of SMC1 and BRCA1 phosphorylation on NBS1. A GM07166 TERT cell line and its NBS1 cDNA-complemented derivative cell line were irradiated and analyzed for SMC1 and BRCA1 phosphorylation.

2c,d) as compared with NBS1 wild-type cells (IMR-90 and TK6; Fig. 2c,d). Interestingly, the defect in SMC1 phosphorylation was better observed at a lower IR dosage, particularly in the lymphoblast cell line JS.

Defective SMC1 phosphorylation in A-T cells was corrected by the introduction of ATM cDNA; therefore, SMC1 phosphorylation is indeed ATM-dependent (Fig. 2e). Phosphorylation of SMC1 and BRCA1 was restored with the introduction of NBS1 cDNA in NBS fibroblasts (Fig. 2f), thus showing that the phosphorylation of SMC1 and BRCA1 in response to IR is NBS1-dependent. Together, these observations suggest that SMC1 and BRCA1 function in the ATM and NBS1 signaling pathway in response to IR.

### *S957 and S966 of SMC1 are phosphorylated in vivo in response to IR, and ATM phosphorylates SMC1 in vitro*

We used mass spectrometry to identify in vivo phosphorylation sites in SMC1. SMC1 was immunoprecipitated from NE prepared from irradiated cells, immunoprecipitates were resolved on SDS-PAGE, and SMC1 was analyzed with mass spectrometry (Zhang et al. 1998). Trypsin digestion of the bottom band of SMC1 identified a phosphopeptide, and mass spectrometric sequencing of the phosphopeptide was used to identify the exact phosphorylation site. The observation of the $y_{10}$ ion, which corresponds to amino acid residues 959–968 without phosphorylation, and the $y_{12}$ ion, which corresponds to residues 957–968 with a phosphate group, unambiguously identified one of the three SQ sites present in the phosphopeptide, S957, as the site of phosphorylation (Fig. 3a). The masses of other fragment ions all agree with this assignment. Asp-N digest of the top band identified another phosphopeptide (Fig. 3b). Mass spectrometric sequencing of this phosphopeptide confirmed phosphorylation and unambiguously identified it as spanning amino acids 961–984 of SMC1 (data not shown). However, owing to the low amount of phosphorylated SMC1 and the lesser propensity of Asp-N peptides to break randomly along the peptide backbone compared with tryptic peptides, we were unable to pinpoint the precise phosphorylation site in this phosphopeptide. Given that this phosphopeptide contains one SQ motif, which confers to the ATM phosphorylation consensus (Kim et al. 1999; O'Neill et al. 2000), and that phosphorylation of SMC1 is ATM-dependent, we tentatively assigned S966 as the phosphorylation site. Because the phosphopeptide recovered from the bottom band contains unphosphorylated S966 (Fig. 3a), and the phosphopeptide recovered from the top band contains phosphorylated S966, the phosphorylation of S966 is likely to contribute to the SDS-PAGE mobility shift.

We raised phosphorylation site-specific antibodies against pS957 and pS966 of SMC1 and affinity-purified them. To show the specificity of these antibodies, we made S957A, S966A, and S957A/S966A mutations in SMC1, transiently expressed Flag-tagged wild-type (WT) and mutant SMC1 in 293T cells, irradiated the cells with 10 Gy of IR, and let them recover for 1 h. Flag-SMC1 proteins were immunoprecipitated and analyzed by Western blotting using phospho-SMC1 antibodies. Phospho-specific antibody against pS957 did not recognize Flag-SMC1-S957A or Flag-SMC1-S957A/S966A, in which S957 was mutated, but recognized Flag-SMC1-WT and Flag-SMC1-S966A (Fig. 3c), showing that the phospho-specific antibody against pS957 specifically recognized S957. Similarly, the phospho-specific antibody against pS966 specifically recognized S966. We then used these antibodies to examine SMC1 phosphorylation in vivo in 293T and HeLa cells in response to IR. Both S957 and S966 were phosphorylated in vivo in response to IR (Fig. 3d; data not shown).

To determine whether ATM directly phosphorylates SMC1 in vitro, we expressed a fragment of SMC1 (amino acids 890–1233) containing the in vivo phosphorylation sites as a GST fusion protein. Wild-type Flag-tagged ATM, immunoprecipitated either by an ATM antibody or a Flag antibody from transiently transfected 293T cells following IR treatment, phosphorylated GST-SMC1, whereas kinase-dead ATM did not (Fig. 3e; data not shown). We conclude that ATM phosphorylates SMC1 in vitro.

### *Dependence of S957 and S966 phosphorylation on ATM and NBS1*

To examine whether ATM is required for the phosphorylation of S957 and S966 in response to IR, we used the A-T fibroblast cell line FT169 that was complemented with either wild-type *ATM* cDNA or the vector. Cycling cells were irradiated with 10 Gy of IR and allowed to recover for different times. Figure 4a shows that both S957 and S966 phosphorylation depended on ATM. To examine whether NBS1 is required for S957 and S966 phosphorylation, we used NBS fibroblasts that were complemented with either wild-type NBS1 or the vector (Fig. 4b, lanes 1–8). Phosphorylation of S957 and S966 both depended on the presence of NBS1. Quantification of the pS966 blot relative to the SMC1 blot indicated that at 1 h after IR, complementation with wild-type NBS1 resulted in a threefold increase in the phosphorylation of S966, whereas at 2 and 4 h after IR, this increase was only about twofold.

It is hypothesized that the M/R/N complex may function as a sensor for DSB (Mirzoeva and Petrini 2001). ATM phosphorylates NBS1 in response to IR on S278 and S343. This phosphorylation is required for the activation of the S-phase checkpoint (Zhao et al. 2000). If the M/R/N complex functions as a sensor, phosphorylation of proteins that are downstream of NBS1 will be defective in NBS cells. This is, indeed, the case for SMC1, which supports the sensor model. The sensor model also predicts that the phosphorylation of ATM substrates should not depend on NBS1 phosphorylation. We tested this prediction using NBS cells that were complemented with S278A/S343A mutant NBS1 (Fig. 4b, lanes 9–12). Phosphorylation of S957 clearly depended on NBS1 phos-

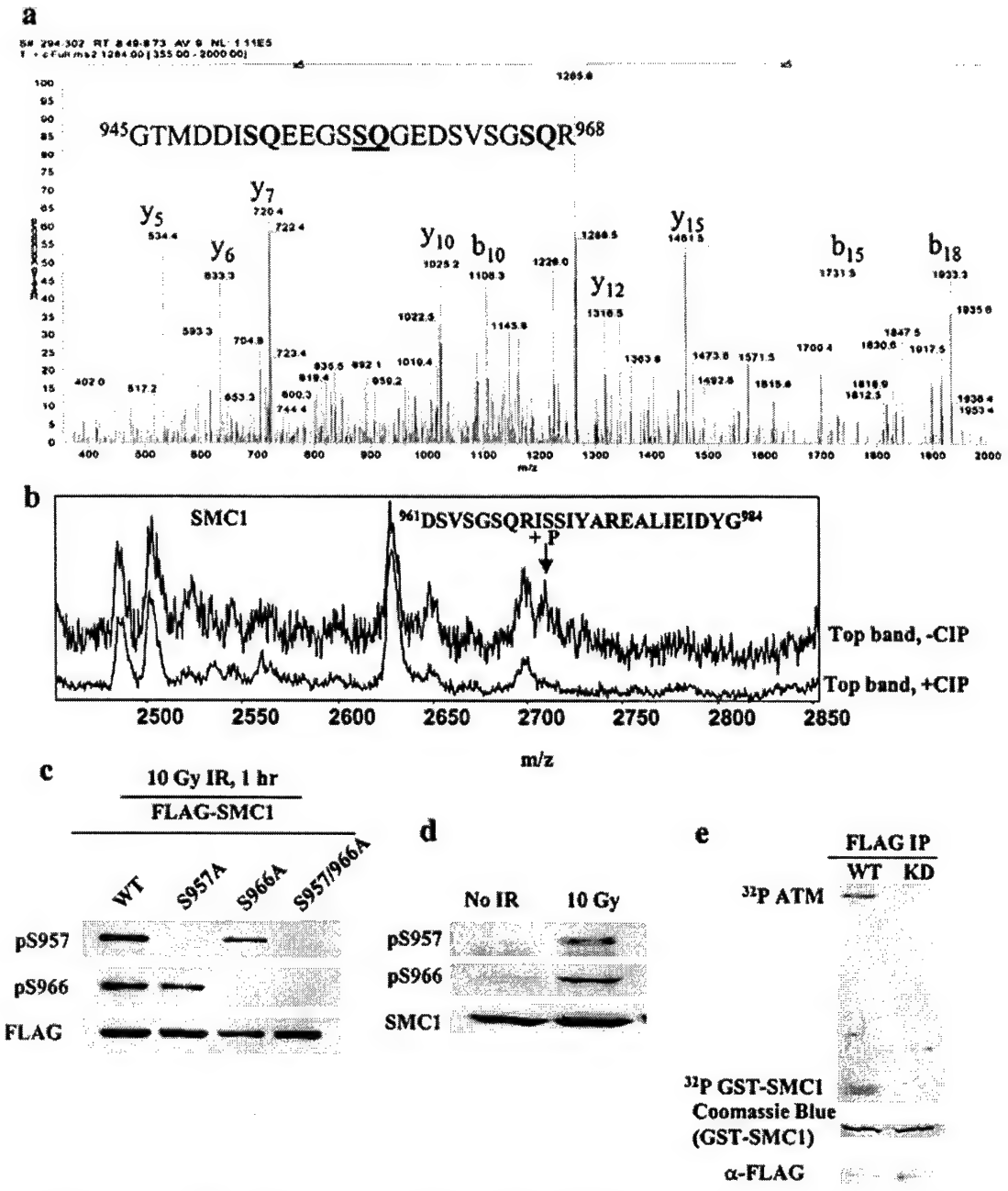


**Figure 3.** S957 and S966 of SMC1 are phosphorylated in vivo in response to IR. SMC1 was immunoprecipitated from HeLa NE prepared from cells that were irradiated with 20 Gy of IR, recovered for 2 h, and resolved on a 6% SDS-PAGE gel. The top and bottom bands of SMC1 were cut out and analyzed separately. Identification of phosphopeptides was carried out as described using mass spectrometry (Zhang et al. 1998). (*a*) The MS/MS spectrum of the tryptic phosphopeptide amino acids 945–968 of SMC1 from the bottom band. The spectrum identifies the site of phosphorylation as S957. (*b*) A portion of the MALDI-TOF spectra of the Asp-N digests of the top band of SMC1 that were treated with (*bottom* panel) and without (*top* panel) calf intestine phosphatase (CIP). The arrow marks the phosphopeptide, in which S966 is tentatively assigned as the site of phosphorylation. (*c*) Test of the specificity of phospho-specific antibodies. Flag-SMC1 WT, S957A, S966A, and S957A/S966A were expressed in 293T cells. Cells were treated with 10 Gy of IR and allowed to recover for 1 h. Flag-SMC1 proteins were immunoprecipitated with a Flag antibody, and Western blotted with phospho-specific antibodies against pS957 and pS966. (*d*) In vivo phosphorylation of S957 and S966 of SMC1 in response to IR. Untreated and IR-treated 293T cells were analyzed by Western blotting using phospho-specific antibodies against pS957 and pS966. (*e*) In vitro phosphorylation of SMC1 by ATM. A GST–SMC1 fragment (amino acids 890–1233) and Flag-tagged ATM (wild-type or kinase dead) immunoprecipitated by Flag antibody from transiently transfected 293T cells following 20 Gy of IR and 1 h of recovery were used to perform the kinase assay.

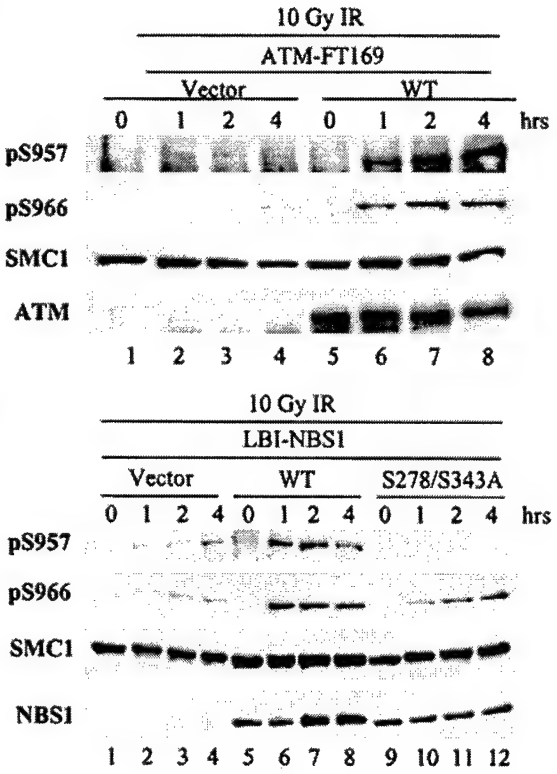


**Figure 4.** Phosphorylation of S957 and S966 of SMC1 depends on ATM and NBS1. (*a*) Vector and wild-type ATM cDNA-complemented A-T cells were irradiated with 10 Gy of IR and allowed to recover for the indicated times. Phosphorylation of S957 and S966 of SMC1 was examined by Western blotting using phospho-specific antibodies against pS957 and pS966 of SMC1. Two identical gels were run, one for blotting pS957, and the other for blotting pS966. Care was taken to load the two gels equally. (*b*) Vector, wild-type NBS1, and phosphorylation mutant S278A/S343A NBS1 cDNA-complemented NBS cells were irradiated with 10 Gy of IR and allowed to recover for the indicated times. Phosphorylations of S957 and S966 of SMC1 were examined by Western blotting using phospho-specific antibodies against pS957 and pS966 of SMC1.

phorylation. However, the dependence of S966 phosphorylation on NBS1 phosphorylation was not as clear. Quantification of the data indicated a nearly twofold difference in S966 phosphorylation 1 h after IR between cells complemented with wild-type and/or S278A/S343A mutant NBS1. Although small, this difference was consistently observed in three different sets of experiment. At 2 and 4 h after IR, no significant difference in S966 phosphorylation was observed between the two cell lines. Therefore, the phosphorylation of S966 depends on NBS1 phosphorylation in the early response (1 h after IR), but not in the late response (2 and 4 h after IR). These observations contradict the prediction of the sensor model. Therefore, the sensor model cannot be strictly correct and needs to be modified. We propose that the M/R/N complex can serve as a sensor, but that NBS1 functions as an adaptor after IR for the phosphorylation of SMC1 in the ATM/NBS1/SMC1 pathway (see below).

### *Phosphorylation of SMC1 is BRCA1- and BLM-independent*

To test the hypothesis that BRCA1 plays an organizer or adaptor role in BASC, we examined the dependence of SMC1 phosphorylation on BRCA1. SMC1 was phosphorylated on S957 and S966 in response to 10 Gy of IR in HCC1937 cells that were complemented with wild-type *BRCA1* cDNA or the vector (Fig. 5a). Quantification of phosphorylated bands relative to total SMC1 indicated a maximum 1.5-fold increase in the phosphorylation of S957 and S966 in the presence of wild-type BRCA1 at 1 and 4 h after IR. We observed no significant difference in the SDS-PAGE mobility shift of SMC1 in the two cell lines after IR treatment (Fig. 5b). Moreover, the phosphorylation of S957 and S966 was independent of BRCA1 when studied in mouse embryonic fibroblasts (MEF) that

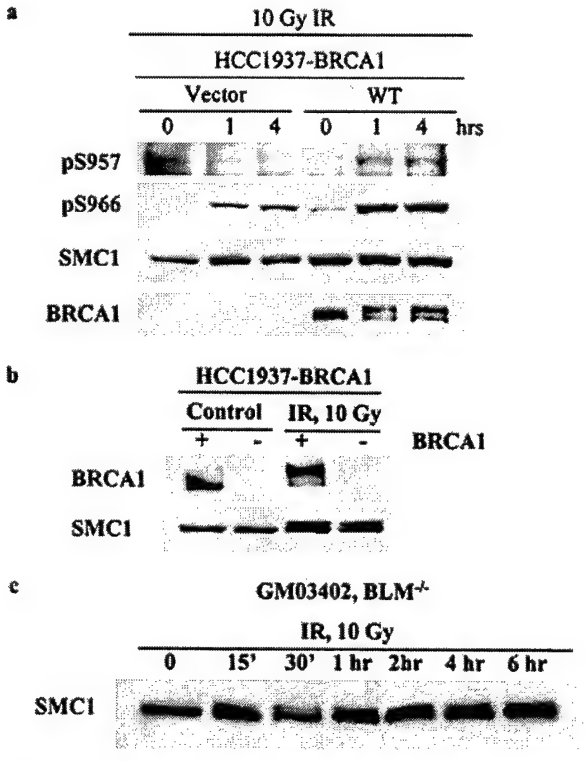


**Figure 5.** Phosphorylation of S957 and S966 of SMC1 does not depend on BRCA1 or BLM. (*a*) Vector and wild-type *BRCA1* cDNA-complemented HCC1937 cells were irradiated with 10 Gy of IR and allowed to recover for the indicated times. Phosphorylation of S957 and S966 of SMC1 was examined by Western blotting using phospho-specific antibodies against pS957 and pS966 of SMC1. (*b*) Phosphorylation of SMC1 was examined by SDS-PAGE mobility shift in the HCC1937 cells that were complemented with vector and wild-type BRCA1 cDNA. (*c*) The BLM-deficient cell line GM03402 was used to examine the kinetics of SMC1 phosphorylation in response to 10 Gy of IR.

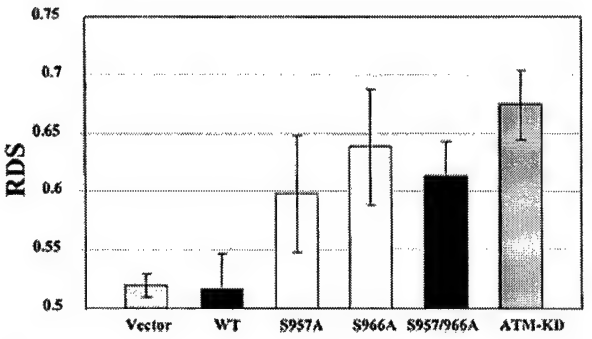


**Figure 6.** Phosphorylation of S957 and/or S966 of SMC1 is required for IR-induced S-phase checkpoint activation. RDS in 293T cells that were transiently transfected with pCDNA3-Flag vector, pCNDA3-Flag–SMC1-WT, S957A, S966A, S957A/S966A, and pCDNA3-Flag–ATM-KD. Incorporated [$^3$H]thymidine was measured following 20 Gy of IR and 1 h of incubation. Data were normalized with respect to untreated (control) cells. Error bars represent the standard deviation. Five independent experiments were carried out.

were either wild type for BRCA1 or contained a BRCA1 exon 11 deletion (data not shown). Therefore, phosphorylation of SMC1 appears to be BRCA1-independent, and BRCA1 does not seem to play an adapter/organizer role in the phosphorylation of SMC1 in response to IR. However, HCC1937 cells are not completely null for BRCA1, and the BRCA1 exon 11 deletion MEF has a truncated BRCA1 protein. Hence, it is formally possible that BRCA1 plays a role in this pathway. Sgs1 of *S. cerevisiae* is required for DNA damage checkpoint activation (Frei and Gasser 2000), and its human homolog, the BLM helicase, is a component of the BASC. BLM also associates with SMC1 (data not shown). The above findings led us to question whether SMC1 phosphorylation depends on BLM. SMC1 was phosphorylated in the BLM-defective cell line GM03402 in response to IR with kinetics similar to those in IMR-90 cells (Fig. 5c). Therefore, SMC1 phosphorylation does not depend on BLM.

### *Phosphorylation of S957 and/or S966 is required for activation of the S-phase checkpoint*

As SMC1 phosphorylation is both ATM- and NBS1-dependent, we tested whether SMC1 phosphorylation participates in the ATM/NBS1-dependent S-phase checkpoint pathway in response to IR. We transiently transfected 293T cells with Flag-epitope-tagged wild-type or mutant S957A, S966A, or S957A/S966A SMC1, and measured RDS 1 h after 20 Gy of IR. Cells expressing both vector and Flag-SMC1-WT showed inhibition of DNA synthesis, but those expressing Flag-SMC1-S957A, Flag-SMC1-S966A, and Flag-SMC1-S957A/S966A showed RDS (Fig. 6). The extent of RDS in the three SMC1 mutant cell lines was intermediate to those in Flag-SMC1-WT and ATM-KD cells (ATM-KD is a kinase-dead mutant of ATM that functions as a dominant negative, interfering with wild-type ATM functions.) Similar amounts of Flag-SMC1 were expressed in 293T cells (data not shown; similar to Fig. 3c). Therefore, phosphorylation of S957 and/or S966 is required for the activation of the S-phase checkpoint.

### *Cohesion per se is not sufficient for the phosphorylation of SMC1*

To help understand the molecular mechanism of SMC1-dependent S-phase checkpoint activation, we examined whether the phosphorylation of SMC1 has an effect on its binding to chromosomes. Untreated or IR-treated U2OS cells were fractionated according to the chromatin fractionation protocol developed in the Stillman laboratory (Mendez and Stillman 2000), and cytoplasmic, nucleoplasmic, and chromatin-bound fractions were analyzed by Western blotting (Fig. 7a). SMC1 was largely chromatin-bound (P3 fraction) before and after IR, and the phosphorylation of S966 did not affect chromatin binding. We could not detect pS957, as the pS957 antibody is significantly weaker than the pS966 antibody.

Because SMC1 is a component of the cohesin complex, it is important to study its phosphorylation in relation to its function in sister chromatid cohesion. The cohesin

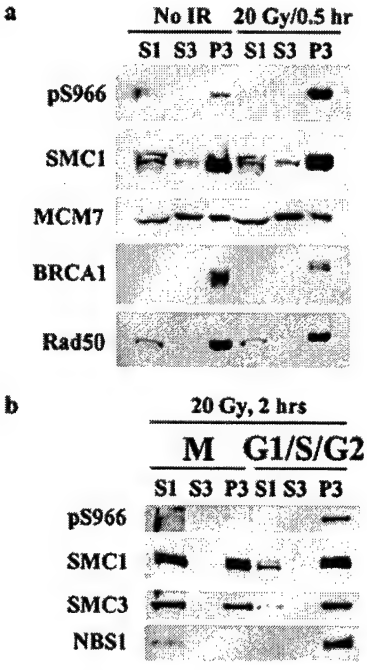


**Figure 7.** Characterization of SMC1 phosphorylation. (*a*) Phosphorylation of S966 does not affect SMC1 chromatin binding. U2OS cells were fractionated into the cytoplasmic (S1), nucleoplasmic (S2), and chromatin (P3) fractions and analyzed by Western blotting. (*b*) Cohesion per se is not sufficient for S966 phosphorylation. U2OS cells were blocked in mitosis with nocodazole, irradiated with 20 Gy of IR, and allowed to recover for 2 h. Cells were then separated into the mitotic fraction (M) and $G_1/S/G_2$ fraction by mitotic shake-off. M and $G_1/S/G_2$ cells were subject to chromatin fractionation.

complex is present on chromosomes in interphase cells even before sister chromatids are made. Most of the cohesin, however, dissociates from chromosomes in prometaphase, leaving only a small fraction of the cohesin on chromosomes to hold the sister chromatids together until the metaphase–anaphase transition (Losada et al. 1998; Hirano 2000). Only this small fraction that is still chromatin-bound in metaphase technically functions as cohesin. To examine the relationship between SMC1 phosphorylation and sister chromatid cohesion, we blocked the cell cycle in mitosis using nocodazole, irradiated the cells with 20 Gy of IR, and allowed cells to recover for 2 h. We then separated the mitotic cells from the rest by mitotic shake-off, and chromatin-fractionated the two cell populations. As shown in Figure 7b, S966 is not phosphorylated in the mitotic population, although a significant amount of SMC1 is still chromatin-bound. In the $G_1/S/G_2$ population, however, the chromatin-bound SMC1 (P3) is phosphorylated on S966. Therefore, cohesion per se is not sufficient for S966 phosphorylation. Consistent with this finding, NBS1 dissociates from chromatin in the mitotic population, but is chromatin-bound in the $G_1/S/G_2$ population. Therefore, the phosphorylation of SMC1 is not likely to regulate cohesion in mitosis, suggesting other functions for SMC1 besides sister chromatid cohesion.

### *The ATM/NBS1/SMC1 S-phase checkpoint pathway is distinct from the ATM/CHK2/CDC25A pathway*

The molecular mechanism for the ATM/NBS1-dependent S-phase checkpoint is not known. Because the ATM/CHK2/CDC25A pathway is known to regulate the S-phase checkpoint in response to IR, we investigated whether the ATM/NBS1 pathway converges to the ATM/CHK2/CDC25A pathway. NBS cells complemented with vector, wild-type NBS1, or S287A/S343A mutant were treated with 10 Gy of IR and analyzed for CDC25A. As shown in Figure 8a, CDC25A is degraded in all three cell lines in response to IR. Therefore, the ATM/CHK2/CDC25A pathway is intact in NBS cells. This is consistent with the activation of CHK2 in the three cell lines (Fig. 8b). In wild-type NBS1-complemented cells, CDC25A starts to accumulate 3 h after IR. In vector and mutant NBS1-complemented cells, however, CDC25A is not detected up to 4 h after IR. This observation implies that the signal that leads to CDC25A degradation is removed shortly after IR in wild-type cells, but persists in the absence of NBS1 or the presence of a phosphorylation-defective mutant. These data suggest that the ATM/NBS1/SMC1 pathway of the S-phase checkpoint is distinct from the ATM/CHK2/CDC25A pathway (Fig. 8c).

## Discussion

In this study, we established that SMC1 of the structural maintenance of chromosomes proteins is a component of the DNA damage response network. Data presented here show that SMC1 is a downstream effector of ATM and NBS1 in the activation of the IR-induced S-phase checkpoint. We also discovered that the phosphorylation of NBS1 by ATM is required for the phosphorylation of SMC1, establishing the role of NBS1 as an adaptor in the ATM/NBS1/SMC1 pathway. The ATM/CHK2/CDC25A pathway is also involved in S-phase checkpoint activation (Falck et al. 2001). We found that this pathway is intact in NBS cells. Our results indicate that the ATM/NBS1/SMC1 pathway is a separate branch of the S-phase checkpoint pathway, distinct from the ATM/CHK2/CDC25A branch (Fig. 8c). Thus, this work establishes the ATM/NBS1/SMC1 branch of the S-phase checkpoint

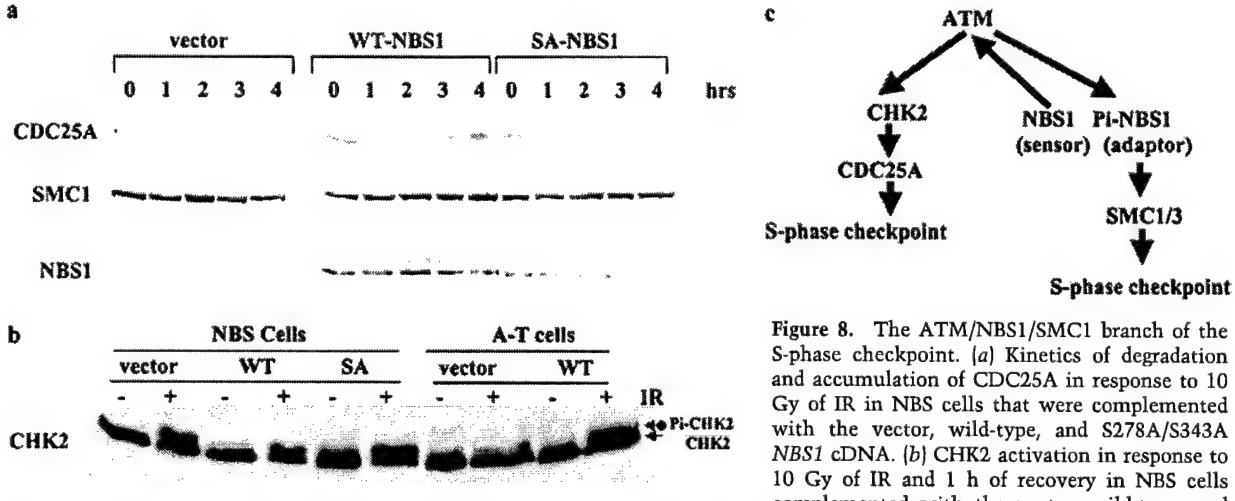


**Figure 8.** The ATM/NBS1/SMC1 branch of the S-phase checkpoint. (*a*) Kinetics of degradation and accumulation of CDC25A in response to 10 Gy of IR in NBS cells that were complemented with the vector, wild-type, and S278A/S343A *NBS1* cDNA. (*b*) CHK2 activation in response to 10 Gy of IR and 1 h of recovery in NBS cells complemented with the vector, wild-type, and S278A/S343A *NBS1* cDNA and A-T cells complemented with the vector and wild-type *ATM* cDNA. CHK2 was detected by Western blotting. The slowly migrating form marked with an arrow is labeled with Pi-CHK2. (*c*) A simplified S-phase checkpoint pathway in response to DSBs in mammalian cells. Phosphorylated NBS1 (Pi-NBS1) is depicted as an adaptor.

in response to IR, and provides a molecular basis for the S-phase checkpoint defect in NBS cells.

### *The distinction between the ATM/CHK2/CDC25A pathway and the ATM/NBS1/SMC1 pathway*

The kinetics of CDC25A degradation and accumulation in response to IR in NBS cells complemented with the vector, wild-type NBS1, or the phosphorylation mutant NBS1 are intriguing. CDC25A is degraded in the early response to IR in the three cell lines, suggesting that the ATM/CHK2/CDC25A pathway is intact in NBS cells (Fig. 8a). Consistently, CHK2 is activated in response to IR in all three cell lines (Fig. 8b). Therefore, NBS1 is not required for the activation of CHK2, at least in response to 10 Gy of IR. This conclusion is in contrast with Delia's results (Buscemi et al. 2001). Whereas Delia and coworkers used an IR dosage of 4 Gy, we used a dosage of 10 Gy. Possibly, different pathways are used for the response to DNA damage of different severity. Moreover, CDC25A does not accumulate to detectable levels after IR in the absence of NBS1 or if NBS1 cannot be phosphorylated by ATM. Therefore, NBS cells are defective in the late stage of the response to IR, possibly in the recovery phase. In the presence of wild-type NBS1, the signal that leads to CDC25A degradation is eliminated in 3 h, whereas in the absence of NBS1 or NBS1 phosphorylation by ATM, this signal is not removed in 3 h, leading to a relatively late accumulation of CDC25A. NBS1 must participate in the elimination of the signal that results in the degradation of CDC25A. This scenario agrees with a role for the M/R/N complex in DNA replication and repair (Maser et al. 2001). Phosphorylated SMC1 may also play a role in removing the signal, perhaps by homologous recombinational repair. Homologous recombinational repair requires the presence of an undamaged copy of the chromosome as a template. Sister chromatids are the preferred partners for this purpose. SMC1, as a subunit of the cohesin complex, may provide the structural scaffold for DSB repair by homologous recombination. This is consistent with the requirement of sister chromatid cohesion for postreplicative DSB repair in *S. cerevisiae* (Sjogren and Nasmyth 2001) and the finding that SMC1 is a component of the recombination complex RC-1 (Jessberger et al. 1996). It has been shown that postreplicative repair requires cohesion that is established only during S phase. When the cohesin complex is expressed after the S phase, despite the fact that the cohesin complex is chromatin-bound, the cells are defective in DNA repair. This finding is in agreement with our observation that the fraction of SMC1 that is still chromatin-bound in mitosis, providing cohesion between sister chromatids, is not phosphorylated. Taken together, it is likely that phosphorylated SMC1 is required for efficient postreplicative repair in human cells. Functionally, the two branches of ATM-dependent S-phase checkpoint pathways diverge to allow the CHK2/CDC25A branch to directly communicate with the cell cycle machinery, and the NBS1/SMC1 branch to directly communicate with the replication/repair machinery.

### *Phosphorylation of SMC1 is required for activation of the S-phase checkpoint*

The exact molecular mechanism by which phosphorylated SMC1 prevents radio-resistant DNA synthesis is not known. CDC25A is degraded and CHK2 is activated in NBS cells. Considering the above observations, phosphorylated SMC1 is not likely to function toward the suppression of the firing of origins in line for firing before encountering DSB, a pathway that is largely controlled by RAD53 (the human counterpart is CHK2) and the cell cycle machinery (Tercero and Diffley 2001). Phosphorylation of SMC1 may participate in the replication elongation process by interfering with the establishment of cohesion between the template and the sister chromatid that is being elongated, thus slowing down the progression of the replication fork. Phosphorylated SMC1 binds tightly to chromosomes in $G_1$/S/$G_2$. Structurally, SMC1 is phosphorylated within the C-terminal coiled-coil domain, and SMC3, the partner of SMC1, is phosphorylated in the N-terminal coiled-coil domain (P. Yazdi and J. Qin, unpubl.). These coiled-coil domains of SMC1 and SMC3 are in the same position of the antiparallel heterodimer of SMC1/3. Hence, phosphorylation of SMC1 and SMC3 may result in a large conformational change, modulating protein–protein interactions, presumably with the replication machinery. The heart of future research in the NBS1 branch of the S-phase checkpoint will be at the identification of the components of the replication machinery that are subject to regulation by the ATM/NBS1 pathway.

### *NBS1 may be an adaptor in response to IR in the ATM/NBS1/SMC1 pathway*

The identities of sensors that detect DNA damage have been elusive. The proposal that the human M/R/N complex functions as a sensor is supported by the observation that in response to DSB, checkpoint activation and *S. cerevisiae* Rad9 phosphorylation, an early event in checkpoint activation, require the Mre11/Rad50/Xrs2 complex (the *S. cerevisiae* counterpart of the human M/R/N complex; D'Amours and Jackson 2001; Grenon et al. 2001). Our finding that SMC1 phosphorylation (as well as BRCA1 phosphorylation) in response to IR depends on ATM and NBS1 may suggest that NBS1 lies upstream of ATM, serving as a sensor for DSB as proposed previously (Mirzoeva and Petrini 2001), or modifying DSB to a form recognizable by ATM. ATM is known to phosphorylate NBS1 in response to IR, suggesting that ATM lies upstream of NBS1. To resolve this paradox, we suggest an alternative model in which the M/R/N complex initially serves as a sensor, leading to the activation of ATM. ATM, in turn, phosphorylates its substrates, including NBS1. Phosphorylation of NBS1 effectively terminates the function of NBS1 as a sensor and

converts NBS1 into an adaptor by conformational change. The adaptor NBS1 then positions NBS1-binding proteins such that ATM can phosphorylate them. This model is consistent with our finding that SMC1 phosphorylation depends on NBS1 phosphorylation. Within this model, the role of NBS1 can be more accurately described as an adaptor that brings the substrate, SMC1, to ATM. This also agrees with the observation that a small population of NBS1 interacts with a small population of SMC1, as shown by coimmunoprecipitation (P. Yazdi and J. Qin, unpubl.). Our duo sensor/adaptor model also imposes specificity on DNA damage response, that is, the transducers can only transduce signals to downstream effectors that bind to the duo sensor/adaptor proteins. This specificity can explain why specific forms of DNA damage elicit specific responses although they all may work through the same transducer. The specificity is imposed by the sensor/adaptor/effector combination.

SMC1 phosphorylation is independent of BLM, suggesting that BLM does not function in the ATM/NBS1/SMC1 pathway. A definitive conclusion is difficult to make for the role of BRCA1 as an organizer or adaptor in the ATM/NBS1/SMC1 signaling pathway. The small increase in SMC1 phosphorylation after stable complementation of HCC1937 cells with *BRCA1* cDNA may be attributable to the low expression level of wild-type BRCA1 in this cell line. A definitive result would be obtained if the HCC1937 cell line could be complemented with higher, yet physiological amounts of BRCA1. The relationship between SMC1 and BRCA1 is not clear. BRCA1 may function as a downstream effector in this pathway, in which its putative E3 ubiquitin ligase activity (Hashizume et al. 2001; Ruffner et al. 2001) is regulated by DNA damage. Many BRCA1-interacting proteins can thus serve as substrates for the E3 activity of BRCA1. We speculate that SMC1 is such a substrate. Therefore, it is conceivable that the BASC, as a genome-surveillance complex, assembles sensors/adaptors, transducers, and effectors in a position to respond promptly to insults on the genome. Understanding the functional relationships among ATM, NBS1, BRCA1, SMC1/3, and other proteins in the BASC complex will provide insights into the mechanism of DNA damage response and the role of each individual protein.

## Materials and methods

### *Antibodies*

Rabbit polyclonal SMC1 antibody was raised against peptide sequence DLTKYPDANPNPNEQ and affinity-purified (Bethyl Laboratories). ATM and NBS1 antibodies were from GeneTex. Monoclonal mouse CDC25A antibody (F-6) was from Santa Cruz Biotechnology. BRCA1 antibody was described before (Wang et al. 2000). Phosphorylation site-specific SMC1 antibodies were raised against QEEGS**p**SQGEDS (S957 of SMC1), and DSVSG**p**SQRISS (S966 of SMC1). Affinity-purified phosphorylation site-specific antibodies recognize phosphorylated and unphosphorylated peptides with ratios >99:1 by ELISA (Bethyl Laboratories). Immunoprecipitation and Western blotting were carried out as described (Wang et al. 2000).

### *Plasmids, recombinant proteins, transient transfection, and in vitro kinase assays*

Fragments of SMC1 cDNA were generated by polymerase chain reaction with reverse transcription (RT–PCR) using RNA isolated from HeLa cells and cloned in pCR-Blunt II-TOPO vectors (Invitrogen). Full-length *SMC1* cDNA was assembled by ligation of SMC1 fragments in pCDNA3.1(–). A GST–SMC1 fusion protein (amino acids 890–1233) plasmid was generated by PCR and cloned in PGEX-4T-2. The fusion protein was expressed and purified according to the standard procedures. Site-specific mutagenesis was performed using a QuickChange site-directed mutagenesis kit (Stratagene), and the results were verified by sequencing. Wild-type, S957A, S966A, and S957A/S966A mutant SMC1 were subcloned in the pCDNA3-Flag vector. Transient transfection of these plasmids was carried out using Lipofectamine 2000 (Invitrogen) according to the manufacturer's suggested protocol. In vitro kinase assays were carried out as described (Cortez et al. 1999).

### *Cell culture*

Control (IMR-90, GM00637, TK6, 293T, and HeLa), A-T (GM05849), NBS (GM07166 and JS), BLM (GM03402), and BRCA1 (HCC1937) cell lines were purchased from either the Coriell Human Mutant cell repository or ATCC and cultured according to directions from the source. Wild-type or mutant S279A/S343A NBS1 was expressed in NBS1-LBI fibroblasts (Zhao et al. 2000) using the retroviral vector pLXIN (Clontech). The 29310A1 retroviral packaging cells (Imgenex) were transfected with pLXIN vector (as a negative control) or pLXIN vectors containing cDNA encoding wild-type NBS1 or mutant S279A/S343A NBS1. Retroviral supernatants were collected 48 h posttransfection. NBS1-LBI cells were incubated in retroviral supernatant plus fresh D-MEM supplemented with 10% fetal calf serum (volume ratio 1:1) for at least 24 h. NBS1-LBI cells were selected with 500 μg/mL G418 72 h after infection. Clones with ectopic expression of NBS1 were tested by Western blotting and immunostaining and maintained in D-MEM supplemented with 10% FCS and 200 μg/mL G418. FT169A ATM fibroblasts and their derivative YZ5 (ATM cDNA-complemented) were provided by Y. Shiloh (Department of Human Genetics and Molecular Medicine, Sackler School of Medicine, Tel Aviv University, Israel); GM07166 telomerase catalytic subunit (TERT) cells and the NBS1 cDNA-complemented GM07166 TERT cell line were provided by D. Livingston (The Dana-Farber Cancer Institute and the Harvard Medical School, Boston, MA); and the BRCA1 cDNA-complemented HCC1937 cell line was provided by J. Chen (Division of Oncology Research, Mayo Clinic, Rochester, MN).

### *Radio-resistant DNA synthesis*

RDS assay was carried out as described (Morgan et al. 1997). Briefly, 293T cells were labeled with 10 nCi/mL of [$^{14}$C]thymidine for 48 h to control for the total DNA content of different samples. Cells were then transfected with plasmids encoding wild-type and mutant Flag-SMC1. Transfection efficiency was estimated to be ~60%–70% using a GFP–SMC1 plasmid and FACS analysis. Sixty hours after transfection, cells were irradiated with 20 Gy of IR and incubated for 1 h. They were then pulse-labeled with 1 μCi/mL [$^{3}$H]thymidine for 30 min, washed twice with PBS, fixed with methanol, and filtered on a GF/C

fiberglass filter. Filters were counted in a liquid scintillation counter. DNA synthesis was calculated using the ratio of $^{3}H/^{14}C$. Overlapping $^{3}H$ and $^{14}C$ emissions were corrected with quenched $^{3}H$ and $^{14}C$ standards. Three replicas were measured for each sample, and five independent experiments were performed to collect data for statistical analysis.

*Mass spectrometry for the identification of phosphorylation sites*

Identification of phosphorylation sites with mass spectrometry was carried out as described previously (Zhang et al. 1998).

## Acknowledgments

We thank Y. Shiloh, D. Livingston, and J. Chen for distribution of cell lines; Z. Songyang for teaching J.Q. molecular biology; and D. Cortez and S. Elledge for discussion and critical reading of the manuscript. This work was supported by grants from the A-T Children Project and NCI (CA84199). J.Q. is a recipient of a career development award from the U.S. Department of Defense Breast Cancer Research program (DAMD17-00-1-0146), and P.T.Y. is a postdoctoral fellow of the U.S. Department of Defense Breast Cancer Research Program (DAMD17-01-1-0148).

The publication costs of this article were defrayed in part by payment of page charges. This article must therefore be hereby marked "advertisement" in accordance with 18 USC section 1734 solely to indicate this fact.

## References

Banin, S., Moyal, L., Shieh, S., Taya, Y., Anderson, C.W., Chessa, L., Smorodinsky, N.I., Prives, C., Reiss, Y., Shiloh, Y., et al. 1998. Enhanced phosphorylation of p53 by ATM in response to DNA damage. *Science* **281:** 1674–1677.

Birkenbihl, R.P. and Subramani, S. 1992. Cloning and characterization of rad21, an essential gene of *Schizosaccharomyces pombe* involved in DNA double-strand-break repair. *Nucleic. Acids. Res* **20:** 6605–6611.

Buscemi, G., Savio, C., Zannini, L., Micciche, F., Masnada, D., Nakanishi, M., Tauchi, H., Komatsu, K., Mizutani, S., Khanna, K., et al. 2001. Chk2 activation dependence on Nbs1 after DNA damage. *Mol. Cell. Biol.* **21:** 5214–5222.

Canman, C.E., Lim, D.S., Cimprich, K.A., Taya, Y., Tamai, K., Sakaguchi, K., Appella, E., Kastan, M.B., and Siliciano, J.D. 1998. Activation of the ATM kinase by ionizing radiation and phosphorylation of p53. *Science* **281:** 1677–1679.

Cortez, D., Wang, Y., Qin, J., and Elledge, S.J. 1999. Requirement of ATM-dependent phosphorylation of brca1 in the DNA damage response to double-strand breaks. *Science* **286:** 1162–1166.

D'Amours, D. and Jackson, S.P. 2001. The yeast Xrs2 complex functions in S phase checkpoint regulation. *Genes & Dev.* **15:** 2238–2249.

Falck, J., Mailand, N., Syljuasen, R.G., Bartek, J., and Lukas, J. 2001. The ATM-Chk2-Cdc25A checkpoint pathway guards against radioresistant DNA synthesis. *Nature* **410:** 842–847.

Frei, C. and Gasser, S.M. 2000. The yeast Sgs1p helicase acts upstream of Rad53p in the DNA replication checkpoint and colocalizes with Rad53p in S-phase-specific foci. *Genes & Dev.* **14:** 81–96.

Gatei, M., Young, D., Cerosaletti, K.M., Desai-Mehta, A., Spring, K., Kozlov, S., Lavin, M.F., Gatti, R.A., Concannon, P., and Khanna, K. 2000. ATM-dependent phosphorylation of nibrin in response to radiation exposure. *Nat. Genet.* **25:** 115–119.

Grenon, M., Gilbert, C., and Lowndes, N.F. 2001. Checkpoint activation in response to double-strand breaks requires the Mre11/Rad50/Xrs2 complex. *Nat. Cell Biol.* **3:** 844–847.

Guacci, V., Koshland, D., and Strunnikov, A. 1997. A direct link between sister chromatid cohesion and chromosome condensation revealed through the analysis of MCD1 in *S. cerevisiae*. *Cell* **91:** 47–57.

Hashizume, R., Fukuda, M., Maeda, I., Nishikawa, H., Oyake, D., Yabuki, Y., Ogata, H., and Ohta, T. 2001. The RING heterodimer BRCA1–BARD1 is a ubiquitin ligase inactivated by a breast cancer-derived mutation. *J. Biol. Chem.* **276:** 14537–14540.

Hirano, T. 2000. Chromosome cohesion, condensation, and separation. *Annu. Rev. Biochem.* **69:** 115–144.

Jessberger, R., Riwar, B., Baechtold, H., and Akhmedov, A.T. 1996. SMC proteins constitute two subunits of the mammalian recombination complex RC-1. *EMBO J.* **15:** 4061–4068.

Kim, S.T., Lim, D.S., Canman, C.E., and Kastan, M.B. 1999. Substrate specificities and identification of putative substrates of ATM kinase family members. *J. Biol. Chem.* **274:** 37538–37543.

Lim, D.S., Kim, S.T., Xu, B., Maser, R.S., Lin, J., Petrini, J.H., and Kastan, M.B. 2000. ATM phosphorylates p95/nbs1 in an S-phase checkpoint pathway. *Nature* **404:** 613–617.

Losada, A., Hirano, M., and Hirano, T. 1998. Identification of *Xenopus* SMC protein complexes required for sister chromatid cohesion. *Genes & Dev.* **12:** 1986–1997.

Maser, R.S., Monsen, K.J., Nelms, B.E., and Petrini, J.H. 1997. hMre11 and hRad50 nuclear foci are induced during the normal cellular response to DNA double-strand breaks. *Mol. Cell. Biol.* **17:** 6087–6096.

Maser, R.S., Mirzoeva, O.K., Wells, J., Olivares, H., Williams, B.R., Zinkel, R.A., Farnham, P.J., and Petrini, J.H. 2001. Mre11 complex and DNA replication: Linkage to E2F and sites of DNA synthesis. *Mol. Cell. Biol.* **21:** 6006–6016.

Matsuoka, S., Huang, M., and Elledge, S.J. 1998. Linkage of ATM to cell cycle regulation by the Chk2 protein kinase. *Science* **282:** 1893–1897.

Mendez, J. and Stillman, B. 2000. Chromatin association of human origin recognition complex, cdc6, and minichromosome maintenance proteins during the cell cycle: Assembly of prereplication complexes in late mitosis. *Mol. Cell. Biol.* **20:** 8602–8612.

Michaelis, C., Ciosk, R., and Nasmyth, K. 1997. Cohesins: Chromosomal proteins that prevent premature separation of sister chromatids. *Cell* **91:** 35–45.

Mirzoeva, O.K. and Petrini, J.H. 2001. DNA damage-dependent nuclear dynamics of the Mre11 complex. *Mol. Cell. Biol.* **21:** 281–288.

Morgan, S.E., Lovly, C., Pandita, T.K., Shiloh, Y., and Kastan, M.B. 1997. Fragments of ATM which have dominant-negative or complementing activity. *Mol. Cell. Biol.* **17:** 2020–2029.

Nelms, B.E., Maser, R.S., MacKay, J.F., Lagally, M.G., and Petrini, J.H. 1998. In situ visualization of DNA double-strand break repair in human fibroblasts. *Science* **280:** 590–592.

O'Neill, T., Dwyer, A.J., Ziv, Y., Chan, D.W., Lees-Miller, S.P., Abraham, R.H., Lai, J.H., Hill, D., Shiloh, Y., Cantley, L.C., et al. 2000. Utilization of oriented peptide libraries to identify substrate motifs selected by ATM. *J. Biol. Chem.* **275:** 22719–22727.

Painter, R.B. and Young, B.R. 1980. Radiosensitivity in ataxia-telangiectasia: A new explanation. *Proc. Natl. Acad. Sci.* **77:** 7315–7317.

Ruffner, H., Joazeiro, C.A., Hemmati, D., Hunter, T., and Verma, I.M. 2001. Cancer-predisposing mutations within the RING domain of BRCA1: Loss of ubiquitin protein ligase activity and protection from radiation hypersensitivity. *Proc. Natl. Acad. Sci.* **98:** 5134–5139.

Shiloh, Y. 2001. ATM and ATR: Networking cellular responses to DNA damage. *Curr. Opin. Genet. Dev.* **11:** 71–77.

Shiloh, Y. and Rotman, G. 1996. Ataxia-telangiectasia and the ATM gene: Linking neurodegeneration, immunodeficiency, and cancer to cell cycle checkpoints. *J. Clin. Immunol.* **16:** 254–260.

Sjogren, C. and Nasmyth, K. 2001. Sister chromatid cohesion is required for postreplicative double-strand break repair in *Saccharomyces cerevisiae*. *Curr. Biol.* **11:** 991–995.

Strunnikov, A.V. and Jessberger, R. 1999. Structural maintenance of chromosomes (SMC) proteins: Conserved molecular properties for multiple biological functions. *Eur. J. Biochem.* **263:** 6–13.

Tercero, J.A. and Diffley, J.F. 2001. Regulation of DNA replication fork progression through damaged DNA by the Mec1/Rad53 checkpoint. *Nature* **412:** 553–557.

Uhlmann, F. and Nasmyth, K. 1998. Cohesion between sister chromatids must be established during DNA replication. *Curr. Biol.* **8:** 1095–1101.

Wang, Y., Cortez, D., Yazdi, P., Neff, N., Elledge, S.J., and Qin, J. 2000. BASC, a super complex of BRCA1-associated proteins involved in the recognition and repair of aberrant DNA structures. *Genes & Dev.* **14:** 927–939.

Weinert, T. 1998. DNA damage and checkpoint pathways: Molecular anatomy and interactions with repair. *Cell* **94:** 555–558.

Wu, X., Ranganathan, V., Weisman, D.S., Heine, W.F., Ciccone, D.N., O'Neill, T.B., Crick, K.E., Pierce, K.A., Lane, W.S., Rathbun, G., et al. 2000. ATM phosphorylation of Nijmegen breakage syndrome protein is required in a DNA damage response. *Nature* **405:** 477–482.

Xu, B., Kim, S., and Kastan, M.B. 2001. Involvement of Brca1 in S-phase and G(2)-phase checkpoints after ionizing irradiation. *Mol. Cell. Biol.* **21:** 3445–3450.

Zhang, X., Herring, C.J., Romano, P.R., Szczepanowska, J., Brzeska, H., Hinnebusch, A.G., and Qin, J. 1998. Identification of phosphorylation sites in proteins separated by polyacrylamide gel electrophoresis. *Anal. Chem.* **70:** 2050–2059.

Zhao, S., Weng, Y.C., Yuan, S.S., Lin, Y.T., Hsu, H.C., Lin, S.C., Gerbino, E., Song, M.H., Zdzienicka, M.Z., Gatti, R.A., et al. 2000. Functional link between ataxia-telangiectasia and Nijmegen breakage syndrome gene products. *Nature* **405:** 473–477.

Zhou, B.B. and Elledge, S.J. 2000. The DNA damage response: Putting checkpoints in perspective. *Nature* **408:** 433–439.

# MSH2 and ATR form a signaling module and regulate two branches of the damage response to DNA methylation

**Yi Wang and Jun Qin***

Verna and Marrs McLean Department of Biochemistry and Molecular Biology and Department of Molecular and Cellular Biology, Baylor College of Medicine, One Baylor Plaza, Houston, TX 77030

Communicated by Stephen J. Elledge, Baylor College of Medicine, Houston, TX, October 21, 2003 (received for review July 20, 2003)

**The mismatch repair proteins function upstream in the DNA damage signaling pathways induced by the DNA methylating agent *N*-methyl-*N*′-nitro-*N*-nitrosoguanidine (MNNG). We report that MSH2 (MutS homolog 2) protein interacts with the ATR (ATM- and Rad3-related) kinase to form a signaling module and regulate the phosphorylation of Chk1 and SMC1 (structure maintenance of chromosome 1). We found that phosphorylation of Chk1 by ATR also requires checkpoint proteins Rad17 and replication protein A. In contrast, phosphorylation of SMC1 by ATR is independent of Rad17 and replication protein A, suggesting that the signaling pathway leading to SMC1 phosphorylation is distinct from that mediated by the checkpoint proteins. In addition, both MSH2 and Rad17 are required for the activation of the S-phase checkpoint to suppress DNA synthesis in response to MNNG, and phosphorylation of SMC1 is required for cellular survival. These data support a model in which MSH2 and ATR function upstream to regulate two branches of the response pathway to DNA damage caused by MNNG.**

By maintaining genome stability, the DNA damage response network plays a significant role in preventing cancer development (1). Many tumor suppressors, such as p53, Chk2, and the breast cancer tumor suppressor BRCA1, are integral components of this network, which regulates cell cycle checkpoint activation and DNA repair. Genetic work from yeast has established the current conceptual framework of DNA damage response (2). In humans, the central checkpoint kinases ATM (ataxia telangiectasia mutated) and ATR (ATM- and Rad3-related), and the RFC (replication factor C)-like checkpoint protein Rad17/RFC2–5 complex have been demonstrated to function upstream of the DNA damage response pathway for the activation of the downstream checkpoint kinase Chk1 by phosphorylation (3). Because different DNA-damaging agents generate different DNA lesions, a key question in damage signaling is how the checkpoint proteins recognize different DNA lesions. One mechanism of DNA damage recognition has been elucidated recently, in which binding of replication protein A (RPA) to single-stranded DNA (ssDNA) results in recruitment of the ATR-interacting protein ATRIP to load the ATR/ATRIP complex to ssDNA, leading to activation of ATR (4). Because ssDNA is a common intermediate for many DNA repair pathways, this model explains nicely how ATR-dependent checkpoint pathways respond to different types of DNA damage.

In contrast to checkpoint pathways, DNA repair pathways use lesion-specific factors to recognize different lesions (5, 6). The mismatch repair (MMR) proteins play key roles in postreplicational mispair correction that is essential for genomic stability (7). Mutations in MMR genes, especially *MSH2* and *MLH1*, are associated with predisposition to hereditary nonpolyposis colorectal cancer (8–10). The MMR reaction is initiated by binding of the MSH2 (MutS homolog 2)/MSH6 heterodimer to the mismatched DNA (11). The MMR proteins also function in signaling DNA damage (7, 11). Upon exposure to MNNG and crosslinking agents, cells deficient in MMR proteins exhibit impaired $G_2$/M cell cycle arrest, reduced activation of the p53/p73 apoptosis pathway, and resistance to the cytotoxicity of these DNA-damaging agents (12–14). Recently, the MMR system has also been implicated in S-phase checkpoint activation in response to low-dosage IR (15). The ability of the MSH2/MSH6 heterodimer to bind a variety of modified DNA structure *in vitro* suggests a possibility that the MMR proteins may signal the DNA damage directly. Alternatively, the checkpoint response can be activated indirectly through recognition of repair intermediates that are generated by MMR. These possibilities have not been thoroughly tested.

In this study, we report a MSH2-dependent signaling pathway in response to DNA damage caused by MNNG. We found that MSH2 protein interacts with the ATR kinase constitutively to form a signaling module that regulates the phosphorylation of downstream effectors including Chk1 and SMC1 (structure maintenance of chromosome 1). Whereas phosphorylation of Chk1 also requires Rad17 and RPA, phosphorylation of SMC1 is independent of Rad17 and RPA. Thus, the pathway leading to SMC1 phosphorylation by ATR seems to branch out the checkpoint pathway mediated by Rad17 and RPA. In addition, both MSH2 and Rad17 are required for the activation of the S-phase checkpoint to suppress DNA synthesis in response to MNNG. Thus, MSH2 and ATR function upstream to regulate two branches of the response pathway to DNA damage caused by MNNG.

## Materials and Methods

**Cell Lines and Antibodies.** TK6 and MT1 cells (provided by P. Modrich, Duke University, Durham, NC) were maintained in RPMI medium 1640 with 10% FBS. 293T and HeLa cells were cultured in DMEM with 10% FBS. Anti-RPA70 antibody was from Oncogene Research Products (La Jolla, CA). Anti-MSH2 (BL323), Rad17 (BL239G), Chk1 (BL234), SMC1 (BL308), MSH6 (BL903), SMC1-pS966 (BL311), Chk1-pS317 (BL229), and Chk1-pS345 (BL231) antibodies were from Bethyl Laboratories (Montgomery, TX). Rabbit anti-ATR was raised against GST-ATR (400–460) and affinity-purified. Anti-ATRIP antibody was provided by S. Elledge (Baylor College of Medicine).

**RNA Interference, *in Vitro* Kinase Assay, *in Vitro* Binding Assays, Immunoprecipitation (IP), and Mass Spectrometry.** The small interfering RNA (siRNA) duplexes were synthesized by Dharmacon Research (Boulder, CO) and prepared by annealing two 21-

Abbreviations: MNNG, *N*-methyl-*N*′-nitro-*N*-nitrosoguanidine; MMR, mismatch repair; ATM, ataxia telangiectasia mutated; ATR, ATM- and Rad3-related; MSH, MutS homolog; ATRIP, ATR-interacting protein; SMC, structure maintenance of chromosome; RPA, replication protein A; ssDNA, single-stranded DNA; siRNA, small interfering RNA; NE, nuclear extracts; IP, immunoprecipitation.

*To whom correspondence should be addressed. E-mail: jqin@bcm.tmc.edu.

ribonucleotide oligonucleotides according to the manufacturer's suggestions. The sequences targeting each gene were as follows: *MSH2*, 5′-AAU CUG CAG AGU GUU GUG CUU-3′; *ATR*, 5′-AAC GAG ACU UCU GCG GAU UGC-3′; *Rad17*, 5′-AAC AGA CUG GGU UGA CCC AUC-3′; and *ATM*, 5′-AAG CAC CAG UCC AGU AUU GGC-3′. The siRPA70 was described in ref. 4. (Throughout, "si" before a gene name indicates gene-specific siRNA.) The si*GFP* and si*Vimentin* were purchased from Dharmacon Research and used as mock controls. HeLa cells were transfected with siRNA duplex by using Oligofectamine (Invitrogen) according to the manufacturer's protocols. Transfected cells were replated 48 h after transfection with a 1:3 ratio and treated with DNA-damaging agents 60–72 h after transfection (16).

The MSH2 and MSH6 proteins were overexpressed in sf9 cells transfected with baculovirus overexpressing MSH2 or MSH6 and purified by IP with antibodies. Flag-ATR was overexpressed in 293T cells, purified with anti-Flag agarose, and eluted with Flag peptide. MSH2 or MSH6 bound to protein A-Sepharose were incubated at 4°C with either purified Flag-ATR or $^{35}$S-labeled, *in vitro* translated SMC1 for 1 h and washed three times with NETN buffer (0.5% Nonidet P-40/1 mM EDTA, pH 8.0/20 mM Tris, pH 8.0/100 mM NaCl). The binding was analyzed with Western blotting or autoradiography.

Purification of MSH2 complex was carried out in 5 ml of HeLa nuclear extracts (NE) (≈10 mg/ml protein) with 50 $\mu$g of MSH2 antibody essentially as described (17). The protein components were separated on a SDS/PAGE and analyzed by mass spectrometry as described (17). An *in vitro* kinase assay using overexpressed Flag-ATR and GST-SMC1 was carried out as described (18).

**Inhibition of DNA Synthesis and Clonogenic Survival Assays.** Inhibition of DNA synthesis assay was carried out as described with some modifications (19). Briefly, 24 h after siRNA transfection, cells were labeled with 50 nCi (1 Ci = 37 GBq) of [$^{14}$C]thymidine per ml for 24 h as a control for the total DNA content of different samples. Sixty to 72 h after transfection, cells were treated with the indicated MNNG concentration for 1 h and allowed to recover for indicated times. They were then pulse-labeled with 1 $\mu$Ci/ml [$^{3}$H]thymidine for 30 min. Labeled cells were harvested, washed twice with PBS, and fixed with 80% ethanol at −20°C overnight. The fixed cells were then pelleted by centrifugation, washed in 80% ethanol, and pelleted again twice. Finally, the washed cell pellets were dissolved in 0.5 ml of 0.25 N NaOH solution, and 10 ml of scintillation counting solution was added for radioactivity counting in a liquid scintillation counter. DNA synthesis was calculated by using the ratio of $^{3}$H/$^{14}$C. Overlapping $^{3}$H and $^{14}$C emissions were corrected with quenched $^{3}$H and $^{14}$C standards. Three replicas were measured for each sample to derive the standard deviation.

Transient transfection of GFP-wt-SMC1 or GFP-S966A-SMC1 in HeLa cells was carried out with Lipofectamine (Invitrogen). Cells overexpressing wild-type or S966A GFP-SMC1 were plated in triplicate at limiting dilutions 30 h after transfection and treated with a range of MNNG 18 h later (48 h after transfection). After incubation in the presence of MNNG for 1 h, cells were replaced with fresh medium and recovered for 7 days. Colonies were then fixed in methanol and stained with Giemsa. A population of >50 cells was counted as one colony.

## Results

**ATR Coimmunoprecipitates with MSH2.** To identify signaling components in the MSH2 pathway, we carried out an IP from HeLa NE using an anti-MSH2 antibody. An IP using a BRCA2 antibody was used as a negative control. We analyzed the immunoprecipitates by mass spectrometry (Fig. 1*A*). Besides MSH6 and MSH3, which are known to be associated with MSH2, we identified a substoichiometrical component with an apparent

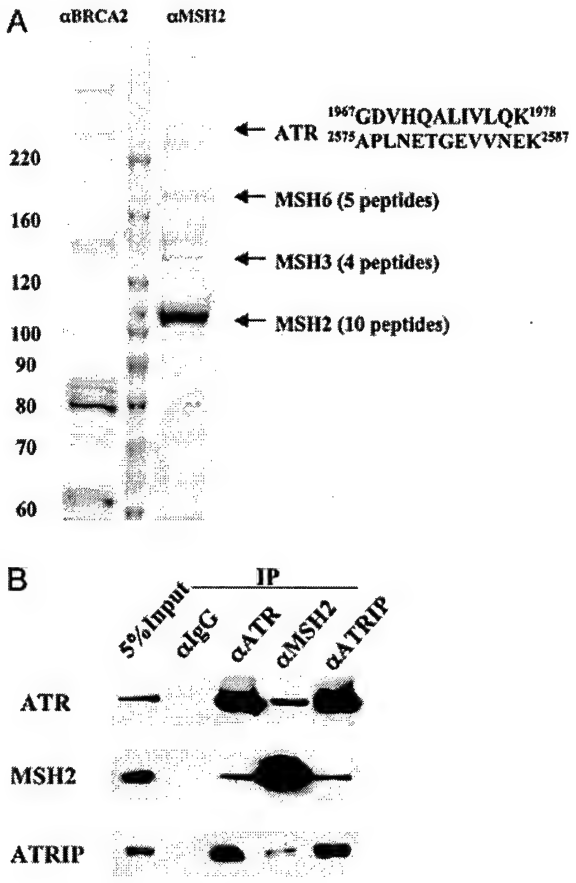


**Fig. 1.** MSH2 associates with ATR in HeLa NE. (*A*) The MSH2 complex was isolated by anti-MSH2 IP and separated on a SDS/PAGE. A parallel IP using a BRCA2 antibody serves as a negative control. Protein bands stained by Coomassie blue were analyzed by mass spectrometry. The sequences of the two ATR peptides identified are shown. (*B*) Coimmunoprecipitations of MSH2, ATR, and ATRIP detected by Western blotting. IPs were carried out in HeLa NE by using indicated antibodies. Five percent of the total protein used in the IP was loaded in the input lane.

molecular mass of ≈250 kDa as the checkpoint kinase ATR. The association between ATR and MSH2 was confirmed by reciprocal IP detected by Western blotting (Fig. 1*B*). The recently identified ATRIP (18), although not detected by mass spectrometry, was also found to be coimmunoprecipitated with MSH2 detected by Western blotting (Fig. 1*B*). Moreover, mass spectrometry analysis of immunoprecipitates of ATR from HeLa NE also identified ATRIP, MSH2, and MSH6 proteins (data not shown), consistent with the IP/Western blot results. This suggests that ATRIP in the MSH2 IP is below the detection limit of Coomassie blue staining because of its lower molecular mass (90 kDa). Elution profiles of MSH2 from ion exchange and gel filtration columns suggest that MSH2 exists in different complexes in the HeLa NE (data not shown). The small percentage of MSH2 and ATR that coimmunoprecipitates suggests that only a small proportion of MSH2 complexes contains ATR.

**SMC1 and Chk1 Are Downstream Effectors in the MSH2/ATR Pathway in Response to MNNG.** The association of ATR with MSH2 implicates ATR as a transducer kinase in the MMR protein-mediated response pathway. SMC1 was recently identified as a component of the ATM/NBS1 branch of the S-phase checkpoint pathway in response to IR (20, 21). SMC1 is phosphorylated at S966 and S957 by ATM in response to IR. To investigate whether

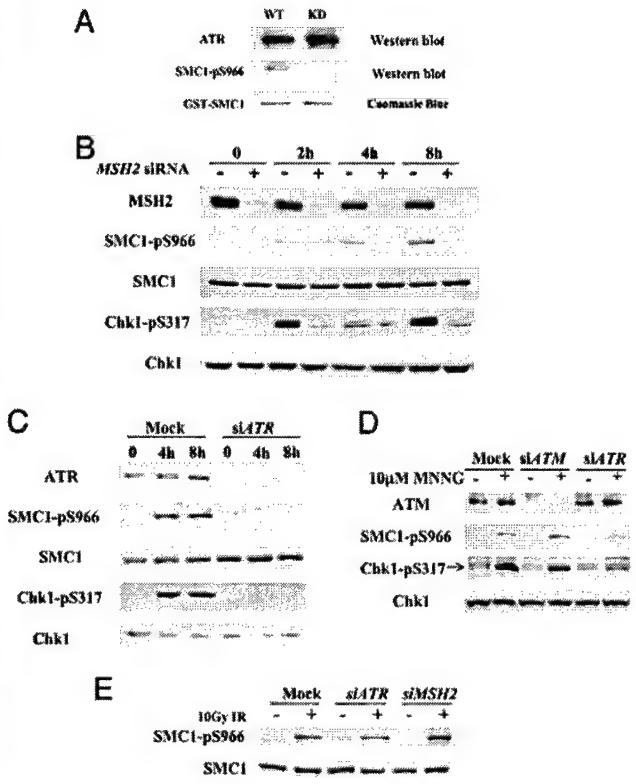


**Fig. 2.** The MSH2/ATR complex is required for MNNG-induced phosphorylation of SMC1 and Chk1. (*A*) *In vitro* kinase assays of SMC1 by ATR. Transiently expressed Flag-tagged ATR (wild type or kinase dead) in 293T cells was used to phosphorylate a GST-SMC1 fragment (amino acids 890-1233). The phosphorylation product was immunoblotted with SMC1 S966 phosphospecific antibody. Equal amounts of GST-SMC1 proteins used in the kinase assays were monitored by Coomassie blue staining. (*B* and *C*) Dependence of SMC1 S966 and Chk1 S317 phosphorylations on MSH2 (*B*) and ATR (*C*) in response to MNNG. HeLa cells transfected with mock (*siGFP*), si*ATR*, or si*MSH2* were treated with 10 $\mu$M MNNG for 1 h and harvested at indicated times. Efficiency of RNA interference was monitored by Western blotting to each protein. (*D*) ATR, not ATM, is the major kinase involved in early response to MNNG-induced damage. Mock, siRNA to *ATM*- or *ATR*-transfected HeLa cells was treated with 10 $\mu$M MNNG for 1 h and harvested after 4 h. Cell lysates were analyzed with indicated antibodies. Chk1 blot also serves as a loading control. (*E*) Independence of SMC1 phosphorylation on ATR and MSH2 in response to $\gamma$ irradiation. HeLa cells transfected with indicated siRNA were treated with 10 Gy of IR and harvested after 1 h.

SMC1 is a downstream effector in response to DNA methylation-induced damage, we treated the cells with MNNG. We found that S966 of SMC1 is phosphorylated in a dosage-dependent manner in HeLa and primary human fibroblast IMR90 cells (data not shown). To determine whether ATR directly phosphorylates SMC1 *in vitro*, we expressed a fragment of SMC1 containing the *in vivo* phosphorylation site (amino acids 890-1233) as a GST fusion protein. Flag-tagged wild-type ATR but not the kinase-inactive form of ATR (kd-ATR) expressed in 293T cells can directly phosphorylate GST-SMC1 at S966 in an *in vitro* kinase assay (Fig. 2*A*).

To determine whether MSH2 and ATR are required in signaling MNNG-induced damage, we used siRNA to inhibit their expression (16). Transfections of si*MSH2* effectively reduced MSH2 protein level and led to defective phosphorylation of both SMC1 at S966 and Chk1 at S317 in response to 10 $\mu$M MNNG treatment (Fig. 2*B*). Similarly, phosphorylation of SMC1 at S966 and Chk1 at S317 were largely abolished in cells depleted of ATR (Fig. 2*C*), consistent with its role as a checkpoint kinase. These results demonstrate that MSH2 and the ATR kinase function upstream in response to MNNG that leads to phosphorylation of SMC1 and Chk1. Defective phopshorylation of SMC1 and Chk1 was also observed in the MSH6-deficient MT1 cell line when compared with the parental TK6 cell line (data not shown), suggesting that a functional MSH2/MSH6 complex is required for SMC1 and Chk1 phosphorylation.

ATM and ATR are the central checkpoint kinases in signaling DNA damage, and they play distinct yet sometimes overlapping roles in signaling different damages (22). To differentiate the role of ATM plays from ATR in signaling MNNG-induced damage, we compared phosphorylation of checkpoint effectors in HeLa cells transfected with siATM or siATR 4 h after 10 $\mu$M MNNG treatment. Phosphorylation of SMC1 and Chk1 remains largely intact in cells lacking ATM and is more defective in cells transfected with siATR (Fig. 2*D*). HeLa cells transfected with siATM under the same conditions are defective in activation of S-phase checkpoint in response to 10 Gy of IR (data not shown), confirming that the ATM function has been compromised by siRNA transfection. Therefore, we conclude that ATR is the major kinase responsible for checkpoint activation in response to MNNG-induced damage.

Because the MSH2/MSH6 heterodimer is a lesion-specific factor that binds DNA mismatches and a variety of modified DNA structures including those caused by MNNG, it has been proposed as a putative damage sensor in the MMR pathway (7, 13). To test whether MSH2 and ATR function in a lesion-specific manner for SMC1 phosphorylation, we examined their roles in response to IR. In contrast to the requirement of MSH2 and ATR in MNNG-induced damage, phosphorylation of SMC1 in response to 10 Gy of IR is normal in siMSH2- or siATR-transfected cells (Fig. 2*E*). Thus, the MSH2/ATR pathway is required to phosphorylate SMC1 specifically in response to damage induced by DNA methylation but not for double-stranded break caused by IR.

**Interaction of MSH2 or MSH6 with ATR and SMC1.** To understand the mechanism of MSH2/MSH6-dependent phosphorylation of SMC1 by ATR, we tested whether ATR and SMC1 interact directly with MSH2 or MSH6. Recombinant MSH2 and MSH6 were expressed in insect cells and purified by IP by using anti-MSH2 or MSH6 antibodies. Flag-ATR was expressed in 239T cells, purified with Flag beads, and eluted with the Flag peptide. As shown in Fig. 3*A*, MSH2 is able to pull down purified ATR *in vitro*, suggesting that they may interact directly. When the same amount of protein A-bound MSH2 or MSH6 was mixed with *in vitro* translated SMC1, more SMC1 was brought down by MSH6 than by MSH2. This suggests that MSH6 may interact directly with SMC1.

The MMR-deficient cell line MT1 was isolated from TK6 by its resistance to killing by MNNG. MT1 expresses a lower level of a mutant MSH6 than TK6 does. To determine whether MSH6 is required for MSH2/ATR association *in vivo*, we compared the coimmunoprecipitation of MSH2/ATR in TK6 and MT1 cells. We found that the MSH2/ATR association in MT1 cells appeared to be intact compared with that in the parental TK6 cells (Fig. 3*B*). The slightly lower amount of coprecipitated ATR in MT1 cells is likely a result of a lower level of MSH2 in the anti-MSH2 IP from MT1. The above result is in agreement with the *in vitro* binding results, suggesting that the MSH2 may directly interact with ATR *in vivo*.

**Phosphorylation of SMC1 Does Not Depend on Rad17or RPA.** The replication factor C-like checkpoint protein Rad17 has been well established as an upstream element in the DNA damage response (2). To test whether phosphorylation of SMC1 and Chk1

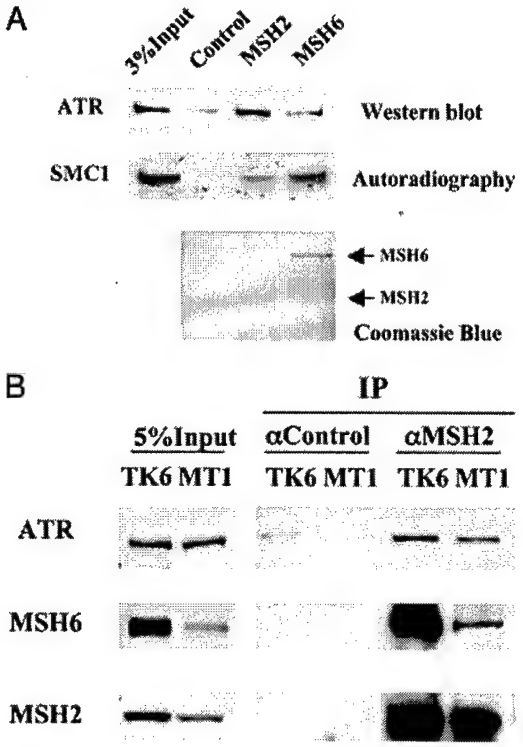


**Fig. 3.** Interaction of MSH2 or MSH6 with ATR and SMC1. (*A*) *In vitro* interactions of MSH2 or MSH6 with ATR and SMC1, respectively. Affinity-purified human MSH2 and MSH6 from sf9 cells were incubated with purified Flag-ATR or $^{35}$S-labeled, *in vitro* translated SMC1. An unrelated antibody incubated with sf9 cell lysate was used as a control. Coomassie blue staining of the membrane after Western blotting shows that human MSH2 and MSH6 used in the binding reactions do not copurify with the insect MSH6 or MSH2. (*B*) MSH6-independent association of MSH2 and ATR. IPs were carried out in NE prepared from lymphoblastoid cell line TK6, which expresses wild-type MSH6, and MT1, which expresses a low level of a mutant form of MSH6.

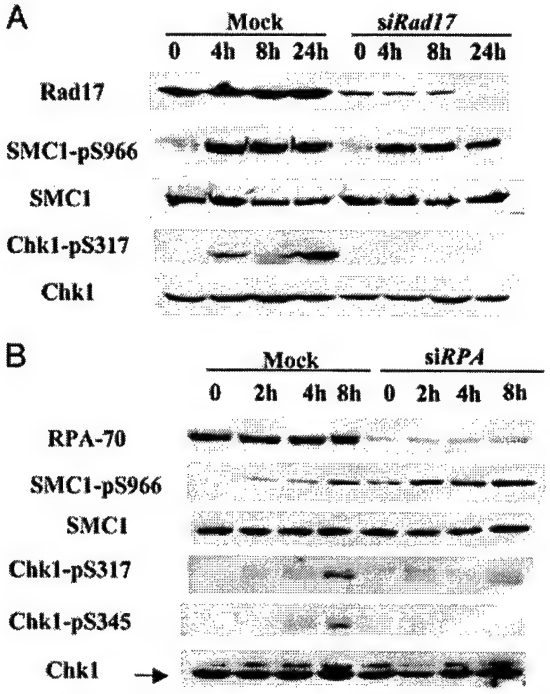


**Fig. 4.** Rad17 and RPA are not required for the phosphorylation of SMC1. Shown is MNNG-induced phosphorylation of SMC1 and Chk1 in the absence of Rad17 (*A*) or RPA (*B*). HeLa cells transfected with indicated siRNAs were treated with 10 $\mu$M MNNG for 1 h and harvested at indicated times. Lysates were analyzed with indicated antibodies.

requires Rad17, we depleted Rad17 by small RNA interference. Surprisingly, phosphorylation of SMC1 remains largely unaffected in the absence of Rad17 (Fig. 4*A*). In contrast, phosphorylation of Chk1 is greatly reduced, as expected. Thus, SMC1 as an ATR substrate can be phosphorylated through a mechanism that is distinct from the Rad17-mediated signaling pathway.

RPA has been shown recently to activate ATR by recruiting the ATRIP to the damaged sites (4). Likewise, we found that RPA is required for the phopshorylation of Chk1 but not for the phosphorylation of SMC1 (Fig. 4*B*). Taken together, these data suggest that, while MSH2 and ATR are required for the MNNG-induced response, the pathway leading to phosphorylation of SMC1 is distinct from that mediated by Rad17 and RPA. Thus, the SMC1 pathway seems to branch out from that mediated by the checkpoint protein Rad17 and RPA.

**MSH2 and Rad17 Both Are Required for Inhibition of DNA Synthesis, and Phosphorylation of SMC1 Is Important for Cellular Survival in Response to MNNG.** In response to DNA damage, eukaryotic cells activate the S-phase checkpoint to slow down DNA synthesis. To investigate whether MSH2 and Rad17 are required for S-phase checkpoint activation in response to MNNG, we monitored DNA synthesis in HeLa cells transfected with si*MSH2*, si*Rad17*, or a control siRNA through a 6-h time course after 10 $\mu$M MNNG treatment. Similar to slowed DNA synthesis in response to IR, DNA synthesis measured by thymidine incorporation in control siRNA-transfected cells was reduced to 20% of that in cycling cells 3 h after MNNG treatment and was 25% at 6 h. Such slowing down of DNA synthesis is characteristic of the activation of the S-phase checkpoint (Fig. 5*A*). In contrast, cells transfected with siMSH2 or siRad17 consistently exhibit a higher level of DNA synthesis after MNNG treatment, indicating that the ability to inhibit DNA synthesis is compromised. We therefore conclude that inactivation of MSH2 or Rad17 leads to defective inhibition of DNA synthesis in response to MNNG.

To determine the long-term effect of damage-induced SMC1 phosphorylation, we evaluated the clonogenic survival of HeLa cells transiently transfected with a wild-type SMC1 or a phosphorylation site mutant of SMC1 after MNNG treatment. HeLa cells expressing S966A of SMC1 (Ser-966 is mutated to Ala-966) display increased sensitivity to MNNG-induced killing compared with those transfected with the wild-type SMC1 (Fig. 5*B*), suggesting that phosphorylation of SMC1 is important for cellular survival. This finding is consistent with the previous report that SMC1 phosphorylation is important for cellular survival in response to IR (21).

## Discussion

**The MSH2/ATR Signaling Module.** In this study, we show that the MSH2 protein physically interacts with ATR to form a signaling module. They are required for the phosphorylation of SMC1 and Chk1. This MSH2-dependent response is lesion-specific, because it responds primarily to MNNG, not IR. The MMR proteins have been implicated as upstream elements in response to MNNG- and cisplatin-induced damage. Our findings further strengthen this notion and establish that ATR is the transducer kinase that participates in the MSH2-dependent DNA damage response pathway. The MSH2/ATR signaling module is analogous to the established signaling

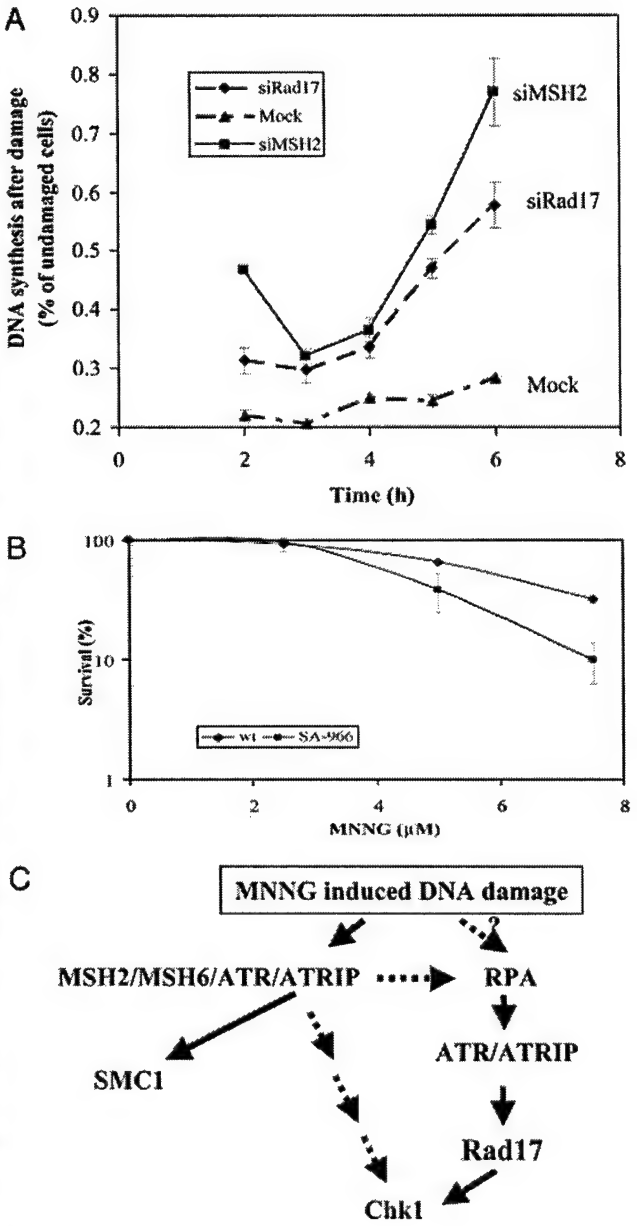


**Fig. 5.** (*A*) Both MSH2 and Rad17 are required for activation of MNNG-induced S-phase checkpoint. HeLa cells transfected with mock, *MSH2*, or *Rad17* siRNA were treated with 10 μM MNNG for 1 h. DNA synthesis measured by [$^3$H]thymidine incorporation was evaluated at time indicated after the treatment and normalized to that in cycling cells. The measurements were performed in triplicate. The error bar represents the standard deviation. (*B*) SMC1 phosphorylation is required for cellular survival after MNNG treatment. HeLa cells expressing either GFP-wt-SMC1 or GFP-SA966-SMC1 were treated with MNNG of indicated concentrations for 1 h and recovered for 1 week before assaying for colony formation. The assay was performed in triplicate. The error bar represents the standard deviation. (*C*) A schematic model of MNNG-induced DNA damage response. Upon exposure to MNNG, binding of the MSH2/MSH6 heterodimer to $O^6$-methyl-G·C activates the checkpoint kinase ATR, leading to the phosphorylation of SMC1 and Chk1. The RPA is also required to recruit the ATR/ATRIP complex to the damaged sites, possibly through binding to MMR intermediates, resulting in Rad17-dependent phosphorylation of Chk1. However, SMC1 can be phosphorylated independent of RPA and Rad17, suggesting the existence of a response pathway through direct interaction between ATR/MSH2 and MSH6/SMC1.

module of the double-stranded break repair complex Mre11/Rad50/NBS1 (M/R/N) with ATM, which responds primarily to double-stranded break (23–25). Such arrangement is intriguing, in that the repair proteins physically associate with transducer kinases constitutively. Because the M/R/N complex binds double-stranded break and MSH2/MSH6 binds the $O^6$-methyl-G·C generated by MNNG, the physical association of these repair proteins with transducer kinases puts them in close proximity for the possibility of direct damage signaling.

**Two Branches of the Damage Response That Are Regulated by MSH2 and ATR.** The participation of Rad17 and RPA as upstream elements for the phopshorylation of Chk1 in the response to MNNG is expected. It is surprising that they are not required for the phosphorylation of SMC1. Although we cannot rule out the possibility that SMC1 lies upstream of Rad17, the current understanding of the mechanism by which Rad17 is recruited to the damaged sites suggests that the pathway that governs SMC1 phosphorylation is likely branched out from the well established checkpoint pathway that is mediated by Rad17 and RPA (Fig. 5*C*). Similar dependence of SMC1 phosphorylation in response to IR was also observed, in which SMC1 phosphorylation depends on the repair protein NBS1 (20, 21) but not the checkpoint protein Rad17 (26).

Although both SMC1 and Chk1 are bone fide ATR substrates, the molecular mechanism by which they are phosphorylated can be different. On the SMC1 branch, the phosphorylation of SMC1 by ATR may be through a mechanism of direct damage signaling. Given that MSH2/MSH6 heterodimer is able to recognize DNA lesions directly, the MSH2/ATR association suggests that ATR kinase can be activated at the site of damaged DNA, leading to SMC1 phopshorylation. The *in vitro* binding of MSH6 with SMC1 raised the possibility that the MSH6 may function as an "adaptor." This is also consistent with the requirement for a functional MSH6 in the MT1 cell line for SMC1 phopshorylation but not for the MSH2/ATR association.

On the Chk1 branch, phosphorylation of Chk1 by ATR may be through an indict mechanism of damage recognition. The requirement for RPA suggests that ssDNA is generated either as a direct result of MNNG damage or, more likely, as a repair intermediate that is processed by the MMR system. Thus, ATR/ATRIP is loaded by RPA-ssDNA, which in turn phosphorylates Chk1 in a Rad17-dependent manner. It is possible that the pool of ATR that phosphorylates Chk1 is different from the pool of ATR that phosphorylates SMC1. The former does not need to associate with MSH2, but the latter does, consistent with our finding that only a small percentage of ATR associates with MSH2 in the cell.

The existence of two branches in damage response to MNNG that are governed by MSH2 suggests that the MMR proteins may be involved in two aspects of damage signaling. (*i*) They generate repair intermediates during MMR, which are recognized by the checkpoint proteins, leading to activation of the Chk1 branch. (*ii*) They signal damage directly to phosphorylate a unique set of substrates, including SMC1, thus are directly involved in checkpoint signaling. A reconstituted *in vitro* system to demonstrate directly the MMR protein-dependent activation of the ATR kinase to phosphorylate SMC1 remains to be established.

**SMC1 Phosphorylation Is Important for Cellular Survival.** Consistent with its role for survival in response to IR (21), we show here that phosphorylation of SMC1 is also involved in the modulation of cellular sensitivity to MNNG damage. In *Schizosaccharomyces pombe*, phosphorylation of Chk1 is also important for cellular survival in response to UV damage (27). Thus, the ATR-dependent pathways are important for cellular survival in response to DNA damage. Paradoxically, a hallmark of

MMR-deficient cells is their resistance to killing by DNA-alkylating agents, including MNNG. Clearly, the inability to phosphorylate SMC1 or Chk1 in MMR-deficient cells is not the cause for such MNNG resistance. Because the MMR proteins function upstream in the DNA damage response, they must also signal to other pathways, which may include the apoptotic pathway, whose components remain to be identified. Elucidation of components in this pathway will provide insights into mechanisms involved in MNNG resistance in MMR-deficient tumors.

We thank P. Modrich, J. Jiricny, and S. Elledge for reagents and cell lines and P. Yazdi for critical reading of the manuscript. This work was supported by National Institutes of Health Grant CA84199 (to J.Q.). J.Q. is the recipient of Career Development Award DAMD17-00-1-0146 from the Department of Defense Breast Cancer Research Program.

1. Myung, K., Datta, A. & Kolodner, R. D. (2001) *Cell* **104,** 397–408.
2. Lydall, D. & Weinert, T. (1995) *Science* **270,** 1488–1491.
3. Zou, L., Cortez, D. & Elledge, S. J. (2002) *Genes Dev.* **16,** 198–208.
4. Zou, L. & Elledge, S. J. (2003) *Science* **300,** 1542–1548.
5. Friedberg, E. C., Walker, G. C. & Sinclair, D. A. (1995) *DNA Repair and Mutagenesis* (Am. Soc. Microbiol., Washington, DC.).
6. Wood, R. D., Mitchell, M., Sgouros, J. & Lindahl, T. (2001) *Science* **291,** 1284–1289.
7. Modrich, P. (1997) *J. Biol. Chem.* **272,** 24727–24730.
8. Fishel, R., Lescoe, M. K., Rao, M. R., Copeland, N. G., Jenkins, N. A., Garber, J., Kane, M. & Kolodner, R. (1993) *Cell* **75,** 1027–1038.
9. Drummond, J. T., Li, G. M., Longley, M. J. & Modrich, P. (1995) *Science* **268,** 1909–1912.
10. Papadopoulos, N., Nicolaides, N. C., Wei, Y. F., Ruben, S. M., Carter, K. C., Rosen, C. A., Haseltine, W. A., Fleischmann, R. D., Fraser, C. M., Adams, M. D., *et al.* (1994) *Science* **263,** 1625–1629.
11. Duckett, D. R., Drummond, J. T., Murchie, A. I., Reardon, J. T., Sancar, A., Lilley, D. M. & Modrich, P. (1996) *Proc. Natl. Acad. Sci. USA* **93,** 6443–6447.
12. Hickman, M. J. & Samson, L. D. (1999) *Proc. Natl. Acad. Sci. USA* **96,** 10764–10769.
13. Duckett, D. R., Bronstein, S. M., Taya, Y. & Modrich, P. (1999) *Proc. Natl. Acad. Sci. USA* **96,** 12384–12388.
14. Gong, J. G., Costanzo, A., Yang, H. Q., Melino, G., Kaelin, W. G. J., Levrero, M. & Wang, J. Y. (1999) *Nature* **399,** 806–809.
15. Brown, K. D., Rathi, A., Kamath, R., Beardsley, D. I., Zhan, Q., Mannino, J. L. & Baskaran, R. (2003) *Nat. Genet.* **33,** 80–84.
16. Elbashir, S. M., Harborth, J., Lendeckel, W., Yalcin, A., Weber, K. & Tuschl, T. (2001) *Nature* **411,** 494–498.
17. Wang, Y., Cortez, D., Yazdi, P., Neff, N., Elledge, S. J. & Qin, J. (2000) *Genes Dev.* **14,** 927–939.
18. Cortez, D., Guntuku, S., Qin, J. & Elledge, S. J. (2001) *Science* **294,** 1713–1716.
19. Morgan, S. E., Lovly, C., Pandita, T. K., Shiloh, Y. & Kastan, M. B. (1997) *Mol. Cell. Biol.* **17,**2020–2029.
20. Yazdi, P. T., Wang, Y., Zhao, S., Patel, N., Lee, E. Y. & Qin, J. (2002) *Genes Dev.* **16,** 571–582.
21. Kim, S. T., Xu, B. & Kastan, M. B. (2002) *Genes Dev.* **16,** 560–570.
22. Abraham, R. T. (2001) *Genes Dev.* **15,** 2177–2196.
23. Lim, D. S., Kim, S. T., Xu, B., Maser, R. S., Lin, J., Petrini, J. H. & Kastan, M. B. (2000) *Nature* **404,** 613–617.
24. Wu, X., Ranganathan, V., Weisman, D. S., Heine, W. F., Ciccone, D. N., O'Neill, T. B., Crick, K. E., Pierce, K. A., Lane, W. S., Rathbun, G., *et al.* (2000) *Nature* **405,** 477–482.
25. Zhao, S., Weng, Y. C., Yuan, S. S., Lin, Y. T., Hsu, H. C., Lin, S. C., Gerbino, E., Song, M. H., Zdzienicka, M. Z., Gatti, R. A., *et al.* (2000) *Nature* **405,** 473–477.
26. Wang, X., Zou, L., Zheng, H., Wei, Q., Elledge, S. J. & Li, L. (2003) *Genes Dev.* **17,** 965–970.
27. Capasso, H., Palermo, C., Wan, S., Rao, H., John, U. P., O'Connell, M. J. & Walworth, N. C. (2002) *J. Cell Sci.* **115,** 4555–4564.

THE JOURNAL OF BIOLOGICAL CHEMISTRY
Vol. 276, No. 12, Issue of March 23, pp. 8734–8739, 2001
Printed in U.S.A.


# Differential Association of Products of Alternative Transcripts of the Candidate Tumor Suppressor *ING1* with the mSin3/HDAC1 Transcriptional Corepressor Complex*

Received for publication, August 22, 2000, and in revised form, December 4, 2000
Published, JBC Papers in Press, December 15, 2000, DOI 10.1074/jbc.M007664200

**Dorota Skowyra‡§, Marija Zeremski¶, Nickolay Neznanov¶, Muyang Li‖, Yongmun Choi§, Motonari Uesugi§, Creig A. Hauser**, Wei Gu‖, Andrei V. Gudkov¶, and Jun Qin‡§ ‡‡**

*From the ‡Department of Molecular and Cellular Biology, §Verna and Mars McLean Department of Biochemistry and Molecular Biology, Baylor College of Medicine, Houston, Texas 77030, the ¶Department of Molecular Genetics, College of Medicine, University of Illinois, Chicago, Illinois 60607, the ‖Institute of Cancer Genetics and Department of Pathology, College of Physicians & Surgeons, Columbia University, New York, New York 10032, and the **Burnham Institute, La Jolla, California 92037*

**The candidate tumor suppressor *ING1* was identified in a genetic screen aimed at isolation of human genes whose expression is suppressed in cancer cells. It may function as a negative growth regulator in the p53 signal transduction pathway. However, its molecular mechanism is not clear. The *ING1* locus encodes alternative transcripts of $p47^{ING1a}$, $p33^{ING1b}$, and $p24^{ING1c}$. Here we report differential association of protein products of *ING1* with the mSin3 transcriptional corepressor complex. $p33^{ING1b}$ associates with Sin3, SAP30, HDAC1, RbAp48, and other proteins, to form large protein complexes, whereas $p24^{ING1c}$ does not. The ING1 immune complexes are active in deacetylating core histones *in vitro*, and $p33^{ING1b}$ is functionally associated with HDAC1-mediated transcriptional repression in transfected cells. Our data provide basis for a $p33^{ING1b}$-specific molecular mechanism for the function of the *ING1* locus.**

Local acetylation and deacetylation of core histones play an important role in the control of eukaryotic gene expression (1,2). Hyperacetylation of histones increases local accessibility of chromatin templates, enabling subsequent activation or repression of transcription by gene-specific factors, while deacetylation is frequently linked with chromatin condensation and gene silencing. Most histone acetyltransferases and histone deacetylases (HDACs)[1] are enzymes that do not bind DNA directly; instead, they are recruited to chromatin through association with distinct proteins in multiprotein complexes (3). One of the conserved proteins that serve as an organizer for the assembly of histone deacetylases with multiple polypeptides in yeast and mammalian cells is Sin3 (4–7). A biochemically purified mammalian Sin3 complex includes HDAC1 and HDAC2, RbAp48 and RbAp46, SAP30, and SAP18 (6–8). The abundance and relative stability of both Sin3 and HDAC1 proteins have led to the proposal that the "core" Sin3 repressor complexes are pre-assembled and available for recruitment by transient association with gene-specific transcription factors, including Mad, MeCP2, Ikaros, p53, PLZF, nuclear hormone receptors, and yeast Ume6 whose abundance and activities are regulated (3).

The *ING1* (inhibitor of growth 1) gene was recently identified as a candidate tumor suppressor in a genetic screen aimed at isolation of human genes whose expression is suppressed in cancer cells (9). The *ING1* gene was localized to chromosome 13q33–34 (10,11), a region that has been implicated in the progression of various tumors (12). Deregulated expression and mutations of *ING1* gene were found in breast carcinomas (11) and in squamous cell carcinomas (13), respectively. Ectopic expression of the originally isolated *ING1* cDNA or suppression of the *ING1* gene expression by antisense RNA demonstrated that *ING1* is a negative regulator of cell proliferation involved in the p53 growth regulatory pathway (9,14).

It has been subsequently found that the *ING1* gene encodes several differentially initiated and spliced mRNAs, which have common 3′ exon and encode at least two distinct proteins in mouse (15), and possibly three distinct proteins in human cells ($p47^{ING1a}$, $p33^{ING1b}$, and $p24^{ING1c}$) (13,16,17). All the known or anticipated ING1 protein isoforms share an identical C-terminal domain with a conserved PHD finger motif. The PHD finger motif was thought to facilitate DNA binding of proteins otherwise unrelated to ING1 (18), suggesting that ING1 proteins might directly interact with DNA. Significantly, missense mutations were detected within the PHD finger and the nuclear localization motif of ING1 in some head and neck squamous cell carcinomas with allelic loss at the 13q33–34 region, suggesting that the PHD finger and the nuclear function of ING1 is important for its tumor suppressor function (13).

All functional analysis of the biological effects of ectopically expressed ING1 was so far done only with the cDNA encoding $p24^{ING1c}$ due to the lack of information on the alternative forms of ING1. Owing to a cloning error, the cDNA that suppressed cell growth was incorrectly termed $p33^{ING1}$ in the original studies (9,14). One candidate mechanism that was proposed to be responsible for the growth suppressor function of the ING1 locus is cooperation with the p53 tumor suppressor (14). Neither p53 nor ING1 can cause growth inhibition when the other one is suppressed, and the $p24^{ING1c}$ expression has been shown to be required for transcriptional activation of the $p21^{WAF1}$ promoter, a key mechanism of p53-mediated growth control. Recent analysis of mouse *ING1* gene structure and function

* This work was supported by National Institutes of Health Grants CA60730 and CA75179 (to A. V. G.) and CA85533 (to W. G.). The costs of publication of this article were defrayed in part by the payment of page charges. This article must therefore be hereby marked "*advertisement*" in accordance with 18 U.S.C. Section 1734 solely to indicate this fact.

‡‡ To whom correspondence should addressed. Tel.: 713-798-1507; Fax: 713-798-1625; E-mail: jqin@bcm.tmc.edu.

[1] The abbreviations used are: HDAC, histone deacetylase; ING1, inhibitor of growth 1; DBD, DNA binding domain; PAGE, polyacrylamide gel electrophoresis; TSA, trichostatin A; SEAP, secreted alkaline phosphatase; PHD, plant homeodomain.

suggests that the shortest of ING1 protein isoforms, the mouse equivalent of human $p24^{ING1c}$, is required for the activation of p53-responsive genes. In contrast, overexpression of the longer form $p37^{ING1}$, an equivalent of the human $p33^{ING1b}$ protein, interferes with the activation of p53-dependent promoters when p53 is stabilized after DNA damage (15). It appears that isoforms of ING1 protein may have different roles in growth control and that their unique N-terminal sequences may determine differences in their function.

In a search for mechanisms of function of the ING1 protein, we explored ING1 associated proteins in human cells. We found differential association of $p33^{ING1b}$ and $p24^{ING1c}$ with nuclear proteins. $p33^{ING1b}$ resides in a complex of ~1–2 MDa, whereas $p24^{ING1c}$ does not. Among $p33^{ING1b}$-associated proteins are known components of the mSin3 transcriptional corepressor complex, including HDAC1. Consistently, $p33^{ING1b}$ is functionally associated with HDAC-dependent transcriptional repression, in reporter gene expression assays *in vivo*, and in histone deacetylation assays *in vitro*. We demonstrate that the mSin3-mediated HDAC1-dependent transcriptional repression requires the unique N-terminal 99-amino acid sequence characteristic of the $p33^{ING1b}$ protein, therefore defining a new, $p33^{ING1b}$-specific mechanism for the function of the ING1 locus.

## EXPERIMENTAL PROCEDURES

*Antibodies*—Rabbit anti-ING1 antibodies were generated using recombinant His-epitope-tagged human $p33^{ING1b}$ protein prepared from *Escherichia coli*. Goat anti-ING1 antibodies were from Santa Cruz (sc-7566). Mouse monoclonal anti-RbAp48 antibodies were from GeneTex (MS-RBP14-PX1), and rabbit anti-Sin3A antibodies were from Santa Cruz (sc-767). Rabbit anti-HDAC1 and anti-SAP30 antibodies were generous gifts of Dr. Glen Humphrey and Dr. Robert Eisenman, respectively. Anti-FLAG M2-agarose affinity gel was from Sigma (A-1205).

*Purification of the $p33^{ING1b}$ Complexes*—The FLAG epitope-tagged $p33^{ING1b}$ used for mammalian expression were constructed by subcloning the full-length cDNA with the tagged sequence into the pCIN4 vector (19). H1299 cells ($1 \times 10^6$) were transfected by calcium phosphate precipitation on a 10-cm plate essentially as previously described with minor modifications. Five μg of pCIN4-Flag-ING1 expression plasmid with 15 μg of carrier DNA (pGEM-3) were used for transfections on each plate. Thirty hours after transfection, the cells were transferred to the same Dulbecco's modified Eagle's medium containing 1000 μg/ml G418 (Life Technologies, Inc.) for selection. After 2 months' selection, single colonies were picked and expanded for Western blot analysis.

The tagged cells were grown in Dulbecco's modified Eagle's medium with 10% fetal bovine serum and 1000 μg/ml G418, and nuclear extracts were prepared as described previously. Forty milliliters of the nuclear extract prepared from different cell lines was adjusted to 200 mM NaCl and 0.2% Nonidet P-40 by addition of 5 M NaCl and 10% Nonidet P-40, and incubated with 300 μl of M2-agrose beads (Sigma) at 4 °C for 10 h by rotation. After five washes with BC200 with 0.2% Nonidet P-40, proteins were eluted from beads by incubation at 4 °C for 30 min with 300 μl of BC100 with 0.2% Nonidet P-40 plus 0.2 mg/ml FLAG peptide.

Large scale immunoprecipitation for mass spectrometric analysis was carried out with 10 mg of crude or fractionated nuclear extracts and 100 μg of affinity-purified rabbit anti-ING1 antibodies, with an excess of the purified $p33^{ING1b}$ antigen as a negative control. Immune complexes were isolated by binding to 100 μl of Sepharose-Protein A beads, washed five times with 100 volumes of NETN buffer, eluted, and separated by SDS-PAGE.

*Identification of Proteins with Mass Spectrometry*—Protein sequencing using mass spectrometry was carried out as described (20). Tryptic peptides that were recovered from in-gel digested protein bands were analyzed using an electrospray ion trap mass spectrometer (LCQ, Finnigan MAT, San Jose, CA) coupled on-line with a capillary high performance liquid chromatography (Magic 2002, Michrom BioResources, Auburn, CA). Data derived from the mass spectrometry/mass spectrometry spectra were used to search a compiled protein data base that was composed of the protein data base NR and a six-reading frame translated expressed sequence tag data base to identify the protein using the program PROWL, which is publicly available on the World Wide Web.

*Immunoprecipitation and Immunoblotting*—Immunoprecipitations were done by incubating 1 mg of HeLa nuclear protein extracts prepared according to the Dignam method, with 5–10 μg of the appropriate antibodies for 2 h at 4 °C, followed by isolation of the immune complexes on Protein A beads (Amersham Pharmacia Biotech.). Immune complexes were washed three times with 1 ml of NETN buffer (50 mM Tris, pH 7.5, 100 mM NaCl, 1 mM EDTA, 0.5% Nonidet P-40, 0.5 mM dithiothreitol) prior to SDS-PAGE and immunoblotting. Immunoblottings were done after low voltage protein transfer (30 V, 12 h) from polyacrylamide gels to nitrocellulose in Tris-glycine buffer, pH 8.0, with 5% methanol. Membranes were blocked with 5% milk in Tris-buffered saline with Tween 20 buffer (100 mM Tris, pH 8.0, 150 mM NaCl, 0.05% Tween 20), incubated with 1:200–1:1000 dilution of the primary antibodies for 1 h at room temperature, washed, and incubated with 1:25000 dilution of horseradish peroxidase-conjugated secondary antibodies. Antibody detection was with ECL (Amersham Pharmacia Biotech), using horseradish peroxidase-conjugated antibodies from Santa Cruz.

*Histone Deacetylase Assays*—Histone deacetylase activity was measured using acid-soluble histones that were isolated from [$^3$H]acetate-labeled HeLa cells, by a published procedure (21, 22). Immune complexes were incubated for 3 h at 37 °C with 40,000 cpm of $^3$H-labeled histones (~2000 cpm/μg) in a total volume of 200 μl of HD buffer (25 mM Tris, pH 7.5, 100 mM NaCl, 2.5% glycerol). Reactions were stopped by addition of 50 μl of STOP buffer (1 M HCl, 0.16 M acetic acid), extracted with two volumes of ethyl acetate, and the supernatant was counted in a scintillation counter. Assays were carried out with or without 10 mM sodium butyrate, as indicated in the figure legends.

*Transcriptional Repression Assays*—NIH3T3 cells ($1 \times 10^6$) were transfected using LipofectAMINE Plus (Life Technologies, Inc.) with a combination of 1 μg of luciferase reporter plasmids 2Py-Luc or 6AP-Luc and 100 ng of the LacZ reporter construct (pCMV-LacZ) to normalize transfection efficiency. One hundred ng of *ras* expression vector (v-Ha-*ras* cDNA cloned in pLXSN vector under the control of the LTR promoter) and 50 ng of each of the test expression vectors FNE2DBD, pCINE2DBD:En, FN-lINGE2DBD, and FN-sINGE2DBD (shown in Fig. 4*A* as *1*, *2*, *3*, and *4*, respectively) were cotransfected with the reporter plasmids. Cells were harvested for luciferase and β-galactosidase assays 40 h after transfection. The luceferase and β-galactosidase enzyme activities from the extracts of transfected NIH3T3 cells were measured according the Promega protocols.

Polymerase chain reaction-derived DNA fragments encoding either human $p33^{ING1}$ or $p24^{ING1}$ were fused individually to the N terminus of the GAL4 DNA-binding domain (amino acids 1–94). 293T cells ($1 \times 10^6$, in 2.5-cm plate), were transiently cotransfected using GenePORTER (Gene Therapy Systems) with 0.5 μg of appropriate pING1-GAL4 expression vector and 1.5 μg of reporter plasmid. The reporter plasmid carried secreted alkaline phosphatase (SEAP) gene under the control of the constitutively active SV40 early promoter with five Gal4 binding sites. Twenty-four hours after transfection, cells were incubated with 50 ng/ml trichostatin A (TSA), where indicated, and 12 h later cells were harvested and assayed. Expression of the GAL4 fusion proteins was determined by Western blotting with the anti-Gal4 antibody.

## RESULTS

*$p33^{ING1b}$ Associates with Known Components of the mSin3 Corepressor Complex*—To acquire an insight to mechanisms of ING1 function, we sought to isolate ING1-associated proteins in human cells. We fractionated HeLa nuclear extracted on a DEAE column and immunoprecipitated the endogenous ING1 protein from the 0.2 M KCl fraction, which contains most of the cellular $p33^{ING1b}$ protein. We used mass spectrometry to identify RBP1, Sin3, and HDAC1 along others as ING1-associated proteins (Fig. 1*A*.). To facilitate protein purification and to alleviate the interference of the antibody, we created an H1299-derived cell line, which stably expressed a FLAG epitope-tagged $p33^{ING1b}$ (19). The FLAG-$p33^{ING1b}$ was overexpressed by 5–10-fold compared with the endogenous $p33^{ING1b}$ protein by Western. The recombinant FLAG-$p33^{ING1b}$ protein complex was isolated from nuclear extracts prepared from the stable line using affinity chromatography. Colloidal Coomassie Blue staining of a SDS-PAGE gel containing the $p33^{ING1b}$ complex revealed that ~10 polypeptides specifically copurify with the FLAG-$p33^{ING1b}$ on the affinity column (Fig. 1*B*). More bands that were masked by antibody are clearly detected in the

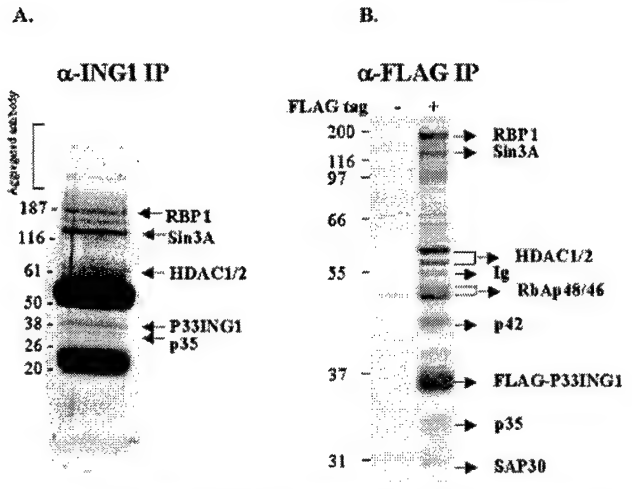


FIG. 1. **Purification and identification of the FLAG-p33$^{ING1b}$ complex.** *A*, the endogenous ING1 complex in HeLa cells was purified by large scale immunoprecipitation (*IP*) from 0.2 M KCl fraction of the DEAE column and resolved on 4–20% gradient SDS-PAGE gel. *B*, the FLAG epitope-tagged p33$^{ING1b}$ was purified from nuclear extracts prepared from H1299 cells that stably expressed the FLAG-p33$^{ING1b}$ protein. As a control, a mock purification was performed from nuclear extracts prepared from the parental H1299 cells. The FLAG-peptide elutes were separated by 10% SDS-PAGE, visualized by staining gels with colloidal Coomassie Blue, and identified by capillary liquid chromatography electrospray ion trap mass spectrometry. p42 and p35 are two novel proteins that are identified from the expressed sequence tag data base.

recombinant complex.

We identified proteins that copurified with p33$^{ING1b}$ in the recombinant p33$^{ING1b}$ complexes using capillary liquid chromatography ion trap mass spectrometry (20). Mass spectrometric analysis of the p33$^{ING1b}$ complexes identified the mSin3 corepressor and the HDAC1/2 histone deacetylases, as well as RbAp48, RbAp46, and SAP30. These proteins are components of a biochemically purified mSin3 complex (6–8). We also identified RBP1 (23) and two novel proteins, p42 and p35, which were not reported as components of the mSin3 complex. RbAp48, RbAp46, SAP30, and p42 were masked by antibody in the endogenous ING1 complex. These data demonstrate that p33$^{ING1b}$ is a component of a Sin3 containing histone deacetylase complex, thus suggesting a role for p33$^{ING1b}$ in transcriptional repression.

We confirmed the association of Sin3 and HDAC1 with p33$^{ING1b}$ by reciprocal immunoblotting of the endogenous p33$^{ING1b}$, HDAC1, and Sin3 immune complexes from HeLa cells (Fig. 2*A*). Although the polyclonal rabbit antibodies that we used in these experiments reacted with both p33$^{ING1b}$ and p24$^{ING1c}$ proteins (Fig. 2*A*, *lane 3*), due to their identical C-terminal end, only p33$^{ING1b}$ was detected in the Sin3 and HDAC1 immune complexes (Fig. 2*A*, *lines 1* and *2*). Pre-incubation of the anti-ING1 antibodies with an excess of purified recombinant His-tagged p33$^{ING1b}$ protein prevented precipitation of the endogenous p33$^{ING1b}$ and p24$^{ING1c}$ as well as Sin3A and HDAC1 (Fig. 2*B*), demonstrating specificity of the observed associations. Approximately the same amounts of Sin3A, the Sin3A-directly associated protein SAP30 (7) and p33$^{ING1b}$ were present in either Sin3A or ING1 immune complexes of the endogenous proteins, suggesting that p33$^{ING1b}$ is a stoichiometric component of the Sin3A/SAP30 complex *in vivo*. Moreover, both p33$^{ING1b}$ and Sin3A immune complexes had similar amounts of histone deacetylase HDAC1 and the histone H4-binding protein RbAp48. Gel filtration analysis of partially purified p33$^{ING1}$ complexes demonstrated that p33$^{ING1b}$,

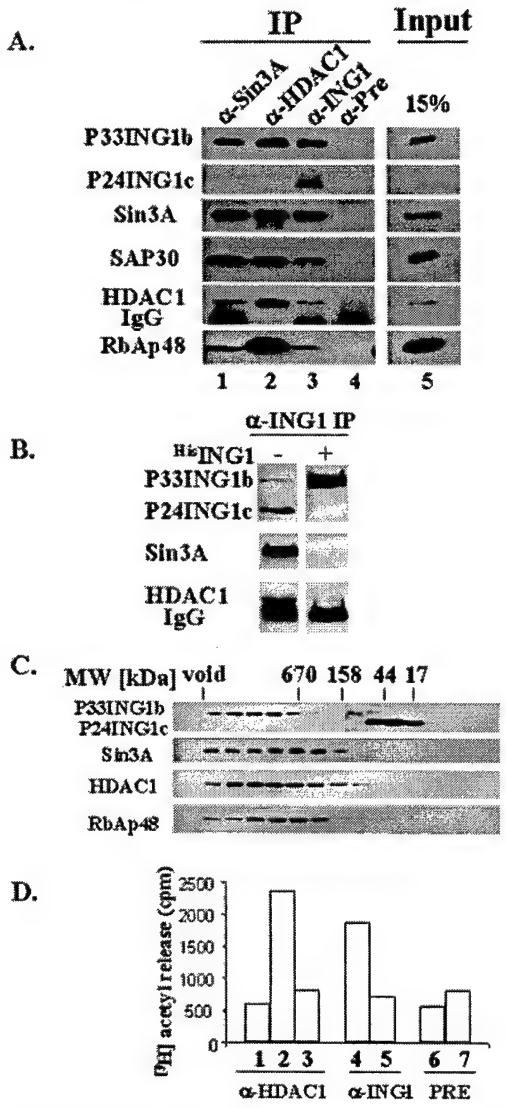


FIG. 2. **Endogenous p33$^{ING1b}$ in HeLa cells associate with Sin3 complexes that contain active HDAC1.** *A*, coimmunoprecipitation of p33$^{ING1b}$ with mSin3 complexes. Immunoprecipitations (*IP*) were performed with 1 mg of HeLa nuclear protein extracts and 2–10 μg of rabbit anti-Sin3A (*lane 1*), rabbit anti-HDAC1 (*lane 2*), rabbit anti-p33$^{ING1b}$ (*lane 3*), or rabbit pre-immune (*lane 4*) antibodies. The amount of individual antibodies was adjusted to obtain approximately the same amount of p33$^{ING1b}$ in all immune complexes. *B*, competition of the purified recombinant His-epitope tagged p33$^{ING1b}$ protein with p33$^{ING1b}$ complexes from HeLa extracts. Immunoprecipitations were done as above, except that the anti-p33$^{ING1b}$ antibodies were pre-incubated with an excess of the purified recombinant His epitope-tagged p33$^{ING1b}$ protein. *C*, coelution of p33$^{ING1b}$ with mSin3 complexes in gel filtration analysis. Partially purified HeLa nuclear protein extracts (0.2 mg, 300 mM KCl elution from CM Sepharose) were separated by gel filtration on Superose 6 PC3.2/30 column, in a buffer with 50 mM Tris, pH 7.5, 200 mM KCl, and 0.5 mM dithiothreitol. Proteins from the gel filtration fractions were precipitated with 10% trichloroacetic acid, separated by SDS-PAGE, and analyzed by immunoblotting, as indicated. *D*, histone deacetylase activity associated with HDAC1 and ING1 immune complexes *in vitro*. HDAC1 immune complexes used in histone deacetylation assays (*bars 1–3*) were identical with those shown in *A* (*lane 2*) and served as a reference. The ING11 immune complexes (*bars 4* and *5*) used in deacetylation assays were isolated with 100 μg of anti-ING1 antibodies, which is 10-fold more than what was used in *A* (*lane 3*), to obtain comparable amounts of HDAC1 to those present in HDAC1 immune complexes. Control reactions were done with 10 μg (*bar 6*) and 100 μg (*bar 7*) of pre-immune rabbit serum, or with HDAC1 (*bar 3*) and ING1 (*bar 5*) immune complexes that were pre-incubated with 10 mM sodium butyrate. *Bar 1* indicates level of nonenzymatic [$^3$H]acetyl release observed in HDAC1 immune complexes incubated at 0 °C.

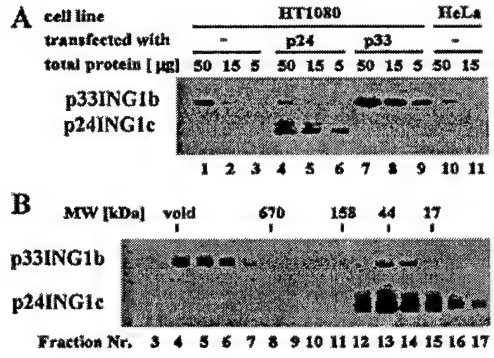


FIG. 3. **Effects of overproduction of $p24^{ING1c}$ on protein complex assembly.** *A*, quantitative Western blotting of ING1 proteins in cell lines. Different amounts of the ING1 proteins were immunoblotted with anti-ING1 antibody from nuclear extracts prepared from parental (*lanes 1–3*), stable HT1080 cells, that overexpress $p24^{ING1c}$ (*lanes 4–6*) and $p33^{ING1b}$ (lanes 7–9) as well as in HeLa cells. *B*, overproduction of $p24^{ING1c}$ does not drive $p24^{ING1c}$ assembly. Nuclear extracts prepared from HT1080 cells that overexpress $p24^{ING1c}$ were analyzed by gel filtration on a Superose 6 column. The ING1 proteins were detected.

Sin3A, HDAC1, and RbAp48 proteins coelute in complexes of an apparent size of 1–2 MDa (Fig. 2*C*), as reported previously for the Sin3 complex (6). It is not clear whether the previously biochemically purified mSin3 complex is a stable subcomplex of this larger $p33^{ING1b}$ complex. It is possible that extensive column fraction may disrupt weaker associations to yield the stable core mSin3 complex.

To establish that $p33^{ING1b}$ associates with functional HDAC1, we prepared the endogenous ING1 immune complexes from HeLa cells, as presented on Fig. 2*A*, and assayed them for histone deacetylase activity. We found that ING1 complexes were active in deacetylating $^3$H-labeled histones *in vitro*, and this activity was comparable with the activity of HDAC1 immune complexes when assays were performed with similar HDAC1 amounts (Fig. 2*D*, *bars 2* and *4*). Addition of 10 mM sodium butyrate, an inhibitor of histone deacetylase activity (24), inhibited the reaction in both HDAC1 and ING1 immune complexes to the level of nonenzymatic [$^3$H]acetyl release (Fig. 2*D*, *bars 3* and *5*, compare with *bar 1*). In contrast, the control immunoprecipitates with various amounts of rabbit preimmune serum alone did not catalyze histone deacetylation (Fig. 2*D*, *bars 6* and *7*). Therefore, $p33^{ING1b}$ associates with enzymatically active HDAC1 complexes, suggesting that $p33^{ING1b}$ may act with Sin3 to mediate transcriptional repression by a mechanism that involves targeted recruitment of histone-modifying activity.

*The Association with Sin3 Complexes Is Specific to the $p33^{ING1b}$ Isoform and Is Defined by Its Unique N-terminal Sequence*—Our analysis of endogenous proteins from HeLa cells suggest that, although we can detect and immunoprecipitate both $p33^{ING1b}$ and $p24^{ING1c}$ isoforms, only $p33^{ING1b}$ associates with Sin3/HDAC1 complexes (Fig. 2). $p24^{ING1c}$ is identical to $p33^{ING1b}$ except for lacking the N-terminal 99 amino acids that are characteristic of the $p33^{ING1b}$ isoform (16), suggesting that the N-terminal fragment of $p33^{ING1b}$ controls its assembly with the Sin3 complex. However, $p24^{ING1c}$ appears to be less abundant than $p33^{ING1b}$ in a variety of cell lines that we tested, and immunodetection of the endogenous $p24^{ING1c}$ in protein extracts was generally poorer or negative (Figs. 2*A*, *lane 5* and 3*A*), unless the extracts were enriched in $p24^{ING1c}$ by partial purification (Fig. 2*C*).

To eliminate the possibility that lower abundance of the $p24^{ING1c}$ protein rather than its different protein structure is responsible for the observed differences in the assembly pattern, we analyzed $p24^{ING1c}$ assembly under the condition of its overexpression, using stably transfected HT1080 fibroblasts (14). Quantitative Western blot analysis of nuclear extracts prepared from the transfected and untransfected HT1080 cells demonstrates that the recombinant $p24^{ING1c}$ was at least as abundant as the endogenous $p33^{ING1b}$ (Fig. 3*A*, compare *lanes 4–6* with *lanes 1–3*). However, overproduction did not force $p24^{ING1c}$ assembly into large protein complexes (Fig. 3*B*). Identical results were also obtained from stably transfected MCF7 cells. Therefore, the association with Sin3 complexes is specific to the $p33^{ING1b}$ isoform and is defined by its unique N-terminal sequence.

*$p33^{ING1b}$ Is Functionally Associated with HDAC1-dependent Transcriptional Repression in Vivo*—We used one reporter system to test whether $p33^{ING1b}$ is functionally associated with transcriptional repression *in vivo*. In this system, the DNA binding domain (DBD) of the transcription factor Ets2 is fused with the mouse $p37^{ING1}$ and $p26^{ING1}$, which are human homologues of $p33^{ING1b}$ and $p24^{ING1c}$, respectively. The structures of expression constructs are shown schematically in Fig. 4*A*. A previously described fusion protein containing Ets2 DBD and the repressor domain of the Engrailed protein of *Drosophila melanogaster* was used as a positive control (*construct 2* in Fig. 4*A*) (25, 26). The reporter plasmid contains the luciferase gene under the control of the minimal promoter of the *ras*-responsive c-*fos* gene and oncogene regulatory elements as described previously (27) (Fig. 4*B*). The reporter (2Py-luc) contains a tandem repeat of a combination of Ets and Ap1 binding sites from the enhancer of polyoma virus. The 6AP-Luc reporter plasmid containing six tandem AP-1 binding sites was used as a control. Both reporters are *ras*-responsive if cotransfected with *ras*-expressing plasmid into NIH 3T3 cells, but 6AP-Luc is insensitive to Ets. Expression plasmids were coexpressed in NIH3T3 cells with activated *ras*, serving as an activator of Ets-directed transcriptional activation of reporter constructs. Protein levels of the chimeric proteins were normalized using a *LacZ* gene reporter. The results of luciferase assays are shown in Fig. 4 (*C* and *D*). The long form of ING1 fused with Ets2 DBD works as a potent repressor similar to the positive control of the Engrailed repressor domain fused to Ets2 DBD (*lanes 5* and *4*). In contrast, the short form of ING1 exhibits a moderate repression (*lane 6*), which is similar to that of the Ets2 DBD alone (*lane 3*). This moderate repression may be due to competition with the endogenous Ets2 protein. Both ING1 fusion proteins and Ets2 DBD are similarly active in gel mobility shift assays with the oligonucleotide corresponding to the Ets2 DNA binding site (data not shown). The repressor effect is specific to Ets2 since none of the plasmids tested show any effect on the control reporter construct (6AP-luc) lacking Ets2-binding sequences (Fig. 4*D*).

We obtained similar results using another reporter system, in which the activity of SEAP was used as a reporter of transcription from a constitutively active SV40 promoter that was cloned next to five Gal4 binding sites. In this system, the chimeric GAL4-$p33^{ING1b}$ fusion protein also mediates transcriptional repression (Fig. 4*E*, compare *lane 3* and *lane 1*). The repression is specific to $p33^{ING1b}$, because the GAL4-$p24^{ING1c}$ fusion protein has little effect on the SV40 promoter. Moreover, treatment of transfected cells with TSA, a specific inhibitor of histone deacetylases, restores the reporter activity, indicating that the transcriptional repression mediated by $p33^{ING1b}$ requires active HDAC. Western blot analysis confirmed that both GAL4-$p33^{ING1b}$ and GAL-$p24^{ING1c}$ fusion proteins were expressed in comparable amounts, regardless of the presence or absence of TSA (Fig. 4*E*). Therefore, tethering $p33^{ING1b}$ to an artificial promoter *in vivo* can confer HDAC-dependent transcriptional repression in reporter gene expression systems.

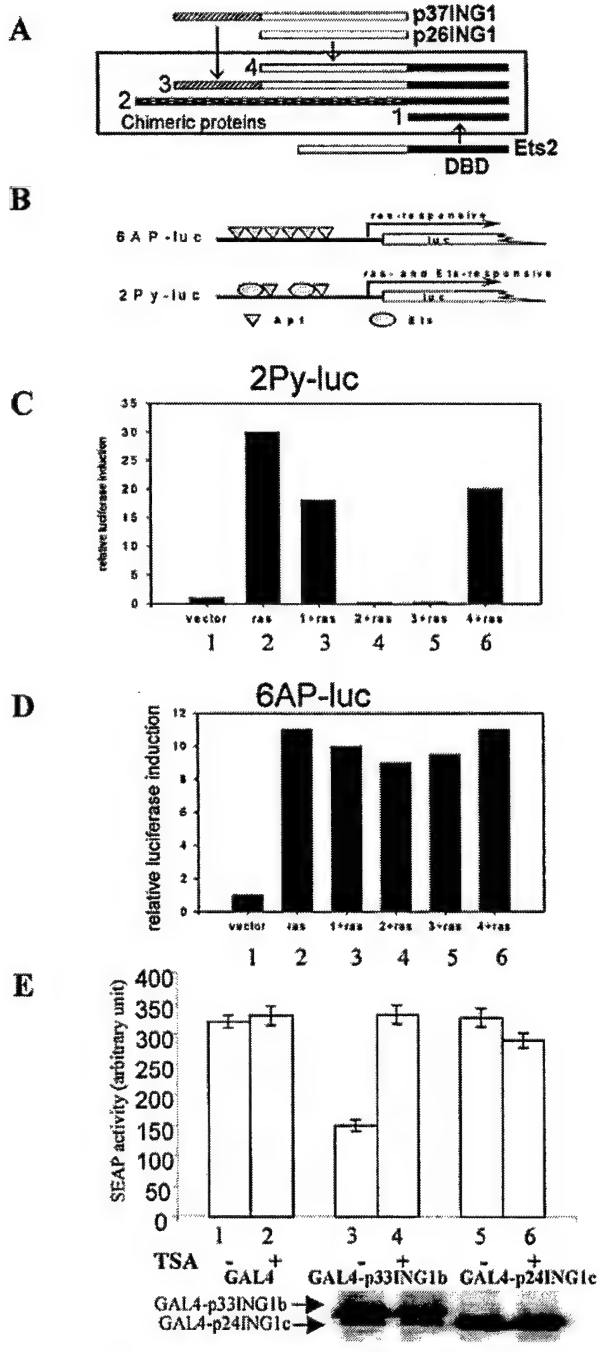


FIG. 4. **$p33^{ING1b}$ is functionally associated with HDAC1-mediated transcriptional repression *in vivo*.** *A*, schematic structures of the expression plasmids of the Ets2 DBD fusion systems. *Construct 1*, DBD of Ets2 alone; *construct 2*, DBD Ets2 fused with the repressor domain of the Engrailed protein of *D. melanogaster* (positive control); *constructs 3* and *4*, DBD Ets2 fused with mouse homologues of human $p33^{ING1b}$ and $p24^{ING1c}$, respectively. *B*, schematic structures of promoter regions of the reporter plasmids. *C* and *D*, transcriptional repression results as measured by the luciferase assays with the indicated systems described in *A* and *B*. The luciferase activity was measured in lysates of NIH 3T3 cells cotransfected with 1 $\mu$g of reporter plasmid, 100 ng of LacZ gene reporter (to normalize transfection efficiency), 100 ng of *ras* expression vector, and 50 ng of one of the test constructs (*1–4*). Three independent experiments yielded similar results. *E*, transcriptional repression assays using the GAL4 fusion system. Plasmids containing the human GAL4-$p33^{ING1b}$ and GAL4-$p24^{ING1b}$ were transiently transfected in 293T cells, and their ability to repress transcription of a SEAP reporter was assayed. The SEAP reporter construct is under the control of the constitutively active SV40 promoter and five Gal4 sites. Treatment of transfected cells with TSA (50 ng/ml) restored the reporter activity. Whole cell lysates from the transfected cells were also analyzed by Western blot with an antibody against the GAL4 DNA-binding domain.

## DISCUSSION

Our finding of differential association of the products of the alternative transcripts of $p33^{ING1b}$ and $p24^{ING1c}$ with the mSin3 transcriptional corepressor complex provides a basis for a molecular mechanism of ING1 function as a growth regulator and a candidate tumor suppressor. It also introduces novel aspects into the understanding of the Sin3/HDAC1-mediated transcriptional repression, by identifying new components that might serve as a link to regulation of growth and cell division.

Our data suggest that $p33^{ING1b}$ is the predominant isoform among ING1 proteins that is associated with the Sin3/HDAC1-mediated transcriptional repression. This is based on the observation that the N-terminal 99 amino acids, which are unique to $p33^{ING1b}$, are required for: 1) the assembly with Sin3/HDAC1 complexes, and 2) the HDAC1-dependent transcriptional corepressor activity in reporter gene assays. $p24^{ING1c}$, which is otherwise identical to $p33^{ING1b}$ except for missing the N-terminal domain, does not seem to interact with the Sin3/HDAC1 complexes even when overproduced. The $p47^{ING1a}$ isoform has a unique N-terminal fragment that is distinct from that of $p33^{ING1b}$. Although in this study we did not rigorously examine the assembly of $p47^{ING1a}$, the putative endogenous $p47^{ING1a}$ protein that we can detect with the affinity purified polyclonal anti-ING1 antibodies does not coelute with the Sin3/HDAC1 complexes in gel filtration experiments. Moreover, $p47^{ING1a}$ cannot be immunoprecipitated by Sin3 and HDAC1 (data not shown). This suggests that $p47^{ING1a}$ may associate with different protein partners, but the nature and roles of the $p47^{ING1a}$ assembly remain to be determined.

The cooperation of ING1 with p53 was the first mechanism that was proposed to account for the growth suppressor function of ING1 (14). Recent analysis of the ING1 isoforms in mouse suggests that the equivalent of the human $p24^{ING1c}$ homologue is required for the activation of p53-dependent promoters. In contrast, the mouse equivalent of the human $p33^{ING1b}$ isoform interferes with the activation of the p53-dependent responses (15). This result is consistent with our finding that $p33^{ING1b}$ functions in transcriptional repression, not activation. Moreover, Sin3-mediated HDAC1 activity was recently indicated in the repression of p53-responsive genes (15). It will be important to test whether $p33^{ING1b}$ plays a role in the negative regulation of the p53-responsive genes in cooperation with Sin3/HDAC1. A model for the function of the ING1 locus can be envisaged from our data and previous studies that the interplay of the ING1 isoforms in collaboration with p53 sets the transcriptional program that determines cell proliferation or arrest. We propose that $p33^{ING1b}$ together with the mSin3 corepressor machinery represses p53-responsive genes that halt cell cycle progression and that $p24^{ING1c}$ serves as an antagonist to relieve this repression. The relative ratio of $p33^{ING1b}$ and $p24^{ING1c}$ thus may determine the proliferate potential of the cell.

Work from a number of laboratories demonstrated that Sin3 serves as scaffold protein for the assembly of multiprotein complexes, which target histone deacetylase activities to selected genes by interacting with specific transcription factors. These complexes facilitate transcriptional repression through a mechanism of induction of local rearrangements of the chromatin structure (3). In contrast to Sin3 and HDAC1, which are relatively stable proteins and do not seem to be cell cycle-

regulated, ING1 is cell cycle-regulated. $p24^{ING1c}$ accumulates in cells that are quiescence or senescence and overexpression of $p24^{ING1c}$ in primary fibroblasts arrests cells in $G_1$ phase of the cell cycle (28). $p33^{ING1b}$ also accumulates in quiescence, but induction of cell division by addition of mitogens leads to rapid decline of the $p33^{ING1b}$ protein.[2] In light of our data presented in this paper, these observations suggest that $p33^{ING1b}$ may serve as a regulatory subunit of the mSin3 complex and together with mSin3 might be involved in repression of some essential cell cycle regulatory genes. The identities of those genes are not known, but our identification of RBP1 as a presumptive subunit of the $p33^{ING1b}$/Sin3 complex suggests that among possible candidates are genes that are regulated by the Rb/E2F pathway through an interaction of RBP1 with Rb. This intriguing possibility agrees with the observation that HDAC1 interacts with the Rb protein and that the HDAC1 activity is required for full transcriptional repression of some of the Rb-regulated genes (29,30). Therefore, our data presented here may also link Sin3/HDAC1 to cell cycle regulation through the association with $p33^{ING1b}$.

*Acknowledgments*—We thank Drs. Glen Humphrey and Robert Eisenman for the generous gift of antibodies. We thank Fannie Huang for establishing the FLAG-$p33^{ING1b}$ stable cell line, Dr. Irina Grigorian for providing the construct of His-epitope-tagged $p33^{ING1b}$ protein, and Dr. Jin Wang for mass spectrometric sequencing. We thank Dr. Jieming Wong for discussion and critical reading of the manuscript.

REFERENCES

1. Struhl, K. (1998) *Genes Dev.* **12,** 599–606
2. Brehm, A., and Kouzarides, T. (1999) *Trends Biochem. Sci.* **24,** 142–145
3. Knoepfler, P. S., and Eisenman, R. N. (1999) *Cell* **99,** 447–450
4. Ayer, D. E., Lawrence, Q. A., and Eisenman, R. N. (1995) *Cell* **80,** 767–776
5. Schreiber-Agus, N., Chin, L., Chen, K., Torres, R., Rao, G., Guida, P., Skoultchi, A. I., and DePinho, R. A. (1995) *Cell* **80,** 777–786
6. Zhang, Y., Iratni, R., Erdjument-Bromage, H., Tempst, P., and Reinberg, D. (1997) *Cell* **89,** 357–364
7. Zhang, Y., Sun, Z. W., Iratni, R., Erdjument-Bromage, H., Tempst, P., Hampsey, M., and Reinberg, D. (1998) *Mol. Cell* **1,** 1021–1031
8. Zhang, Y., Ng, H. H., Erdjument-Bromage, H., Tempst, P., Bird, A., and Reinberg, D. (1999) *Genes Dev.* **13,** 1924–1935
9. Garkavtsev, I., Kazarov, A., Gudkov, A., and Riabowol, K. (1996) *Nat. Genet.* **14,** 415–420
10. Garkavtsev, I., Demetrick, D., and Riabowol, K. (1997) *Cytogenet. Cell Genet.* **76,** 176–178
11. Toyama, T., Iwase, H., Watson, P., Muzik, H., Saettler, E., Magliocco, A., DiFrancesco, L., Forsyth, P., Garkavtsev, I., Kobayashi, S., and Riabowol, K. (1999) *Oncogene* **18,** 5187–5193
12. Maestro, R., Piccinin, S., Doglioni, C., Gasparotto, D., Vukosavljevic, T., Sulfaro, S., Barzan, L., and Boiocchi, M. (1996) *Cancer Res.* **56,** 1146–1150
13. Gunduz, M., Ouchida, M., Fukushima, K., Hanafusa, H., Etani, T., Nishioka, S., Nishizaki, K., and Shimizu, K. (2000) *Cancer Res.* **60,** 3143–3146
14. Garkavtsev, I., Grigorian, I. A., Ossovskaya, V. S., Chernov, M. V., Chumakov, P. M., and Gudkov, A. V. (1998) *Nature* **391,** 295–298
15. Zeremski, M., Hill, J. E., Kwek, S. S., Grigorian, I. A., Gurova, K. V., Garkavtsev, I. V., Diatchenko, L., Koonin, E. V., and Gudkov, A. V. (1999) *J. Biol. Chem.* **274,** 32172–32181
16. Garkavtsev, I. (1999) *Nat. Genet.* **23,** 373
17. Saito, A., Furukawa, T., Fukushige, S., Koyama, S., Hoshi, M., Hayashi, Y., and Horii, A. (2000) *J. Hum. Genet* **45,** 177–181
18. Aasland, R., Gibson, T. J., and Stewart, A. F. (1995) *Trends Biochem. Sci.* **20,** 56–59
19. Gu, W., Malik, S., Ito, M., Yuan, C. X., Fondell, J. D., Zhang, X., Martinez, E., Qin, J., and Roeder, R. G. (1999) *Mol. Cell* **3,** 97–108
20. Ogryzko, V. V., Kotani, T., Zhang, X., Schlitz, R. L., Howard, T., Yang, X. J., Howard, B. H., Qin, J., and Nakatani, Y. (1998) *Cell* **94,** 35–44
21. Ausio, J., and van Holde, K. E. (1986) *Biochemistry* **25,** 1421–1428
22. Carmen, A. A., Rundlett, S. E., and Grunstein, M. (1996) *J. Biol. Chem.* **271,** 15837–15844
23. Fattaey, A. R., Helin, K., Dembski, M. S., Dyson, N., Harlow, E., Vuocolo, G. A., Hanobik, M. G., Haskell, K. M., Oliff, A., and Defeo-Jones, D. (1993) *Oncogene* **8,** 3149–3156
24. Candido, E. P., Reeves, R., and Davie, J. R. (1978) *Cell* **14,** 105–113
25. Li, J., Thurm, H., Chang, H. W., Iacovoni, J. S., and Vogt, P. K. (1997) *Proc. Natl. Acad. Sci. U. S. A.* **94,** 10885–10888
26. Han, K., and Manley, J. L. (1993) *EMBO J.* **12,** 2723–2733
27. Galang, C. K., Der, C. J., and Hauser, C. A. (1994) *Oncogene* **9,** 2913–2921
28. Garkavtsev, I., and Riabowol, K. (1997) *Mol. Cell. Biol.* **17,** 2014–2019
29. Luo, R. X., Postigo, A. A., and Dean, D. C. (1998) *Cell* **92,** 463–473
30. Magnaghi-Jaulin, L., Groisman, R., Naguibneva, I., Robin, P., Lorain, S., Le Villain, J. P., Troalen, F., Trouche, D., and Harel-Bellan, A. (1998) *Nature* **391,** 601–605

[2] K. V. Gurova and A. V. Gudkov, unpublished data.

THE JOURNAL OF BIOLOGICAL CHEMISTRY
Vol. 279, No. 10, Issue of March 5, pp. 9539–9546, 2004
Printed in U.S.A.


# Components of a Pathway Maintaining Histone Modification and Heterochromatin Protein 1 Binding at the Pericentric Heterochromatin in Mammalian Cells*

Received for publication, October 22, 2003, and in revised form, November 19, 2003
Published, JBC Papers in Press, December 9, 2003, DOI 10.1074/jbc.M311587200

**Huawei Xin‡§¶, Ho-Guen Yoon§, Prim B. Singh‖, Jiemin Wong§, and Jun Qin‡§****

*From the ‡Verna and Marrs McLean Department of Biochemistry and Molecular Biology and §Department of Molecular and Cellular Biology, Baylor College of Medicine, Houston, Texas 77030 and ‖Nuclear Reprogramming Laboratory, Division of Gene Expression and Development, The Roslin Institute (Edinburgh), Midlothian, EH25 9PS, United Kingdom*

**Heterochromatin is a higher order chromatin structure that is important for transcriptional silencing, chromosome segregation, and genome stability. The establishment and maintenance of heterochromatin is regulated not only by genetic elements but also by epigenetic elements that include histone tail modification (*e.g.* acetylation and methylation) and DNA methylation. Here we show that the p33ING1-Sin3-HDAC complex as well as DNA methyltransferase 1 (DNMT1) and DNMT1-associated protein 1 (DMAP1) are components of a pathway required for maintaining proper histone modification and heterochromatin protein 1 binding at the pericentric heterochromatin. p33ING1 and DMAP1 interact physically and co-localize to heterochromatin in the late S phase, and both are required for heterochromatin protein 1 binding to heterochromatin. Although the p33ING1-Sin3-HDAC and DMAP1-DNMT1 complexes are recruited independently to pericentric heterochromatin regions, they are both required for deacetylation of histones and methylation of histone H3 at lysine 9. These data support a cooperative model for histone deacetylation, methylation, and DNA methylation in maintaining pericentric heterochromatin structure throughout cell divisions.**

Heterochromatin is that portion of the genome that generally remains condensed throughout the cell cycle and replicates late in the S phase because of its unique, higher order chromatin structure. Heterochromatic DNA is predominantly present in the centromeric and telomeric regions of the chromosome that are composed of repetitive DNA sequence elements. In general, heterochromatic DNA sequences are heavily methylated on cytosine of the CpG dinucleotides. It is suggested that the chief DNA methyltransferase DNMT1[1] is important for the maintenance of DNA methylation in mammalian cells (1, 2). In addition to methylated DNA, histones are found to be hypoacetylated and hypermethylated at heterochromatin. These distinct covalent modifications are thought to be important for heterochromatin structure and function and are faithfully transmitted to daughter cells during cell division (3).

Among the enzymes that modify histone tails, the histone methyltransferase Suv39h was found to be specifically required for maintaining pericentric heterochromatin structure and genome stability (4). Methylation of histone H3K9 creates binding sites for heterochromatin protein 1 (HP1) (5, 6), a marker of heterochromatin that is thought to reinforce the structure of heterochromatin. Loss of Suv39h leads to delocalization of HP1 from the pericentric heterochromatin (4). On the other hand, prolonged treatment of cells with trichostatin A, a general histone deacetylase (HDAC) inhibitor, also disrupts the normal localization pattern of HP1 (7), suggesting that the localization of HP1 to heterochromatin also requires histone deacetylase activity to maintain histone hypoacetylation at pericentric heterochromatin. It remains unknown, however, which of the many HDAC complexes in the cell is responsible for such an effect.

DNMT1 may provide a functional link between DNA methylation and histone deacetylation because DNMT1 was reported to interact and co-localize with HDAC2 at replication foci in the late S phase when heterochromatin was replicated (8). However, it remains unknown how HDAC2 is targeted to DNMT1 and the late replication foci, whereas DNMT1 and DNMT1-associated protein 1 (DMAP1) interact and co-localize to DNA replication foci throughout the S phase. This discrepancy raises the possibility that other factors may be involved in targeting HDAC activity specifically to heterochromatin during heterochromatin duplication in the late S phase.

In this paper we report the components of a pathway that maintain histone modification for HP1 binding. We find that the candidate tumor suppressor p33 inhibitor of growth family 1 (ING1) complex, which includes the core Sin3-HDAC1/2 complex, physically and functionally interacts with the DNMT1-DMAP1 complex to maintain histone hypoacetylation and methylation of histone H3 of K9 at pericentric heterochromatin during cell division in human cells.

## EXPERIMENTAL PROCEDURES

*Cell Culture, Antibodies, Plasmids, and Transfections*—293T and HeLa cells were cultured in Dulbecco's modified Eagle's medium with 10% fetal bovine serum. The stable HeLa cell line expressing FLAG-DMAP1 was cultured in medium supplemented with 1 μg/ml puromycin. The M2 anti-FLAG antibody was from Sigma. Anti-acetyl-histone H3, H4, and anti-dimethyl-histone H3K9 antibodies were from Upstate Cell Signaling Solutions. Anti-trimethyl-histone H3K9 antibody was described previously (9). The DNMT1 monoclonal antibody was from

* The costs of publication of this article were defrayed in part by the payment of page charges. This article must therefore be hereby marked "*advertisement*" in accordance with 18 U.S.C. Section 1734 solely to indicate this fact.

¶ Postdoctoral Fellow of the U. S. Department of Defense Breast Cancer Research Program (DAMD17-01-1-0148).

** Supported in part by a Career Development Award from the U. S. Department of Defense Breast Cancer Research Program (DAMD17-00-1-0146). To whom correspondence and requests for reagents should be addressed. Tel.: 713-798-1507; Fax: 713-798-1625; E-mail: jqin@bcm.tmc.edu.

[1] The abbreviations used are: DNMT1, DNA methyltransferase 1; HP1, heterochromatin protein 1; HDAC, histone deacetylase; DMAP1, DNMT1-associated protein 1; ING1, inhibitor of growth family 1; GST, glutathione *S*-transferase; siGFP, small interfering green fluorescence protein; siRNA, small interfering RNA.

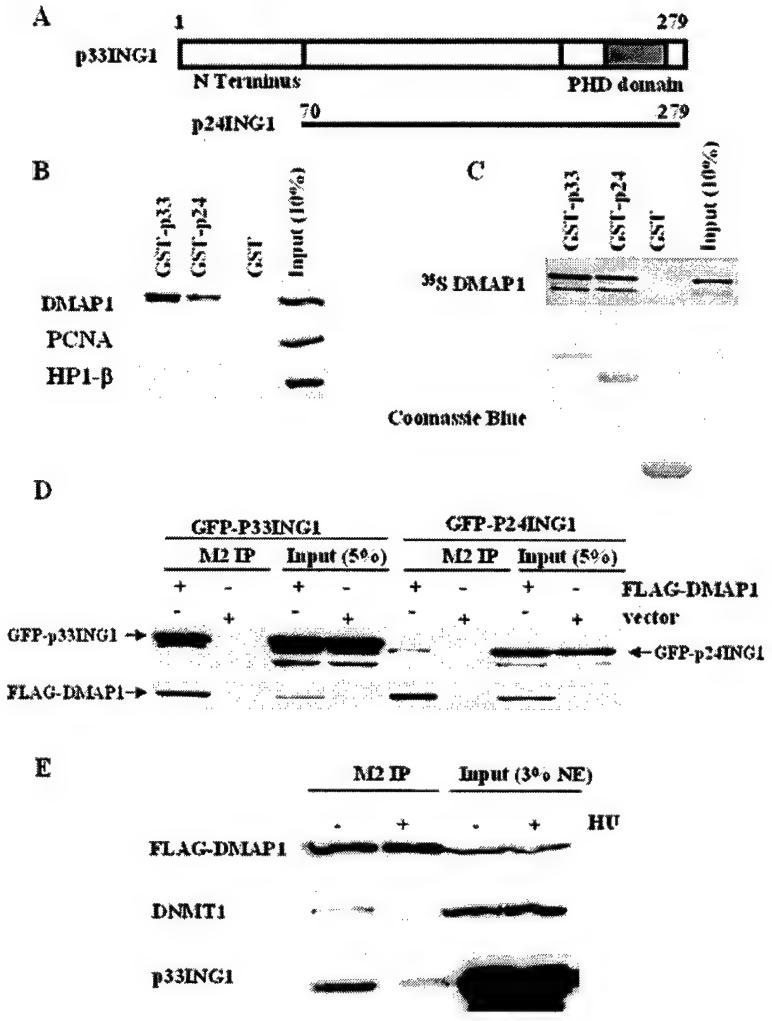


FIG. 1. **Interaction of ING1 with DMAP1.** *A*, the schematic shows ING1 domains and the p24ING1 isoform. *B*, a GST pull-down is shown of DMAP1 by recombinant GST-p33ING1 and GST-p24ING1 from nuclear extract (*NE*) prepared from a stable HeLa cell line that expresses FLAG-DMAP1. The *lower band* of the doublet is the endogenous DMAP1. *C*, a GST pull-down of DMAP1 translated *in vitro* by various GST-ING1 proteins is shown. *D*, a co-immunoprecipitate of overexpressed ING1 and DMAP1 is shown. Plasmids encoding GFP-p33ING1 or GFP-p24ING1 together with FLAG-DMAP1 were co-transfected in 293T cells. The cell lysates were used to immunoprecipitate FLAG-DMAP1 protein by the M2 anti-FLAG antibody. Co-immunoprecipitated GFP-ING1 proteins were detected by Western blotting using ING1 C terminus antibody. *E*, a co-immunoprecipitation of endogenous p33ING1 and FLAG-DMAP1 from cycling HeLa cells is shown. FLAG-DMAP1 was immunoprecipitated from cycling and 1 mM hydroxyurea (*HU*)-treated cells, respectively, and co-immunoprecipitated DNMT1 and ING1 were detected by Western blotting. PCNA, proliferating cell nuclear antigen; *IP*, immunoprecipitate.

Imgenex. Anti-Sin3 and proliferation cell nuclear antigen antibodies were from Santa Cruz Biotechnology. Anti-HP1α and anti-HP1β antibodies were from Chemicon International. The M31 anti-HP1β rat antibody was from Serotec. Rabbit ING1 and DMAP1 antibodies were raised against bacterially produced His-ING1 and GST-DMAP1 (Bethyl Laboratories) and affinity-purified.

ING1 and DMAP1 were cloned into pET or pGEX4T-1 vectors and were expressed as $His_6$ or GST fusion proteins in *E. coli* BL21 (DE3). For transient transfection in 293T cells, ING1 was cloned into a pEGFP-C2 vector (Clontech Laboratories), and FLAG-DMAP1 was cloned into a pcDNA3 vector (Invitrogen).

Transient transfection of GFP-ING1 and FLAG-DMAP1 in 293T cells was carried out with LipofectAMINE (Invitrogen). Cells were harvested 48 h after transfection. To establish the FLAG-DMAP1-stable cell line, FLAG-DMAP1 was cloned into a pBabe vector and then transfected into PT67 cells for a retrovirus particle package. The virus-containing medium was used for HeLa cell transduction.

*In Vitro Pull-down Assay, Immunoprecipitation, Mass Spectrometry, and Cell Cycle Synchronization*—An *in vitro* pull-down assay was performed using Sepharose-immobilized $His_6$-ING1 or GST-ING1 to pull down interacting proteins from HeLa nuclear extract, or DMAP1 translated *in vitro* (TNT, Promega). Immunoprecipitation, Western blotting, protein identification with mass spectrometry, and immunostaining were described previously (10). For cell cycle synchronization, cells were first blocked in mitosis using 100 ng/ml nocodazole for 12 h. Mitotic cells were collected by mitotic shake-off, washed twice with phosphate-buffered saline, and cultured in medium containing 80 μg/ml mimosine to block cells at the $G_1$/S boundary. Twelve hours later, cells were released into fresh medium to allow entry into the S phase, and cells were collected at different times.

*RNA Interference*—The siRNA duplexes were synthesized by Dharmacon Research and prepared by annealing two 21-ribonucleotide oligonucleotides according to the manufacturer's suggestions. The sequences targeting each gene were *ING1*, 5′-AAGGAGCUAGACGAGUGCUAC-3′; *Sin3*, 5′-AAGCAGUGUCUGAGACCAUGC-3′; *DMAP1*, 5′-AAGUCUAUGCCUUGCUCUACU-3′; and *DNMT1*, 5′-AACGGUGCUCAUGCUUACAAC-3′. siGFP and siVimentin were purchased from Dharmacon Research and used as controls. HeLa cells were transfected with siRNA duplex using Oligofectamine (Invitrogen) according to the manufacturer's protocols. All experiments described in this paper were carried out on cells 3 or 4 days after siRNA transfections.

*Chromatin Immunoprecipitation Assays*—Chromatin immunoprecipitation assays were performed as described (11). PCR primer sequences used for amplification of specific chromosome regions were chromosome 4 centromere 5′ primer, CTGTCCATAAAATATCGAAATACCCTA, and 3′ primer, GTACAGTATATAAATACATAATTTGGGC; a human X chromosome α-satellite DNA 5′ primer, CCGCAAGGGATATTTGGACCTCTTTG, and 3′ primer, GCCACTTGCACATTGTAGAAAAAGTG; an MTA2 gene promoter region 5′ primer, CCGGGCAGCCCCAGCCTAGGCCTTGACTCC, and 3′ primer, TCCGTCGCAGCTCGGCCCCACCCCTTTTC; and a deiodinase (*D3*) promoter region 5′ primer, ACCTTCATTCAGCTCCGCCCAGTGTTG, and 3′ primer, CCACGACCACATGCACAGCCACCTC.

## RESULTS AND DISCUSSION

*p33ING1 Interacts and Co-localizes with DMAP1 in the Late S Phase at Heterochromatin*—Recent studies have shown that the human candidate tumor suppressor p33ING1 resides in an HDAC complex that includes Sin3-HDAC1/2 (12, 13). In a search for p33ING1-binding proteins, we carried out a $His_6$-p33ING1 pull-down assay in HeLa nuclear extract followed by mass spectrometric identification. We found DMAP1 as a

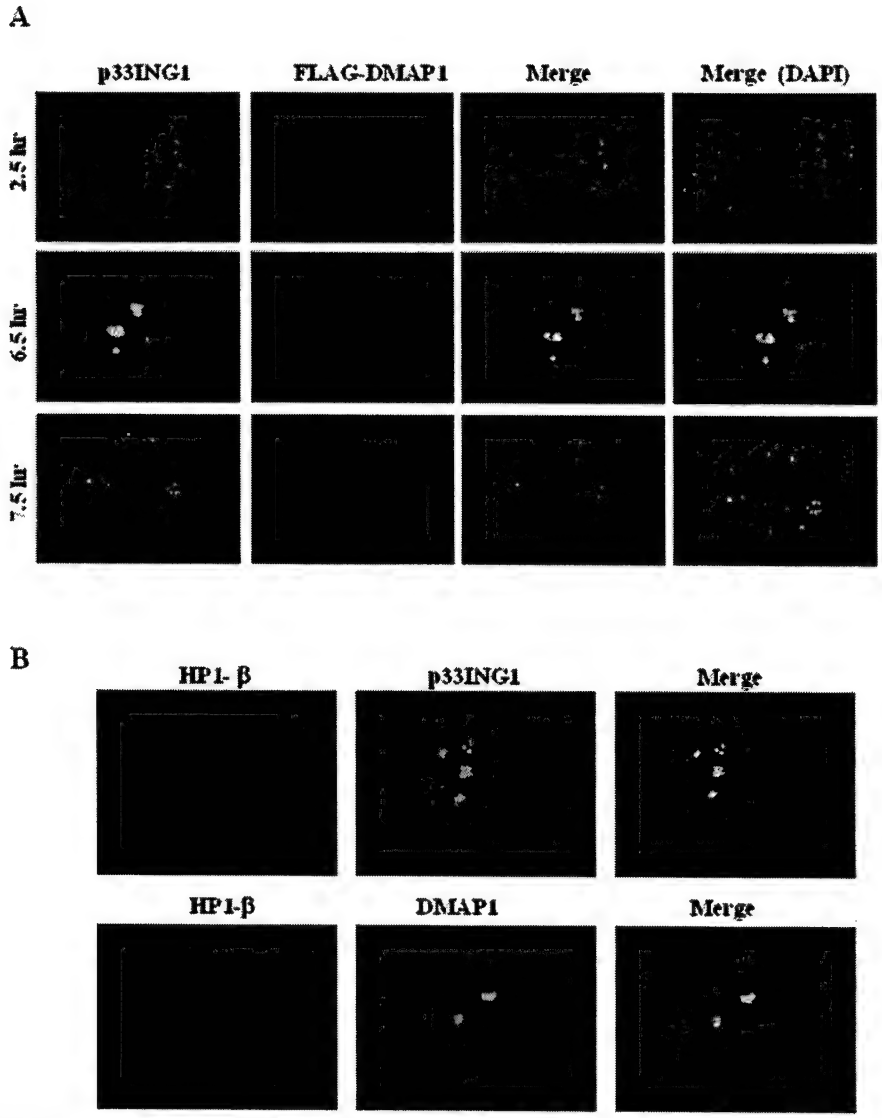


FIG. 2. **Cell cycle-regulated localization of ING1 and DMAP1 to heterochromatin.** *A*, co-localization of ING1 and DMAP1 was regulated by the cell cycle. HeLa cells that stably express FLAG-DMAP1 were synchronized by a double block procedure. At different times after release, cells were fixed with cold methanol/acetone (90:10 in volume) and double immunostained with a mouse M2 antibody (*red*) and a rabbit anti-ING1 N terminus antibody (*green*) as described previously (10). DNA was stained with 4′,6′-diamidino-2-phenylindole (*DAPI*) (*blue*). *B*, ING1 and DMAP1 co-localize with HP1$\beta$ in the late S phase. Co-immunostaining is shown of ING1 or DMAP1 with HP1$\beta$ in the late S phase cells 6.5 h after release from the double block procedure.

p33ING1-interacting protein (data not shown). The specific binding of DMAP1 to ING1 (both p33 and p24ING1 isoforms, Fig. 1*A*) in HeLa nuclear extract was verified by a GST pull-down assay and by Western blotting (Fig. 1*B*), whereas proliferation cell nuclear antigen and HP1$\beta$ as controls cannot bind p33ING1 or p24ING1. *In vitro*-translated DMAP1 also binds to ING1 (Fig. 1*C*), and the conserved plant homeodomain is not required for binding (data not shown). In addition, DMAP1 can interact with ING1 within cells. When GFP-p33ING1 or p24ING1 and FLAG-DMAP1 are co-transfected into 293T cells, immunoprecipitation of DMAP1 by the FLAG antibody (M2) co-precipitates GFP-p33ING1 and GFP-p24ING1 but to a lesser extent (Fig. 1*D*). Furthermore, a small percentage of endogenous p33ING1 can also be co-immunoprecipitated with FLAG-DMAP1 from a cycling stable HeLa cell line that expresses FLAG-DMAP1 at a similar level to endogenous DMAP1. Importantly, the amount of co-immunoprecipitated p33ING1 is diminished when cells are blocked at the $G_1$/S boundary using hydroxyurea. Similarly, DNMT1 is co-immunoprecipitated with DMAP1 from cycling cells but not from hydroxyurea-treated cells (Fig. 1*E*), in agreement with the observation that DNMT1 and DMAP1 interact throughout the S phase. These results show that DMAP1 and p33ING1 physically interact, and their interaction may be cell cycle-regulated (see below).

Because DNMT1 associates with DMAP1 at replication foci throughout the S phase but associates only with HDAC2 in the late S phase (8), our finding that DMAP1 physically interacts with p33ING1 raises the possibility that DMAP1 may bring p33ING1-Sin3-HDAC1/2 to DNMT1 in the late S phase. We examined p33ING1 and DMAP1 localization during the cell cycle by indirect immunostaining. To facilitate this analysis, we used the stable HeLa cell line that expresses FLAG-DMAP1 at a level similar to the endogenous DMAP1 (see Fig. 1*B*). We synchronized HeLa cells by a double block procedure in which nocodazole-arrested mitotic cells enriched by mitotic shake-off were blocked in mimosine and then released into drug-free medium. Cells were fixed and immunostained at different

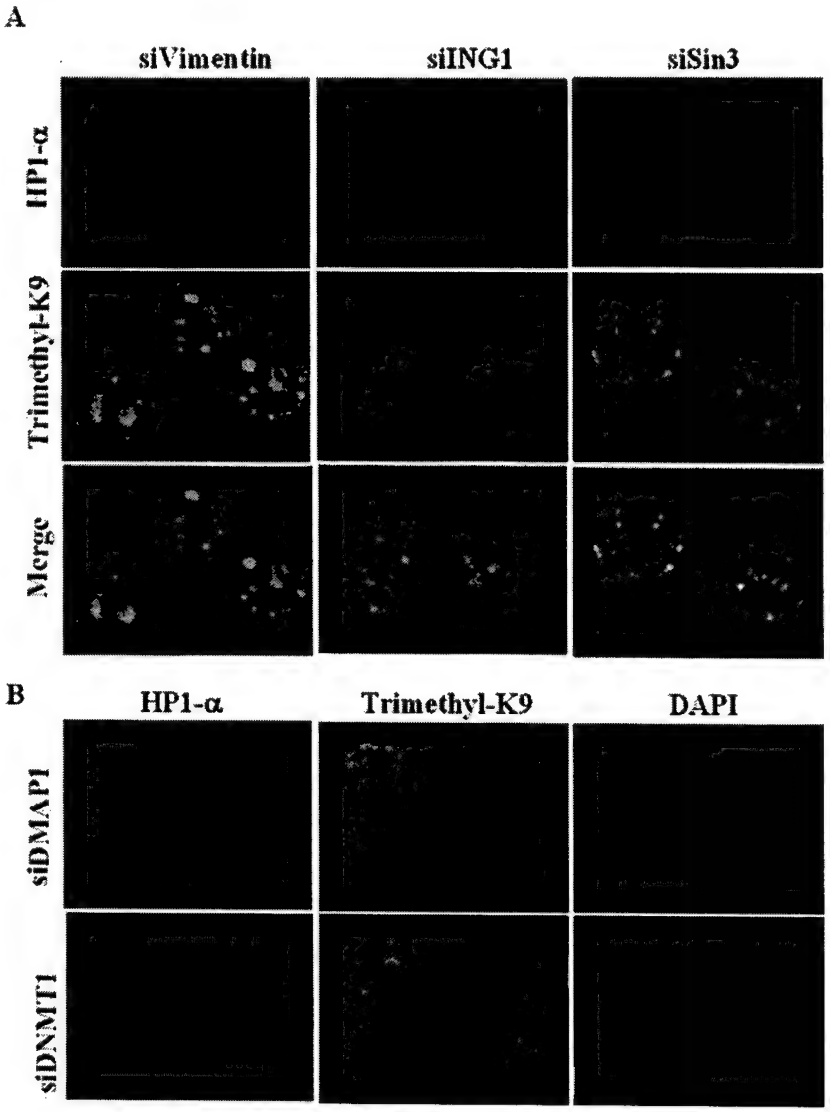


FIG. 3. **The requirement of the p33ING1-Sin3 complex and the DNMT1-DMAP1 complex for binding of HP1 and trimethyl-H3K9 to heterochromatin.** *A*, HP1$\alpha$ and trimethyl-H3K9 were immunostained in cells transfected with siVimentin, siING1, or siSin3. *B*, HP1$\alpha$ and trimethyl-H3K9 were immunostained in cells transfected with siDMAP1 or siDNMT1. *C*, HP1$\alpha$ and $\beta$ were immunostained in cells transfected with siVimentin, siING1, or siDMAP1. *D*, p33ING1, DMAP1, Sin3, or DNMT1 proteins were depleted by RNAi. *DAPI*, 4′,6′-diamidino-2-phenylindole.

times after release from mimosine using a mouse anti-FLAG antibody and a rabbit anti-p33ING1 N terminus antibody. Cell cycle progression was monitored by flow cytometry (data not shown). As shown in Fig. 2*A*, both FLAG-DMAP1 and p33ING1 were stained in a speckle pattern during early S phase (2.5 h after mimosine release), but they do not co-localize. Starting in mid S phase (4.5–5.5 h), the two proteins appear to begin forming bright foci and partially co-localize (data not shown). When cells enter late S phase (6.5 h), they form large foci and co-localize to the highest extent. The large DMAP1 and ING1 foci disappear when cells exit the S phase (7.5 h) and resume the speckled pattern in the $G_2$ phase. These results indicate that p33ING1 and DMAP1 interaction is regulated and confined to the late S phase.

Because heterochromatin is replicated in the late S phase, we examined whether DMAP1 or p33ING1 co-localizes with a heterochromatin maker, HP1$\beta$, in the late S phase cells. HP1$\beta$ shows distinct, large foci and co-localizes with DMAP1 or p33ING1 foci in the late S phase, *i.e.* 6.5 h after release (Fig. 2*B*). This observation supports the idea that DMAP1 and p33ING1 are recruited to the heterochromatin region during the late S phase and suggests that the two proteins and possibly their interaction may be involved in heterochromatin duplication.

*p33ING1-Sin3 and DNMT1-DMAP1 Complexes Are Required for Heterochromatin Protein 1 to Form Foci and for Trimethyl-H3K9 to Concentrate on Heterochromatin*—As hyperacetylated histones are deposited onto the newly synthesized DNA during DNA replication, these histones must be deacetylated to form heterochromatin (14). Our finding that p33ING1 localizes to heterochromatin during the late S phase raises the possibility that the p33ING1-Sin3-HDAC1/2 complex may be responsible for histone deacetylation in heterochromatin, and loss of p33ING1 (and the Sin3 complex) may lead to incomplete deacetylation of histones and eventually affect proper heterochromatin formation. To test this possibility, we used small RNA interference to silence ING1 and Sin3 and examined the effect of siRNA on the organization of heterochromatin by analyzing localization of two heterochromatin markers, HP1$\alpha$ and trimethylated histone H3 at K9. Recent work on heterochromatin histone modifications found that the trimethylated H3K9 may also be used as a heterochromatin marker in immunofluorescence (9, 15).

HP1$\alpha$ and trimethyl-K9 form distinct, large and small foci and co-localize in siVimentin-transfected control cells (Fig. 3*A*). These large foci may correspond to the pericentric heterochromatin region. In contrast, these large foci are significantly disrupted, and HP1$\alpha$ and trimethyl-K9 are uniformly distributed throughout the nucleus with some small foci remaining in

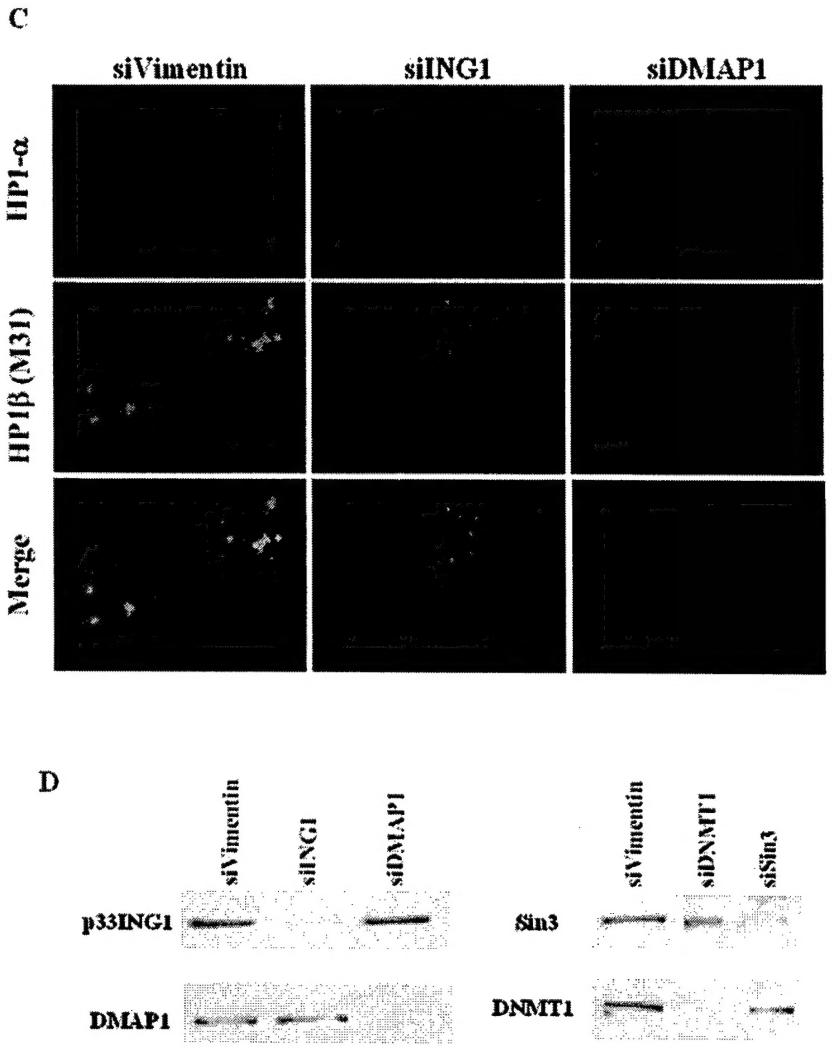


FIG. 3—*continued*

siING1- and siSin3-transfected cells, a pattern similar to that seen in trichostatin A-treated cells (7). These results demonstrate that the p33ING1-Sin3 complex is required for the localization of HP1$\alpha$ and for the concentration of trimethyl-H3K9 to the heterochromatin region. This is consistent with a recent study showing that an mSin3-associated protein, mSds3, is essential for pericentric heterochromatin formation in a mouse knock-out model (16). The human SDS3 protein is an integral component of the p33ING1-Sin3 complex.[2]

The interaction and co-localization of DMAP1 and p33ING1 to heterochromatin during the late S phase (Figs. 1 and 2) suggest that they may function in a pathway maintaining the heterochromatin structure. Indeed, transfection of HeLa cells with siDMAP1 leads to delocalization of HP1$\alpha$ and trimethyl-H3K9 foci (Fig. 3*B*). Therefore, DMAP1 is also required for HP1$\alpha$ and trimethyl-H3K9 association with heterochromatin. Given the previous observation that recruitment of DMAP1 to replication foci throughout the S phase requires DNMT1 (8), we next tested the role of DNMT1 in localizing HP1$\alpha$ and trimethyl-H3K9 to heterochromatin. A similar effect was observed when DNMT1 was down-regulated (Fig. 3*B*). Therefore, the DNMT1-DMAP1 complex also functions in the pathway of maintaining heterochromatin structure.

To corroborate the above results, we examined HP1$\beta$, another heterochromatin marker. To co-stain HP1$\alpha$ and -$\beta$, we used mouse anti-HP1$\alpha$ and rat anti-HP1$\beta$ (M31) antibodies for immunostaining. As shown in Fig. 3*C*, HP1$\alpha$ and -$\beta$ form similar foci, and more importantly, they co-localize to a large degree in siVimentin-transfected control cells. Similarly to HP1$\alpha$, the large HP1$\beta$ foci are also significantly disrupted, and HP1$\beta$ stains uniformly throughout the nucleus with some small foci remaining when cells are transfected with siING1 or siDMAP1. As shown in Fig. 3*D*, the protein levels of ING1, DMAP1, Sin3, and DNMT1 are significantly reduced by siRNA transfection. Collectively, these results demonstrate that the loss of these proteins in the cell has a dramatically adverse effect on the localization of heterochromatin markers to heterochromatin.

*Both p33ING1-Sin3 and DMAP1-DNMT1 Complexes Are Required to Maintain Histone Deacetylation and H3K9 Methylation at the Pericentric Heterochromatin*—We first investigated the global changes in histone acetylation and methylation using total extracted histones from siING1- and siDMAP1-transfected cells. As shown in Fig. 4*A*, neither acetylation nor H3K9 methylation of bulk histones is significantly affected by the loss of ING1 or DMAP1 (Fig. 3*D*), suggesting that they may have only a restricted effect on histone modification of specific chromosome regions, such as the pericentric heterochromatin. Chromatin-associated HP1$\beta$ is somewhat decreased in the absence of ING1 or DMAP1, but the total HP1$\beta$ level in whole cell

[2] J. Qin, M. Li, and W. Gu, unpublished data.

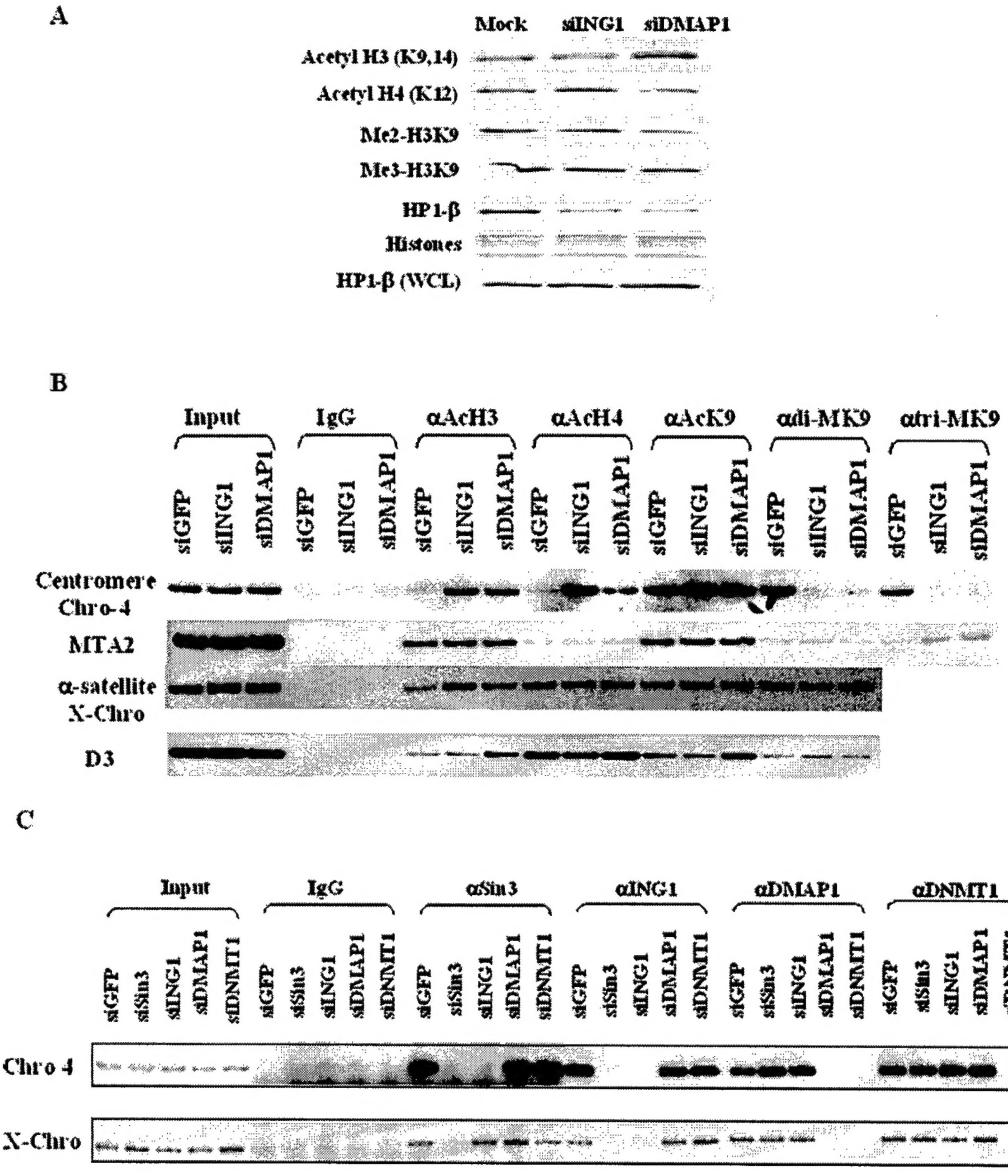


FIG. 4. **Regulation of histone acetylation and methylation by and recruitment of the p33ING1-Sin3 and DNMT1-DMAP1 complexes at pericentric heterochromatin.** *A*, the knockdown of ING1 or DMAP1 does not grossly change histone acetylation and methylation. Total histones and chromatin-associated proteins from mock-, siING1-, and siDMAP1-transfected cells were resolved on SDS-PAGE, and the status of histone acetylation and methylation was measured with acetylation- and methylation-specific antibodies by Western blotting. Note the decreased association of HP1$\beta$ on chromatin in siING1- and siDMAP1-transfected cells, but the HP1$\beta$ total protein level does not change. *B*, increased histone acetylation and diminished histone methylation at pericentric heterochromatin in siING1- and siDMAP1-transfected cells are shown. DNA immunoprecipitated by various antibodies (specific for all acetylated histone H3, all acetylated H4, acetylated H3K9, dimethylated H3K9, and trimethylated H3K9) in the chromatin immunoprecipitation experiments was amplified by specific primers for the chromosome 4 centromere region, a promoter of the *MTA2* gene, the $\alpha$-satellite of the X chromosome, and a promoter of the *D3* gene. *C*, independent recruitment is shown of the p33ING1-Sin3 complex and the DNMT1-DMAP1 complex to the pericentric heterochromatin. Chromatin immunoprecipitation analysis shows associations of Sin3, ING1, DMAP1, and DNMT1 with pericentric heterochromatin in mock, and various siRNA transfected cells. *WCL*, whole cell lysate; *IgG*, immunoglobulin G; *Chro-4*, chromosome 4; *X-Chro*, X chromosome.

lysate does not change. This is consistent with the dynamic nature of HP1 binding to heterochromatin (9, 17, 18). The loss of ING1 or DMAP1 impinges on the integrity of heterochromatin, which in turn is likely to change the dynamics of HP1 binding.

Next we made use of chromatin immunoprecipitation assays to directly examine the role of p33ING1-Sin3 and DMAP1-DNMT1 in regulating histone acetylation and methylation in pericentric heterochromatin (11). For this purpose, specific pairs of PCR primers were designed to allow the amplification of the chromosome 4 centromeric regions and X chromosome-linked $\alpha$-satellite repetitive DNA (19). These two types of centromeric DNA are found in the pericentric heterochromatin territories of chromosome 4 and X, respectively. The *MTA2* and *D3* genes were chosen as control euchromatin loci. As shown in Fig. 4*B*, a knockdown of ING1 or DMAP1 results in elevated levels of acetylated H3 and H4, diminished dimethylated and trimethylated H3K9, and a concomitant increase in acetylated H3K9 in the chromosome 4 centromeric region. Similar results were obtained when the chromosome 10 centromeric region was analyzed (data not shown). In contrast, the knockdown of ING1 and DMAP1 has no significant effect on the acetylation or methylation patterns over the euchromatic *MTA2* and *D3* gene promoter regions. On the other hand, the effect on the X

chromosome-linked α-satellite region is less dramatic with little effect on both acetylation and methylation, which is consistent with the observation that facultative heterochromatinization of the X chromosome may affect the histone modifications differently at the X centromere when compared with the other chromosomes (4). We also found that a knockdown of Sin3 or DNMT1 led to a similar change in histone modifications (data not shown). These results establish an essential role of the p33ING1-Sin3 and DMAP1-DNMT1 complexes for histone deacetylation in pericentric heterochromatin and demonstrate that the p33ING1-Sin3-HDAC and DMAP1-DNMT1 complexes are required for maintaining histone H3K9 methylation in pericentric heterochromatin. In addition, it demonstrates that DNA methyltransferase is also important for maintaining histone hypoacetylation and methylation in pericentric heterochromatin. These results and published work indicate that histone deacetylation and histone and DNA methylation may be interdependent at the pericentric heterochromatin region in maintaining a heterochromatin structure that is conducive for HP1 binding.

*Independent Recruitment of p33ING1 and DMAP1 to Pericentric Heterochromatin*—Because our data demonstrate a physical interaction between p33ING1 and DMAP1, we used a chromatin immunoprecipitation assay to investigate their recruitment to specific pericentric heterochromatin loci. As shown, Sin3, p33ING1, DMAP1, and DNMT1 all associate with the centromeric region of chromosome 4 (Fig. 4*C*, *top row*). Interestingly, although p33ING1 and Sin3 show interdependence for binding to the chromosome 4 centromeric region, a clear difference can be seen when examining their binding to the X chromosome α-satellite sequence. The binding of Sin3 to the X chromosome α-satellite is independent of p33ING1. In contrast, DNMT1 recruits DMAP1 to heterochromatin, consistent with the previous finding that DNMT1 recruits DMAP1 to DNA replication foci (8). Despite the fact that ING1 and DMAP1 physically interact and co-localize to heterochromatin in the late S phase (Figs. 1 and 2), they independently associate with heterochromatin at the chromosome 4 centromeric and X chromosome-linked α-satellite regions.

The three epigenetic elements that characterized heterochromatin are hypoacetylation and hypermethylation of histones, and hypermethylation of DNA (3). The relationships among them are beginning to be understood. Previous studies have shown that a histone H3-specific HDAC, Clr3, is required for H3K9 methylation in fission yeast (20), an H3K9 methyltransferase can direct DNA methylation in fungi and plants (21, 22), and a DNA methyltransferase and a SWI/SNF-like protein that regulates DNA methylation are required for deacetylation of histone H4 in plants (23, 24). Therefore, these three characteristics may be interdependent, and all may be required for maintenance of heterochromatin structure.

In this study, we found that the loss of the p33ING1-Sin3-HDAC complex and the DMAP1-DNMT1 proteins also leads to hyperacetylation and hypomethylation of histones at pericentric heterochromatin. Thus, in addition to the H3K9-specific methyltransferase Suv39h, our data demonstrate that a histone deacetylase complex as well as a DNA methyltransferase complex are required for maintaining histone modifications at the pericentric heterochromatin in human cells. The mechanism of maintaining heterochromatin seems to be evolutionally conserved. The loss of any one of these three enzymes that are important to maintain the characteristics of pericentric heterochromatin can lead to destabilization of the higher order structure that is necessary for binding of HP1 proteins. Although it is clear that both DMAP1-DNMT1 and p33ING1-Sin3 are required for H3K9 methylation at pericentric heterochromatin, it remains to be established whether they are required for DNA methylation of the cytosine residue at pericentric heterochromatin.

Because p33ING1 and DMAP1 are recruited independently to heterochromatin, DMAP1 does not appear to be necessary for localizing the p33ING1-Sin3-HDAC complex to heterochromatin. Thus, the functional significance of the interaction between p33ING1 and DMAP1 is not yet clear. One possibility is that DMAP1 activates the HDAC activity of the p33ING1 complex localized at the pericentric heterochromatin by interacting with the p33ING1 subunit. This model is suggested by the requirements of both p33ING1-Sin3 and DMAP1 for deacetylation of histones at the pericentric heterochromatin. Alternatively, DNMT1-DMAP1 could recruit HDAC2 independently of their interaction with the p33ING1-Sin3 complex. In this scenario, DMAP1 may stimulate the DNMT1-associated HDAC2 activity or stabilize their interaction and/or heterochromatin binding because the binding of DNMT1 to heterochromatin is independent of DMAP1 but is required for deacetylation of histones. Nevertheless, the activities of a histone deacetylase and a DNA methyltransferase need to cooperate at pericentric heterochromatin regions to bring out histone methylation for HP1 binding.

Data presented here reveal components of a pathway for maintaining histone modification at the pericentric heterochromatin during cell division in HeLa cells. Our findings may also provide a molecular mechanism for the links between DNA hypomethylation, genomic instability, and cancer (25, 26). Mice with a hypomorphic allele of *Dnmt1* that retains 10% of wild type DNA methyltransferase activity develop cancer because of genomic instability (25). This instability may be caused by a failure to maintain histone modification at pericentric heterochromatin when DNMT1 activity is low. Similarly, the requirement of the p33ING1-Sin3-HDAC and DNMT1-DMAP1 complexes for this process suggests that other components in these complexes may also be important for preventing cancer development.

*Acknowledgment*—We thank Dr. S. Sazer for critical reading of the manuscript.

REFERENCES

1. Rhee, I., Jair, K. W., Yen, R. W., Lengauer, C., Herman, J. G., Kinzler, K. W., Vogelstein, B., Baylin, S. B., and Schuebel, K. E. (2000) *Nature* **404,** 1003–1007
2. Rhee, I., Bachman, K. E., Park, B. H., Jair, K. W., Yen, R. W., Schuebel, K. E., Cui, H., Feinberg, A. P., Lengauer, C., Kinzler, K. W., Baylin, S. B., and Vogelstein, B. (2002) *Nature* **416,** 552–556
3. Richards, E. J., and Elgin, S. C. (2002) *Cell* **108,** 489–500
4. Peters, A. H., O'Carroll, D., Scherthan, H., Mechtler, K., Sauer, S., Schofer, C., Weipoltshammer, K., Pagani, M., Lachner, M., Kohlmaier, A., Opravil, S., Doyle, M., Sibilia, M., and Jenuwein, T. (2001) *Cell* **107,** 323–337
5. Bannister, A. J., Zegerman, P., Partridge, J. F., Miska, E. A., Thomas, J. O., Allshire, R. C., and Kouzarides, T. (2001) *Nature* **410,** 120–124
6. Lachner, M., O'Carroll, D., Rea, S., Mechtler, K., and Jenuwein, T. (2001) *Nature* **410,** 116–120
7. Maison, C., Bailly, D., Peters, A. H., Quivy, J. P., Roche, D., Taddei, A., Lachner, M., Jenuwein, T., and Almouzni, G. (2002) *Nat. Genet.* **30,** 329–334
8. Rountree, M. R., Bachman, K. E., and Baylin, S. B. (2000) *Nat. Genet.* **25,** 269–277
9. Cowell, I. G., Aucott, R., Mahadevaiah, S. K., Burgoyne, P. S., Huskisson, N., Bongiorni, S., Prantera, G., Fanti, L., Pimpinelli, S., Wu, R., Gilbert, D. M., Shi, W., Fundele, R., Morrison, H., Jeppesen, P., and Singh, P. B. (2002) *Chromosoma (Berl.)* **111,** 22–36
10. Wang, Y., Cortez, D., Yazdi, P., Neff, N., Elledge, S. J., and Qin, J. (2000) *Genes Dev.* **14,** 927–939
11. Li, J., Lin, Q., Wang, W., Wade, P., and Wong, J. (2002) *Genes Dev.* **16,** 687–692
12. Skowyra, D., Zeremski, M., Neznanov, N., Li, M., Choi, Y., Uesugi, M., Hauser, C. A., Gu, W., Gudkov, A. V., and Qin, J. (2001) *J. Biol. Chem.* **276,** 8734–8739
13. Kuzmichev, A., Zhang, Y., Erdjument-Bromage, H., Tempst, P., and Reinberg, D. (2002) *Mol. Cell. Biol.* **22,** 835–848
14. Sobel, R. E., Cook, R. G., Perry, C. A., Annunziato, A. T., and Allis, C. D. (1995) *Proc. Natl. Acad. Sci. U. S. A.* **92,** 1237–1241
15. Tamaru, H., Zhang, X., McMillen, D., Singh, P. B., Nakayama, J., Grewal, S. I., Allis, C. D., Cheng, X., and Selker, E. U. (2003) *Nat. Genet.* **34,** 75–79

16. David, G., Turner, G. M., Yao, Y., Protopopov, A., and DePinho, R. A. (2003) *Genes Dev.* **17,** 2396–2405
17. Cheutin, T., McNairn, A. J., Jenuwein, T., Gilbert, D. M., Singh, P. B., and Misteli, T. (2003) *Science* **299,** 721–725
18. Festenstein, R., Pagakis, S. N., Hiragami, K., Lyon, D., Verreault, A., Sekkali, B., and Kioussis, D. (2003) *Science* **299,** 719–721
19. Waye, J. S., and Willard, H. F. (1985) *Nucleic Acids Res.* **13,** 2731–2743
20. Nakayama, J., Rice, J. C., Strahl, B. D., Allis, C. D., and Grewal, S. I. (2001) *Science* **292,** 110–113
21. Tamaru, H., and Selker, E. U. (2001) *Nature* **414,** 277–283
22. Jackson, J. P., Lindroth, A. M., Cao, X., and Jacobsen, S. E. (2002) *Nature* **416,** 556–560
23. Gendrel, A. V., Lippman, Z., Yordan, C., Colot, V., and Martienssen, R. A. (2002) *Science* **297,** 1871–1873
24. Soppe, W. J., Jasencakova, Z., Houben, A., Kakutani, T., Meister, A., Huang, M. S., Jacobsen, S. E., Schubert, I., and Fransz, P. F. (2002) *EMBO J.* **21,** 6549–6559
25. Gaudet, F., Hodgson, J. G., Eden, A., Jackson-Grusby, L., Dausman, J., Gray, J. W., Leonhardt, H., and Jaenisch, R. (2003) *Science* **300,** 489–492
26. Eden, A., Gaudet, F., Waghmare, A., and Jaenisch, R. (2003) *Science* **300,** 455